

SKB

**TECHNICAL
REPORT**

86-05**Preliminary investigations of fracture
zones in the Brändan area, Finnsjön
study site**

Kai Ahlbom, Peter Andersson, Lennart Ekman,
Erik Gustafsson, John Smellie.
Swedish Geological Co, Uppsala
Eva-Lena Tullborg, Swedish Geological Co, Göteborg

February 1986

PRELIMINARY INVESTIGATIONS OF FRACTURE ZONES IN THE BRÄNDAN
AREA, FINNSJÖN STUDY SITE

Kaj Ahlbom, Peter Andersson, Lennart Ekman, Erik Gustafsson,
John Smellie, Swedish Geological Co, Uppsala

Eva-Lena Tullborg, Swedish Geological Co, Göteborg

February 25, 1986

This report concerns a study which was conducted for SKB. The conclusions and viewpoints presented in the report are those of the author(s) and do not necessarily coincide with those of the client.

A list of other reports published in this series during 1986 is attached at the end of this report. Information on KBS technical reports from 1977-1978 (TR 121), 1979 (TR 79-28), 1980 (TR 80-26), 1981 (TR 81-17), 1982 (TR 82-28), 1983 (TR 83-77), 1984 (TR 85-01) and 1985 (TR 85-20) is available through SKB.

SWEDISH GEOLOGICAL CO
Division of Engineering Geology
Client: SKB

REPORT
ID-no: IRAP 85222
Date: 1986-02-25

PRELIMINARY INVESTIGATIONS OF
FRACTURE ZONES IN THE BRÄNDAN AREA,
FINNSJÖN STUDY SITE

BY

Kaj Ahlbom
Peter Andersson
Lennart Ekman
Erik Gustafsson
John Smellie
Eva-Lena Tullborg

CONTENTS

	Page
ABSTRACT	
1. BACKGROUND	1
2. MAJOR FRACTURE ZONES AT THE BRÄNDAN AREA	3
3. GENERAL DESCRIPTION OF THE FINNSJÖN STUDY SITE	6
3.1 Topography and Quaternary deposits	6
3.2 Geological setting	7
3.3 Lineaments from air-photo interpretation	11
3.4 Outcrops within the central Brändan area	12
4. GROUND GEOPHYSICAL MAPS AND PROFILES	14
4.1 Resistivity and slingram surveys, measured 1978-79	14
4.2 Refraction seismic measurements	15
4.3 Slingram and VLF-measurements in the Brändan area .	15
5. LITHOLOGY AND FRACTURE LOGS	23
5.1 Core mapping of Fi 5	27
5.2 Core mapping of Fi 6	28
5.3 Core mapping of Fi 9	30
5.4 Core mapping of Fi 10	31
5.5 Drilling characteristics and sampling of drilling debris of the percussion borehole HFi 1	33
5.6 Core samples obtained by the Borros sampler	36
5.7 Thin section microscopy	38
6. GEOPHYSICAL LOGGING	41
6.1 Geophysical logging of boreholes in the Brändan area	41
6.2 Geophysical logging of the boreholes outside the Brändan area but within the Finnsjön study site . .	44
7. BOREHOLE RADAR MEASUREMENTS	54
7.1 General	54
7.2 Radar measurements of boreholes in the Brändan area	55
7.3 Wulff net plots	57
7.4 Conclusion	58
8. MEASUREMENTS OF HYDRAULIC CONDUCTIVITY AND ESTIMATES OF STORATIVITY66
8.1 Measurements of hydraulic conductivity by single- hole injection tests and interference tests	66
8.2 Estimates of specific storage	104
9. PIEZOMETRIC MEASUREMENTS108
9.1 Background108
9.2 Equipment	108

9.3 Methods	110
9.4 Results	112
10. DRILLING FLUID AND DRILLING DEBRIS	123
10.1 Drilling fluid and tracers	123
10.2 Water sampling and collection of drilling debris during gas-lift pumping128
11. WATER CHEMISTRY	131
11.1 Earlier hydrochemical studies in the Finnsjön area	131
11.2 Water chemical investigations in the Brändan area	.132
11.3 Chemistry of the groundwaters137
11.4 Discussion of results140
11.5 Conclusions of the water chemistry studies	147
12. CONCLUSIONS	148
REFERENCES151

ABSTRACT

The investigations in the Brändan area have defined two major fracture zones.

Zone 1, the Brändan fracture zone, is 20 m wide, strikes NNE and dips 75 degrees towards east. Characteristic for the zone is a high frequency of coated and sealed fractures, 12 and 50 fr/m respectively. Infillings of hematite and asphaltite are common. Hydraulic conductivity determined by single-hole water injection tests varies between $1.2 \cdot 10^{-6}$ and $4.8 \cdot 10^{-5}$ m/s measured at vertical depths between 57 and 76 m.

Zone 2, a subhorizontal fracture zone, is about 70 m wide and strikes N-S with a westerly dip of 17 degrees. The zone is defined in all 4 cored boreholes in the Brändan area, which gives a minimum lateral extent of about 500 m. The boreholes intersect the zone at depths ranging from 100 to 300 m. Characteristic for Zone 2 are sections with mylonite and breccia. Within the zone, the frequency of sealed fractures is high in all boreholes, about 40 fr/m compared to 14 fr/m in the country rock. The frequency of coated fractures varies greatly between different boreholes, 3 to 9 fr/m compared to 2 to 5 fr/m in the country rock. In spite of low frequency of coated fractures for the Zone 2 in some boreholes, the hydraulic conductivity is high in all boreholes. Several values higher than 10^{-4} m/s have been observed. Interference tests have established hydraulic connections in Zone 2 between four investigation boreholes at distances up to 450 m.

Saline water of about 5000 mg/l of chlorine is found below the Zone 2. The saline water encountered at such shallow levels indicates that the subhorizontal Zone 2 functions as a hydraulic barrier against draining out and replacement of the saline water by non-saline groundwater.

Zone 2 is recommended for the detailed investigations planned for the Fracture Zone Project.

1. BACKGROUND

The only probable mechanism by which radionuclides can reach the biosphere and the human environment is by transportation with the flowing groundwater, which in crystalline rock is restricted to fractures and especially fracture zones. A detailed knowledge of the characteristics of fracture zones is therefore needed. Previous model calculations of groundwater flow at potential repository sites in Sweden have regarded existing fracture zones as completely open, resulting in an improbably rapid radionuclide transportation between repository depth and the surface. Such an assumption is definitely over-conservative since rock - mineral interactions, dilution, dispersion and sorption are retarding the transportation of nuclides along the zones. A generic study, where detailed geological, geophysical, hydrogeological and geochemical investigations of a fracture zone are carried out, has therefore been initiated by the Swedish Nuclear Fuel and Waste Management Co (SKB).

The investigation covers a four year period and is divided into several phases. The purpose of the first phase of the fracture zone study is a preliminary investigation of a site where a 3-D model of the tectonic pattern can be established including hydraulic properties of the fracture zones and the country rock. The result from the first phase, described in this report, will be evaluated in order to decide whether the area is feasible for further investigations. Phase two will focus on detailed hydrogeological and geochemical characterization and migration properties of the selected fracture zone and the surrounding country rock. Phase three, finally, will concentrate on rock mechanical studies in connection to the fracture zone and will also include a final evaluation of the project.

The Finnsjön study site is located in northern Uppland, central Sweden, figure 1.1. The geology and hydrogeology of the bedrock was investigated during the years 1977-1982 within the site selection studies for a repository for spent nuclear fuel (Olkiewicz et al. 1979, Carlsson et al. 1980, Carlsson and Gidlund, 1983, among others). Within the Brändan area, figure 1.1,

two cored boreholes, Fi 5 (751 metres) and Fi 6 (691 metres), were drilled during 1978. Results from the core loggings and hydrogeological tests, together with surface geophysical measurements and topography, indicated the presence of a water conductive, steeply dipping, fracture zone.

The investigations were at first concentrated to this steeply dipping fracture zone, Zone 1. However, after the discovery of a major subhorizontal fracture zone, Zone 2, which appeared to have a strong influence on the hydrology and geochemistry of the site, the major part of the investigations was focused on the Zone 2.

Results from the preliminary investigations are accounted for in this report. In addition, data have been compiled in an internal SKB-report: "Ahlbom, K., Melkersson, K., Strähle, A. (1985): Fracture zone project, core logging and technical data for boreholes Fi 5, Fi 6, Fi 9 and Fi 10."

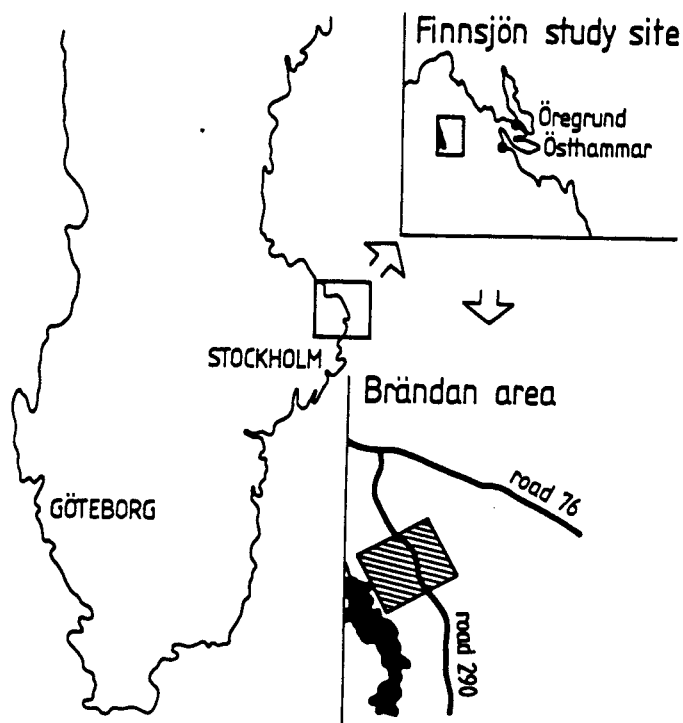


Figure 1.1. Location of the Finnsjön study site.

2. MAJOR FRACTURE ZONES AT THE BRÄNDAN AREA

Most studies within this project have been aimed to define and characterize fracture zones. The results from the different studies have been concentrated on two of the three major fracture zones which have been defined within the area, figures 2.1 and 2.2. In order to facilitate reading of this report, these fracture zones are presented below.

Zone 1, the Brändan fracture zone, has a NNE strike with a dip of about 75 degrees to the east. The width is about 20 m. The fracture zone is topographically expressed as a minor gully, 30-50 m wide and covered with till and peat, surrounded by lowlying outcrops. The lineament representing the fracture zone is traceable for more than 500 m. The fracture zone is well defined by surface geophysical measurements for more than 1 km.

Zone 2, the subhorizontal fracture zone, is only defined in the boreholes. It trends north with a dip of about 17 degrees to the west. However, since the zone is only defined in boreholes which are located along a more or less straight line, the precise orientation is not known.

In the figures 2.1 and 2.2 the location of Zone 2 is taken from data from borehole Fi 6 extrapolated to the other boreholes, with the orientation mentioned above. This agrees well with the interpreted location of the fracture zone in all boreholes, possibly with the exception of borehole Fi 10. Here, the core within the upper part of the extrapolated location of Zone 2 does not show indications of increased fracturing.

Zone 3, the Gåvastbo fracture zone, is a regional zone defined earlier (Carlsson and Gidlund, 1983). The Zone 3 strikes NNW with a vertical dip. This zone has not been included in the detailed studies.

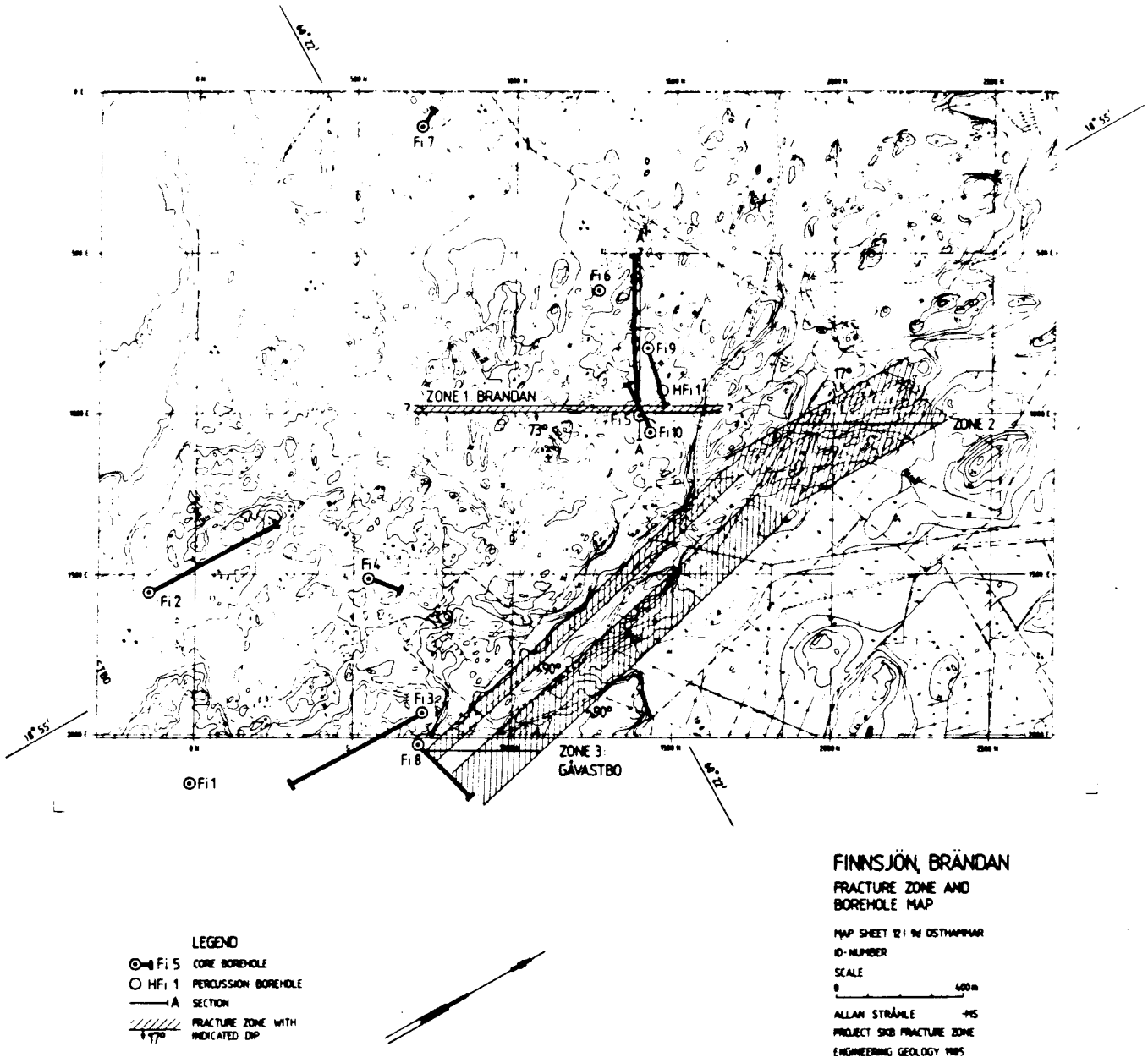


Figure 2.1 Location of boreholes and major fracture zones at the Brändan area. The vertical section A-A is marked.

SE
A

5

NW
A'

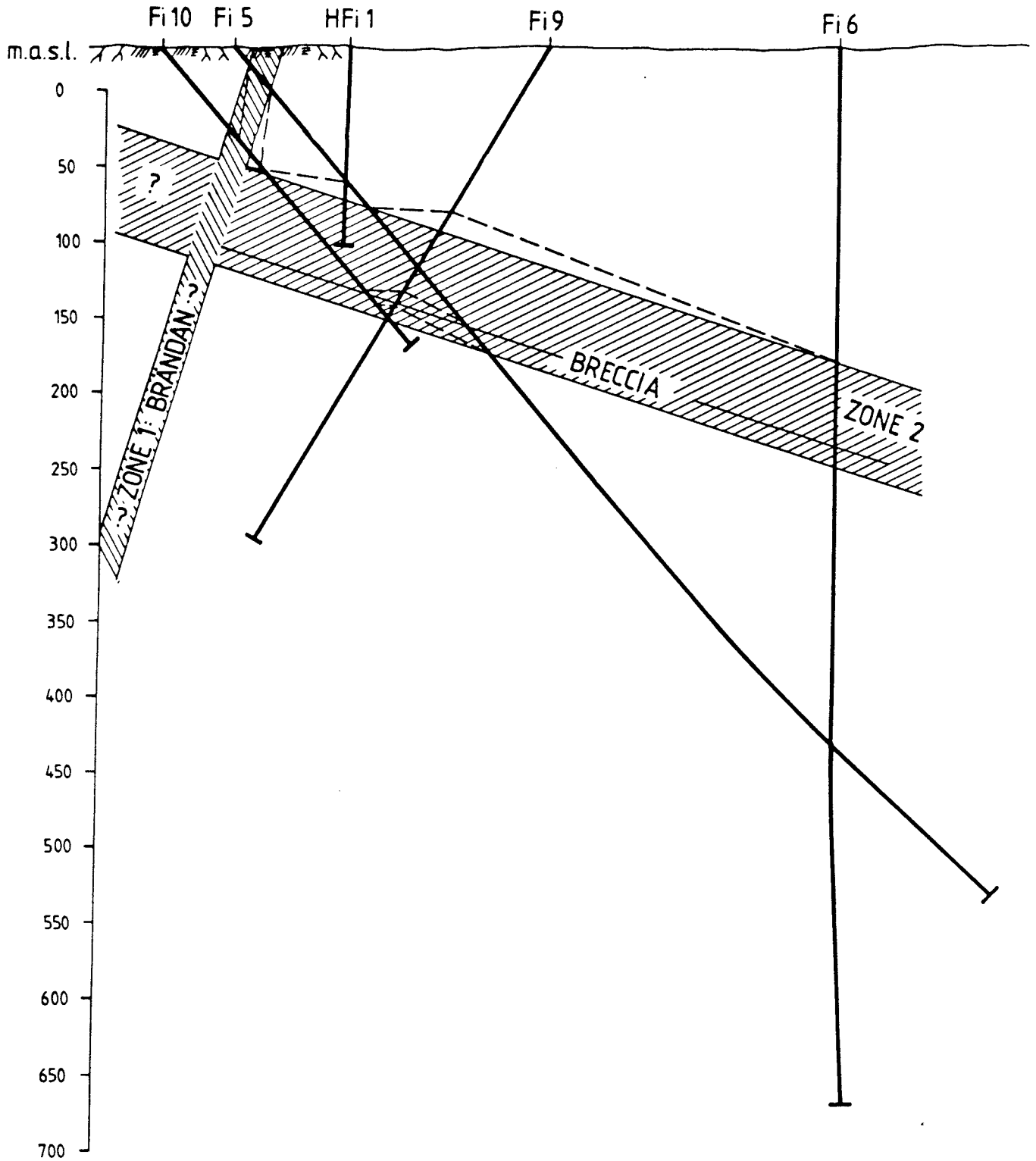


Figure 2.2 Vertical section A-A through the Brändan area. Dashed lines show the extrapolated intersection between the fracture zones and the boreholes. The boreholes are projected into the section.

3. GENERAL DESCRIPTION OF THE BRÄNDAN AREA, FINNSJÖN STUDY SITE

3.1 Topography and Quaternary deposits.

The dominating impression of the topography of the Finnsjön site is the flatness. The western parts of the site are situated at levels between about 25 and 45 m.a.s.l., while the eastern parts are lower, mainly between 20 and 25 m.a.s.l.

Within the study site, the Brändan area displays a variation in altitude of less than 15 m, from about 20 to less than 34 m.a.s.l. A slight dip in altitude creates the drainage direction of the area towards northeast.

The middle and south-western parts of the Brändan area, where most of the studies for the fracture zone project are performed, is dominated by exposed rock. Between the outcrops, the soil is often thin, consisting primarily of till and peat. Under the peat there is generally a thin layer of outwashed material, e.g. sand, sometimes resting on clay. The clay is always underlain by till. Clay or outwashed material is exposed at the surface only in small areas.

The CaCO_3 -content of the till is rather high, between 10 and 20 % of the fine material.

In the eastern part of the Brändan area the percentage of outcrops is much smaller than in the western part. Instead till, bogs, clay and outwashed material is more dominating both as to area and depth. Soundings have here shown a maximum soil depth of 8.5 m, Almén et al., (1978) and Jacobsson, (1980). Typical layering found in the soundings is peat, outwashed sand, glacial clay and till.

In Almén et al. (1978) a short review of the Quaternary history of the Finnsjön study site is given. It is supposed that the latest inland ice movement direction in the area was between north and northeast (N 30 E). The inland ice left the

area about 7 600 B.C. The recession rate was 250 m/year. The Finnsjön area was lifted up above the sea level between about 3 200 B.C. and 800 B.C. Corresponding values for the Brändan area should be about 2 300 B.C. to 1 300 B.C. The average rate of land-uplift at that time was approximately 10 mm/year. Today the rate for the Finnsjön site is 5.5 mm/year.

3.2 Geological setting

The following text is a short summary of an internal SKB-report (81-35) describing a geological mapping of the Finnsjön study site performed in 1980-81: "Olkiewics, A. and Arnefors, J. (1981): Berggrundsbeskrivning av undersökningsområdet vid Finnsjön i norra Uppland." The central part of the geologic map is shown in figure 3.1.

The bedrock within the Finnsjön study site is of Svecokarelian age, about 1800-2100 Ma. The site consists mainly of four rock types: leptite, basites, granodiorite and late-orogenic granite (young granite).

The oldest rock types are some varieties of leptite. This is a supracrustal acidic volcanic rock that mainly consists of quartz, potassium feldspar and plagioclase. The leptites are fine grained and have a greyish red to grey colour. Leptite is found in the northern and northeastern part of the site.

The leptite is bounded to the south by ultra basic to basic rock types. Hornblende is the main mineral of the ultra basic rock. The grain size varies from fine to coarse and the colour is dark green to black. The basic rock types have a dioritic to gabbroic composition with the main minerals plagioclase, hornblende and biotite. The colour is dark grey to black and the rock is fine to medium grained. These basic rocks have intruded into the bedrock before and during a deformation phase which has folded the supracrustal rocks.

Dykes of metabasites are common in all major rock types, excluding the late-orogenic granite. The width of the dykes

is in most cases less than 1 m.

All boreholes within the Finnsjön study site, including the boreholes at the Brändan area, are drilled within a granodiorite which dominates in the central and western part of the site. The granodiorite brecciates the older leptites and basites. Xenolites of these rock types are frequent within the granodiorite. Dykes of younger rock types, i.e. granite, pegmatite and aplite are common.

The SiO_2 content of the granodiorite is 66 weight per cent. The mean mineral content expressed as volume per cent of the granodiorite is (5 samples): plagioclase 32 %, quartz 30 %, microcline 18%, hornblende 11%, biotite and chlorite 9%. In some samples biotite is absent. Minor amounts of chlorite, epidote, apatite, titanite and sericite are common.

Chemical analysis of granodioritic samples are presented in tables 3.1 and 3.2.

The colour varies from grey to greyish red, and the grains are medium sized. Red granodiorite occurs in areas which are tectonically affected. Mylonites are common and epidote occurs frequently in the area.

The foliation of the granodiorite has a northwesterly strike and dips steeply eastwards.

Late-orogenic granite is found as a large rock body in the eastern and southern parts of the site. This rock type consists mainly of plagioclase, quartz and microcline with minor amounts of biotite and chlorite. The colour is red to greyish red, locally grey. The grains are fine to medium sized. The granite has commonly phenocrysts of feldspar. Aplitic pink dykes associated with the granite occur in the granodiorite and the gabbro.

Pegmatite dykes associated with both the granodiorite and the granite occur.

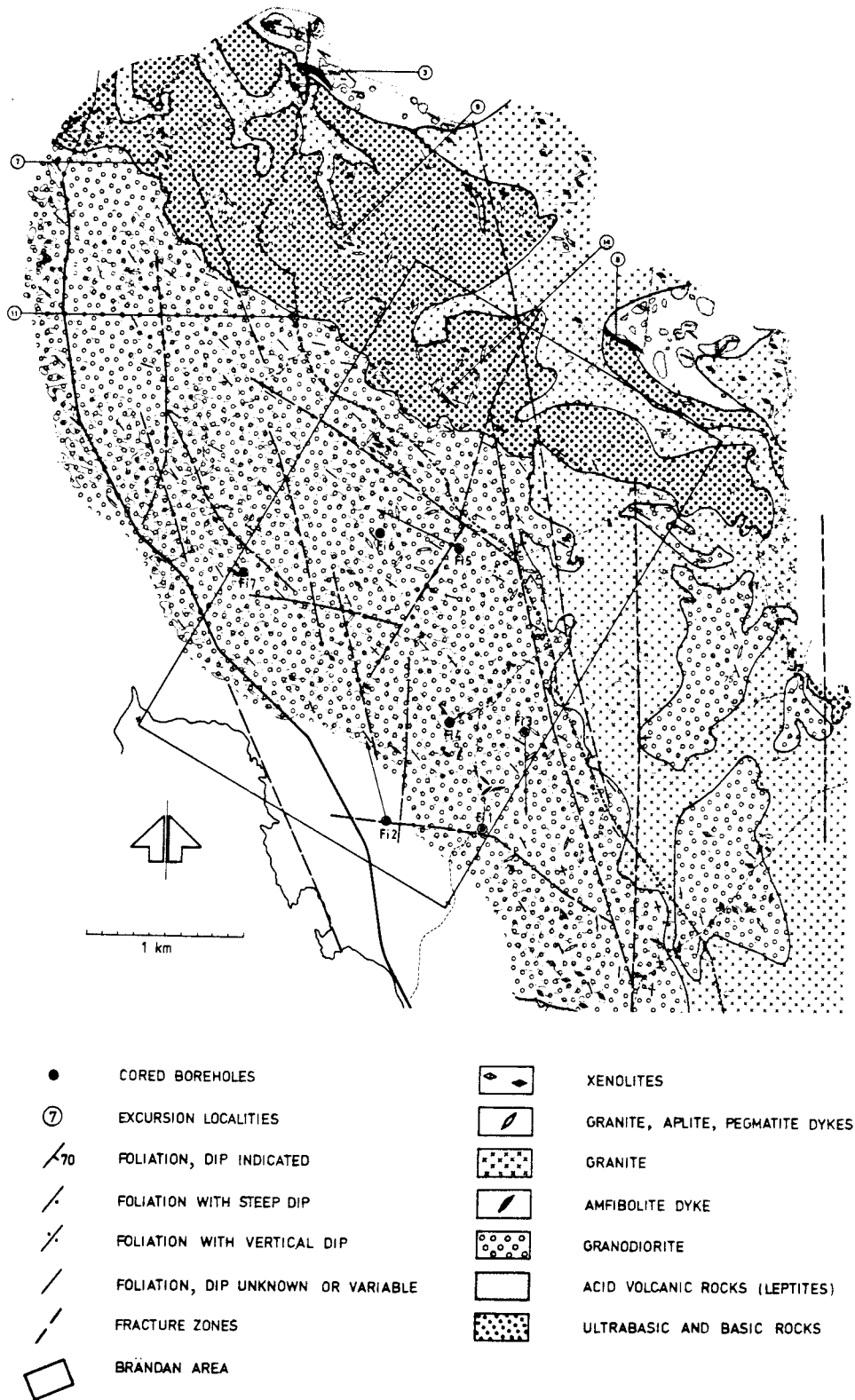


Figure 3.1 Map of precambrian rocks at the Finnsjön study site.

Table 3.1 Chemical analyses of the granodiorite at Finnsjön.

Vikt % Weight %	011-0789	011-0790	011-0791	011-1928	011-1929	011-1930	011-1931	011-1932	011-1933	011-1934	011-1935	BKBA79028	BKBA79029
SiO ₂	64.2	66.0	63.9	64.4	64.6	64.7	66.9	65.2	65.9	66.0	65.5	68.1	75.5
TiO ₂	0.52	0.49	0.57	0.46	0.44	0.42	0.40	0.43	0.42	0.38	0.44	0.42	0.24
Al ₂ O ₃	12.4	12.7	12.6	13.3	14.3	13.9	14.0	14.1	14.3	13.9	13.7	14.3	13.5
Fe ₂ O ₃	1.7	1.4	1.4	2.0	1.5	1.4	1.2	1.4	1.3	1.3	1.3	1.6	0.8
FeO	3.7	3.4	3.9	3.0	3.4	3.2	3.2	3.5	3.3	2.9	3.4	3.1	1.7
MnO	0.11	0.14	0.12	0.10	0.09	0.09	0.10	0.09	0.09	0.08	0.12	0.11	0.08
CaO	4.6	2.0	4.7	3.9	4.1	4.0	2.5	4.0	4.2	3.7	2.0	3.5	2.7
MgO	1.9	2.3	2.1	1.86	1.87	1.74	1.80	1.90	1.74	1.50	2.2	1.93	0.61
Na ₂ O	2.5	3.0	2.6	2.8	2.5	2.5	2.6	2.5	2.6	2.5	3.3	2.4	2.8
K ₂ O	3.5	3.5	3.3	3.3	3.5	3.6	3.9	3.6	3.6	3.9	3.3	3.9	2.5
H ₂ O<105												1.3	1.1
H ₂ O<105												0.2	0.1
P ₂ O ₅												0.11	0.05
CO ₂												0.05	0.02
F												0.09	0.02
S	0.03	< 0.02	0.02	< 0.02	0.02	< 0.02	< 0.02	0.13	< 0.02	< 0.02	0.02	< 0.02	< 0.02
BaO	0.1	0.12	0.13	0.09	0.09	0.08	0.11	0.08	0.08	0.07	0.13	0.11	0.16
U	< 0.005	< 0.005	< 0.005										
SUMMA	95.26	95.05	95.34	95.21	96.41	95.63	96.71	96.93	97.53	96.23	95.41	101.02	101.78
CIPW-norm													
q	24.9	26.6	23.9	25.2	24.6	25.2	27.6	24.9	24.9	26.3	25.1	27.4	41.3
c	0.0	0.3	0.0	0.0	0.0	0.0	0.9	0.0	0.0	0.0	1.0	0.3	1.4
or	21.7	21.8	20.5	20.5	21.5	22.2	23.8	21.9	21.8	23.9	20.4	22.8	14.5
ab	22.2	26.7	23.1	24.9	21.9	22.1	22.7	21.8	22.6	22.0	29.3	20.1	23.3
an	12.9	10.7	13.6	14.7	18.1	16.8	13.0	17.1	17.1	15.8	10.6	15.8	12.9
Sällsk / Sällc	81.7	86.0	81.0	85.2	86.1	86.4	88.2	85.8	86.4	88.0	86.4	86.4	93.4
Femisk / Femic	18.3	13.9	19.0	14.7	13.9	13.6	11.8	14.1	13.6	11.9	13.5	12.2	5.4

Table 3.2 Chemical analyses of granodiorite, trace elements.

Prov nr	Nivå	CU	PB	ZN	MO	NI	CR	CO	FE203	MNO	AS	AG	CAO	MGO	V	SR	TIO	BAO	SN	BE	BI	W
		PPM	PPM	PPM	PPM	PPM	PPM	PPM	%	%	PPM	PPM	%	%	PPM	PPM	%	%	PPM	PPM	PPM	PPM
0111928	316.0-316.3 m Fi 6	18	16	70	<10	<10	37		8.4	0.18	<50	<3	7.5	3.2	162	271	0.59	0.094	<5	<3	<5	
0111929	461.1-461.3 m Fi 5	17	14	45	<10	10	26		6.8	0.14	<50	<3	4.5	2.4	174	450	0.58	0.102	<5	<3	<5	
0111930	140.6-140.9 m Fi 4	14	15	41	<10	<10	23		6.2	0.13	<50	<3	4.8	2.2	148	360	0.47	0.086	<5	<3	<5	
0111931	485.4-485.6 m Fi 4	11	18	48	<10	<10	27		7.4	0.18	<50	<3	3.4	2.7	172	286	0.46	0.068	<5	<3	<5	
0111932	258.6-258.8 m Fi 5	98	13	43	<10	<10	31		7.4	0.15	<50	<3	4.3	2.6	186	380	0.53	0.080	<5	<3	<5	
0111933	181.0-181.3 m Fi 7	27	15	43	<10	<10	22		5.9	0.13	<50	<3	3.8	1.9	149	339	0.35	0.084	<5	<3	<5	
0111934	498.4-498.6 m Fi 7	27	14	33	<10	<10	21		5.6	0.12	<50	<3	3.4	1.7	137	362	0.35	0.083	<5	<3	<5	
0111935	288.7-288.9 m Fi 4	19	21	80	<10	10	35		8.5	0.23	<50	<3	5.3	3.8	196	261	0.63	0.095	<5	<3	<5	
BKBA79028		9	15	28	<10	<10	14	18	4.2	0.11	<50	<3	2.5	1.2	117	218	0.24	0.048	<5	<3	<5	<50
BKBA79029		<5	13	41	<10	<10	<5	<10	2.8	0.08	<50	<3	2.1	0.5	23	263	0.27	0.085	<5	<3	<5	<50

3.3 Lineaments from air-photo interpretation

The lineaments shown in figure 3.2 have been interpreted from black and white air-photos in the scale 1:10 000. Fracture zones are possible to detect due to the thin soil cover and the erosional effect caused by the ice movement during the glaciation. In the interpretation it is important to take into account, that fracture zones parallel to the ice movement are more eroded than fracture zones perpendicular to it. Furthermore, interpretation in different scales pronounces different sizes of fracture zones. Thus the scale 1:10 000 suppresses large features as the Brändan or Gåvastbo fracture zones, but enhances indications of minor fracture zones.

The most common and persistent lineaments are trending N-S and N 50-60 W. North-south trending lineaments are most pronounced in the western upper and eastern lower part of the map. Both the Gåvastbo fracture zone and the subhorizontally dipping Zone 2 are oriented within 10 degrees deviation from this direction.

Lineaments trending N 50 W could to some extent be caused by different erosional properties due to plastic deformation of the rock. The strike of the foliation within the granodiorite is generally N 50 W.

Less persistent but common lineament directions are N 25-35 E and E-W. The Brändan fracture zone is one example of a fracture zone with a N 30 E orientation.

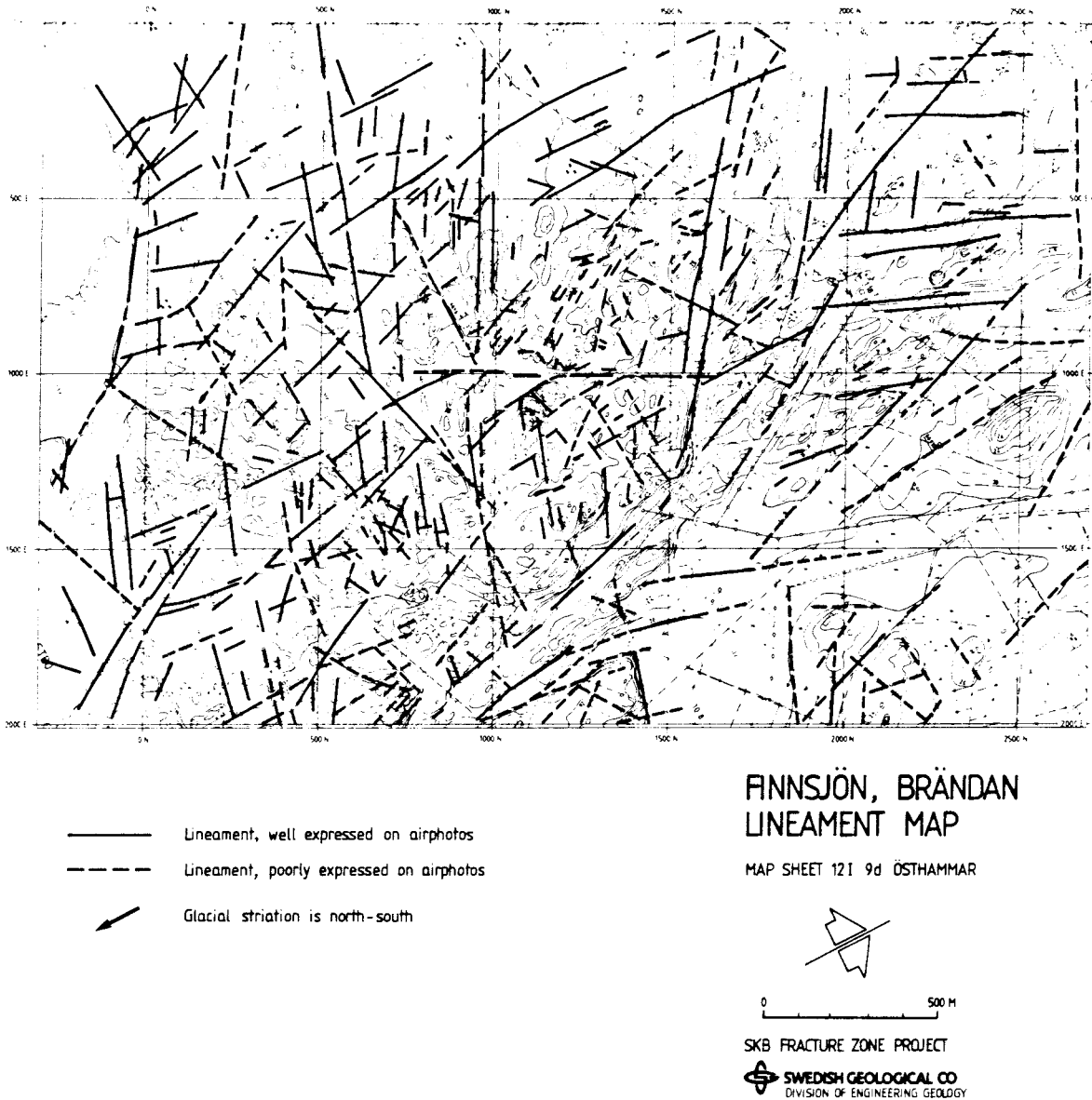


Figure 3.2 Lineaments at the Finnsjön study site.

3.4 Outcrops within the central Brändan area.

Using an aviograph type Wild TC-1, a detailed map of outcrops was made for the central part of the Brändan area, figure 3.4. The map has been used together with the ground geophysical measurements and air-photos to locate possible fracture zones.

The location of the Brändan fracture zone is from topography and geophysical measurements interpreted to be close to the 1000 E line, figures 3.3 and 4.1. There is also a lack of outcrops close to this line. In the southwestern part of the 1000

E line the distance between outcrops is only 10 m. The horizontal width of the fracture zone is calculated from borehole data to be about 20 m. Thus, detailed geologic and tectonic studies of some of the southwestern outcrops might give additional information about the fracture zone.

The topography and lack of outcrops close to borehole HFi 1 may indicate a minor fracture zone trending north-south.

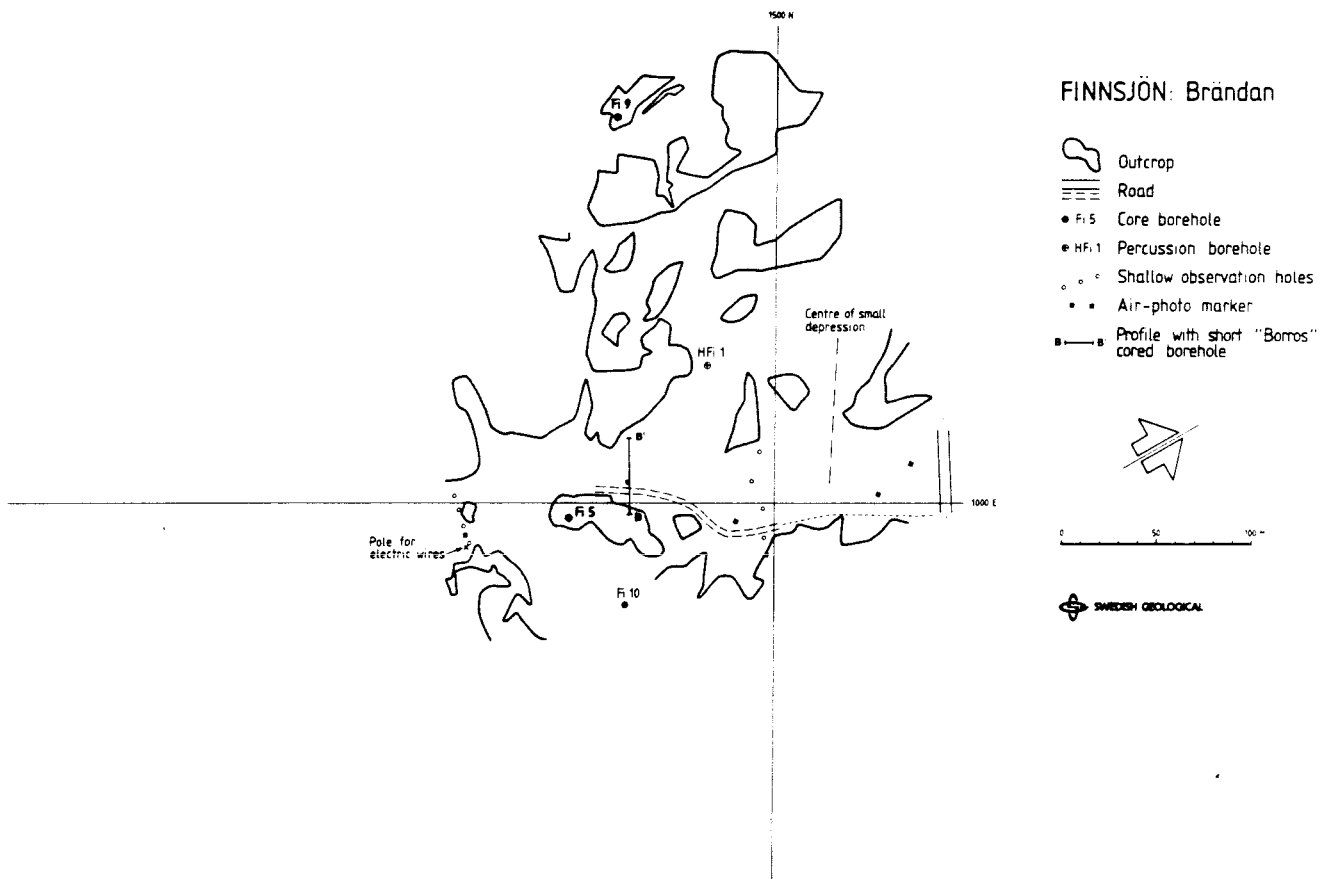


Figure 3.3 Outcrops within the Brändan area.

4. GROUND GEOPHYSICAL MAPS AND PROFILES

Ground geophysical profiles and maps have been studied in order to define the location and, if possible, the dip of fracture zones within the Brändan area. The investigations have been concentrated to the lineament representing Zone 1 (the Brändan fracture zone). However, efforts have also been made to define other fracture zones in the vicinity of this lineament.

4.1 Resistivity and slingram surveys made 1978-1979

During the site investigation 1978-1979, slingram (horizontal loop EM), resistivity, IP and magnetic surveys were carried out within the Finnsjön study site. The measurements were made in profiles oriented in NNW-SSE (N 20 W), with a separation of 20 m between the measuring points and 80 m between the profiles. The results were presented in hand-drawn maps. Within this project the measurements from the slingram (imaginary component) and resistivity surveys were digitized and high resolution maps have been produced using a colour ink-plotter. In this report the maps are presented in black and white, figures 4.1 and 4.2.

Both maps show frequent anomalies perpendicular to the profiles. This is an effect of the interpolation algorithm used by the computer during plotting of data due to the short distance between the measuring points relative to the distance between the profiles. Anomalies caused by fracture zones or other geological structures with the orientation perpendicular to the profiles are therefore hard to discover.

Zone 1 (Brändan) was earlier interpreted to be located around the 1000 E line. This is also indicated by the resistivity and slingram maps. The anomalies are strongest between 900 N to 1600 N. At 900 N the resistivity map indicates an offset or a bend of the zone, 50-100 m, either to the east or to the west. Anomalies indicating minor fracture zones are also indicated

in this area. These fracture zones strike N 80 W. The geophysical interpretation of the location of the fracture zones in the Brändan area is presented together with the resistivity map in figure 4.2.

The Zone 1 divides the bedrock into two blocks of different resistivity. The northeastern block has a higher resistivity than the southeastern block.

4.2 Refraction seismic measurements

Refraction seismic measurements were carried out during 1979 in the Brändan area. Within this project some of the seismic profiles have been interpreted in greater detail. The results indicated a fracture zone, about 25-35 m wide, at the same location as indicated by the resistivity measurements. However, the p-wave velocity within the fracture zone is surprisingly high, 4500-4700 m/s. P-wave velocities measured in the country rock are between 4500-5700 m/s.

One refraction seismic profile was located in the same section in which the soil depth was determined with short boreholes (Borros core sampler, section 5.6). This gives an opportunity to compare the results from the two studies. The width of the fracture zone determined from Borros drillings is 20 m and the soil depth is between 2.0 - 3.4 m. The seismic measurements indicate a width of 25 m of the fracture zone and a soil depth of 2.0 - 2.5 m. Thus, there is a good correlation between the two studies.

4.3 Slingram and VLF-measurements in the Brändan area

In order to define Zone 1 (Brändan), 10 profiles with VLF and Slingram measurements were carried out. The profiles, 500 m in length, were made perpendicular to the Zone 1 with the center at the lineament representing the zone (1000 E line). For some profiles electric cables have distorted the measurements.

The VLF-measurements strongly indicate the presence of the Brändan fracture zone around the 1000 E line. By using the inflexion point for the anomalies caused by the fracture zone, the center of the zone is defined, figure 4.3. As seen from this figure, the fracture zone is slightly windling from the 1500 E line to the 800 E line. The two lines 560 E and 325 E also show a shift in the location of the fracture zone of about 70 m to the west.

The Slingram measurements, figure 4.4, show similar anomalies as the VLF measurements. For the profile at 1500 N a dip of 70 degrees towards west was calculated for Zone 1, which should be compared with the dip interpretation from core logging of 75 degrees towards east. This discrepancy might possible be explained by interference with Zone 2. The anomalies of the fracture zone at other profiles are distorted and no attempt has been made to make dip calculations from these profiles.

Slingram and VLF-profiles were also measured parallel to the Brändan fracture zone at 1075 E line (east of Brändan) and at 925 E (west of Brändan), figure 4.5. Unfortunately electric cables distorted the measurements between 1250-1350 N. Appart from the distorted sections, the slingram and VLF-GBR measurements show only minor anomalies. These occur at 800N, 1015 N and at 1125 N for the 1075 E line and at 860 N, 1010 N and 1530 N for the 925 E line. More geophysical profiles parallel to the Brändan fracture zone are needed in order to define the orientation and extent of these minor fracture zones.

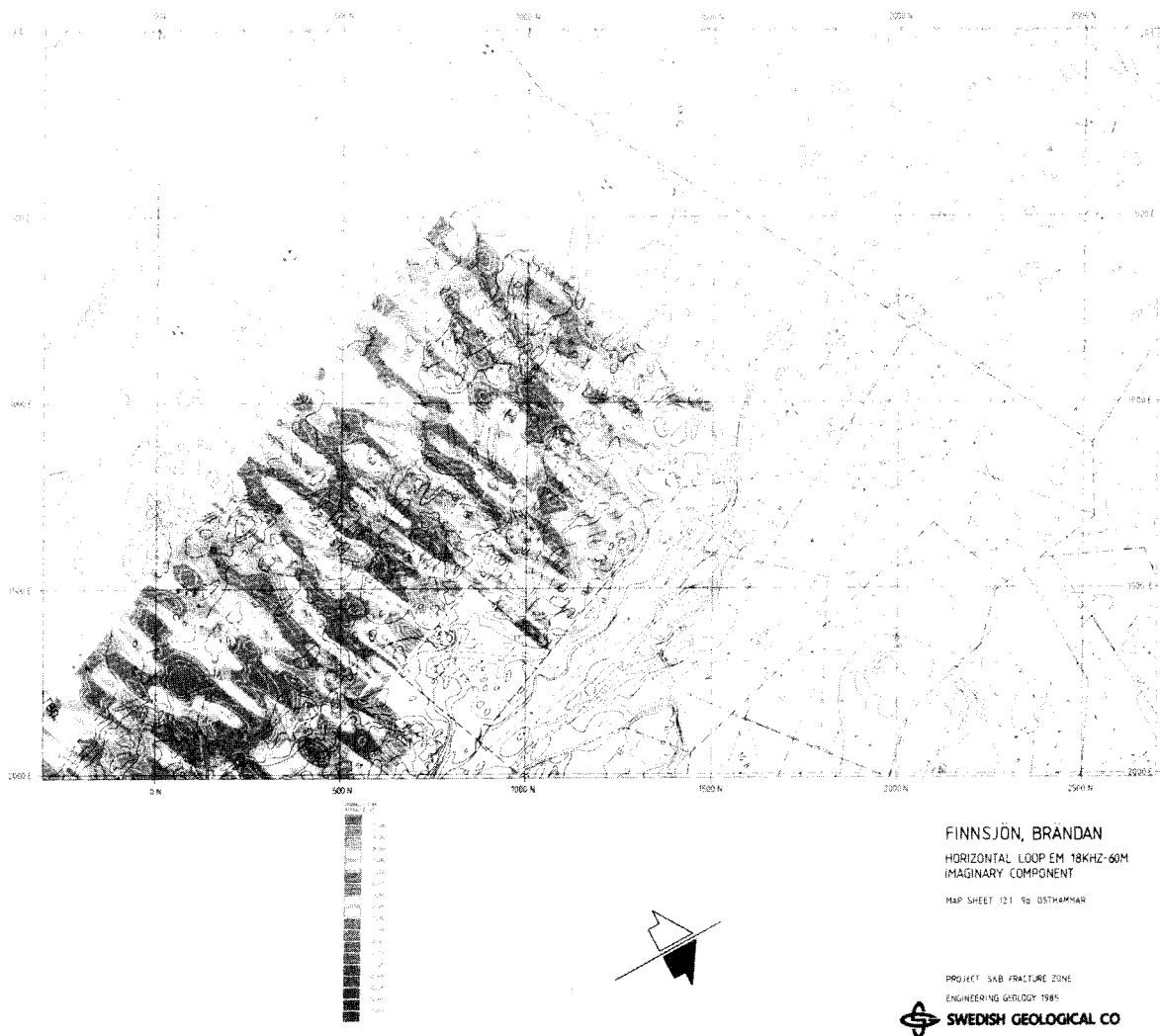


Figure 4.1 Slingram imaginary measurements at the Finnsjön study site.

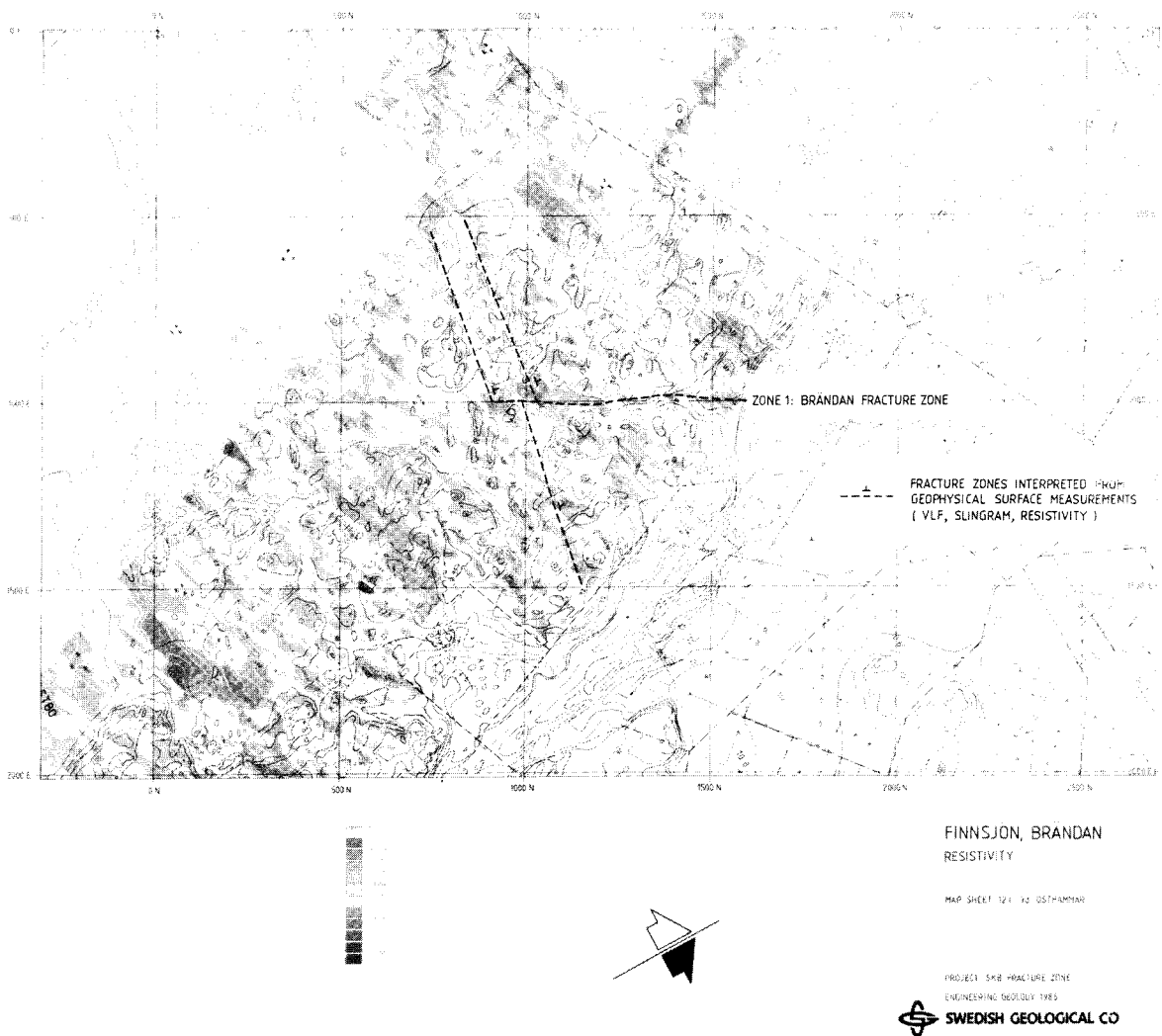


Figure 4.2 Resistivity measurements at the Finnsjön study site. Interpreted fracture zones are marked.

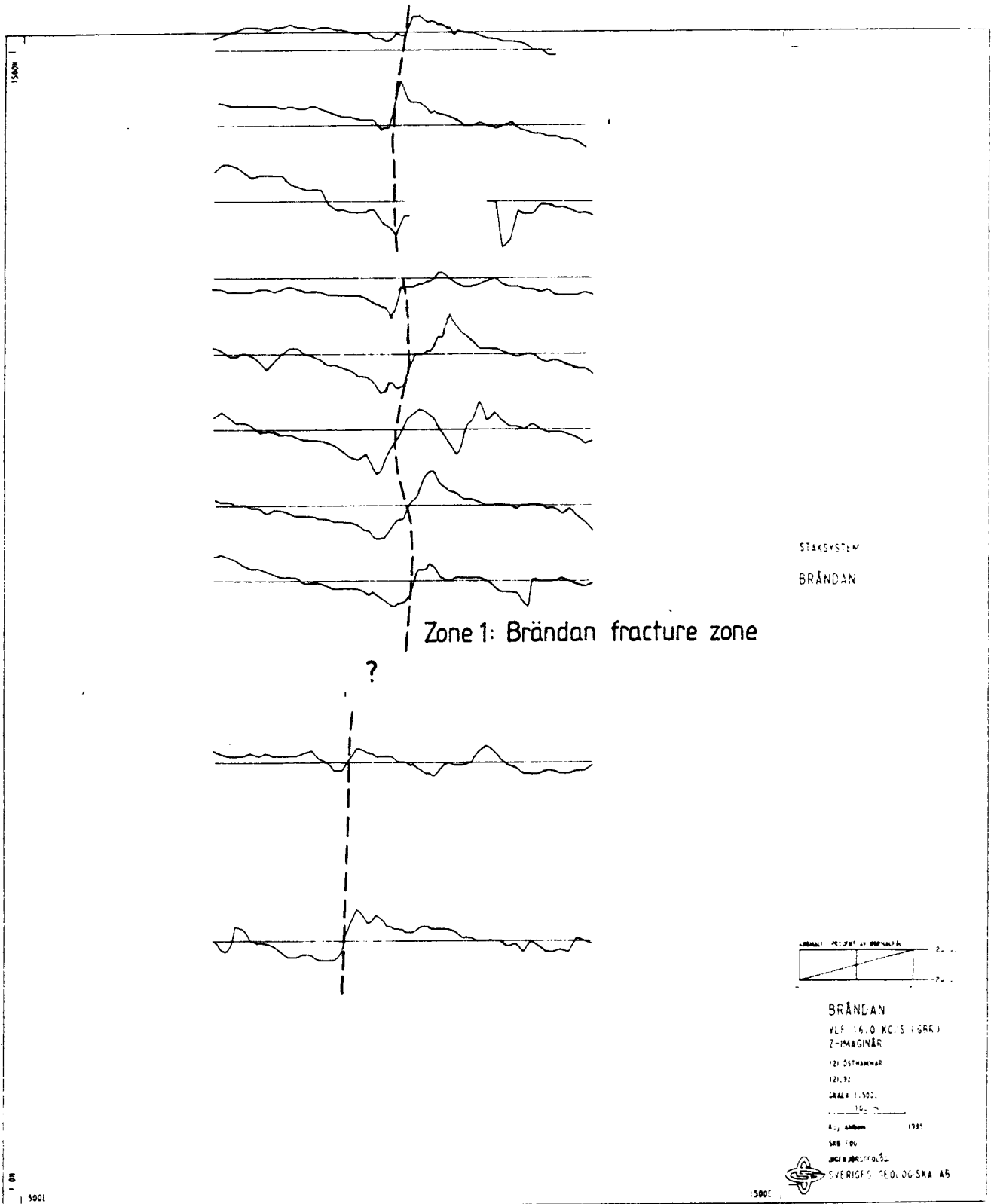


Figure 4.3 VLF imaginary (GBR) measurements at profiles across the Zone 1 (Brändan).

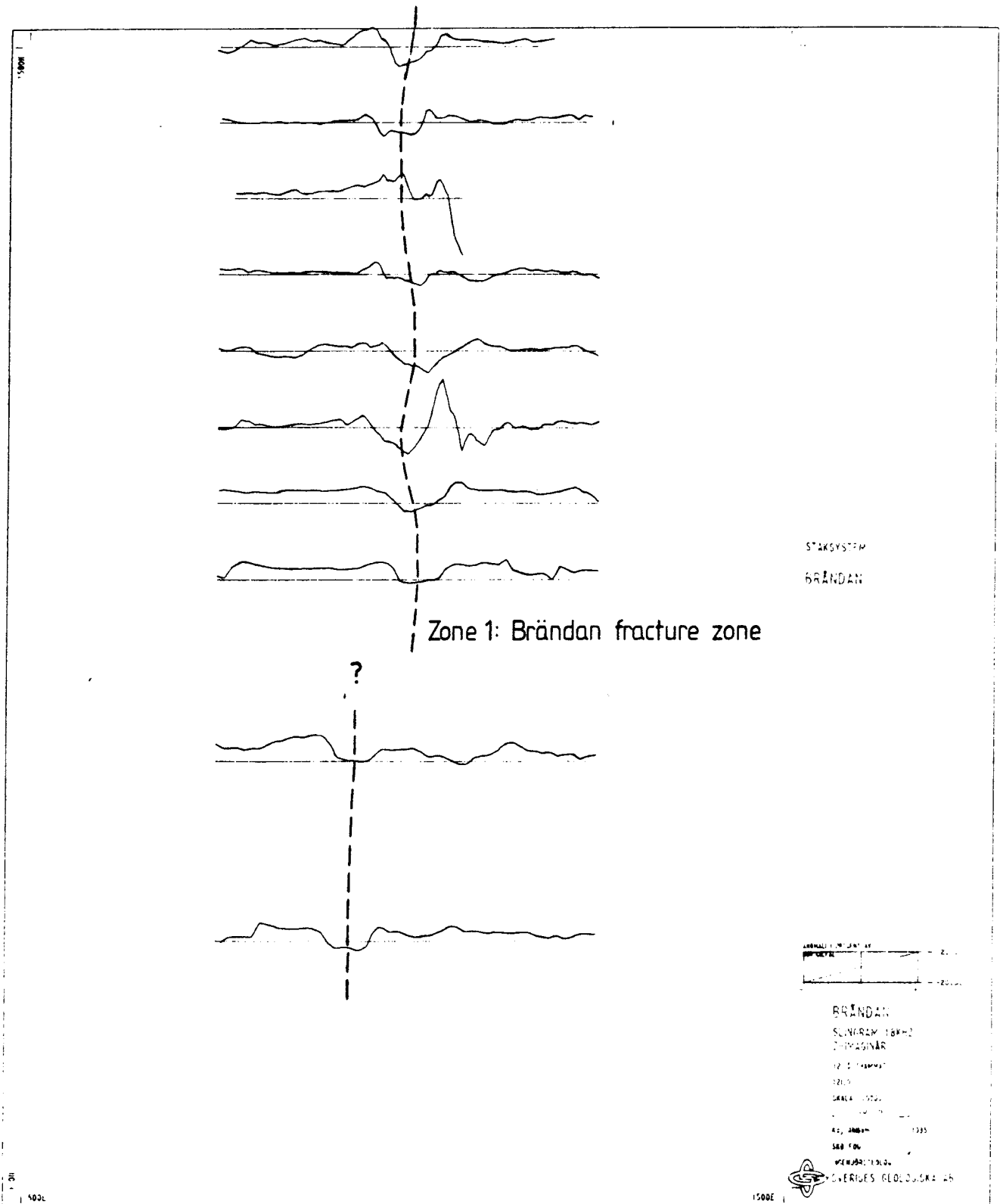
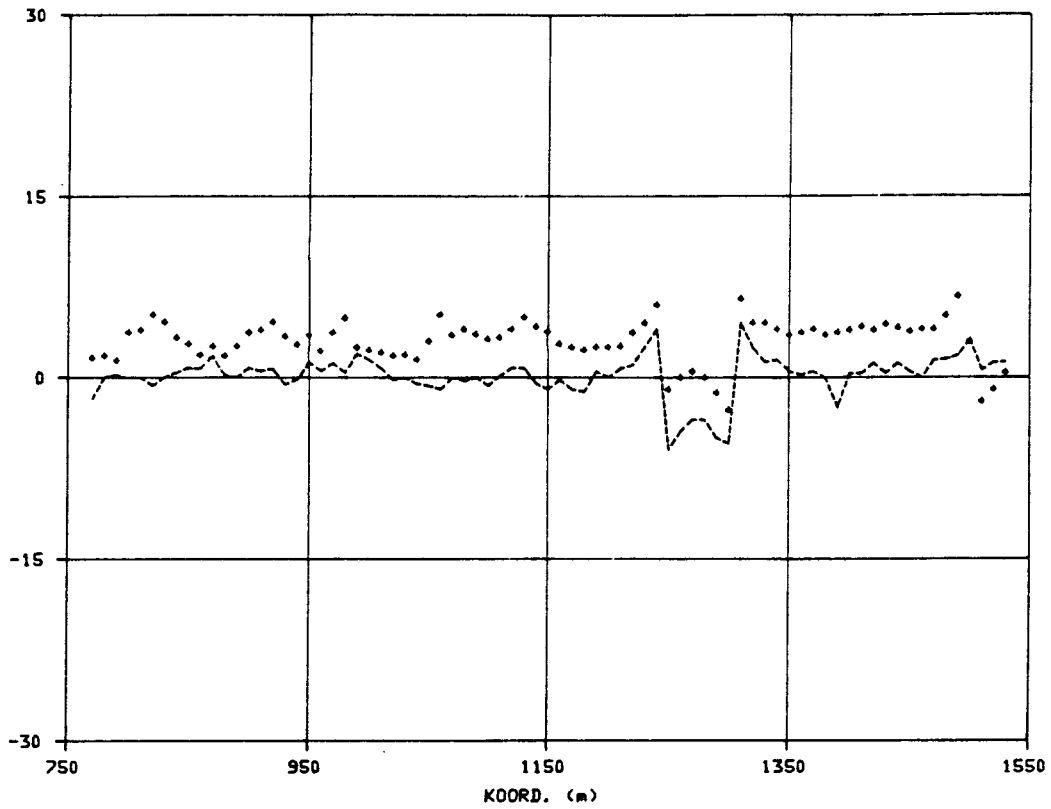


Figure 4.4 Slingram imaginary measurements at profiles across the Zone 1 (Brändan).



PROFIL 1075E SR₁(Re₁--- , Im₁+++)

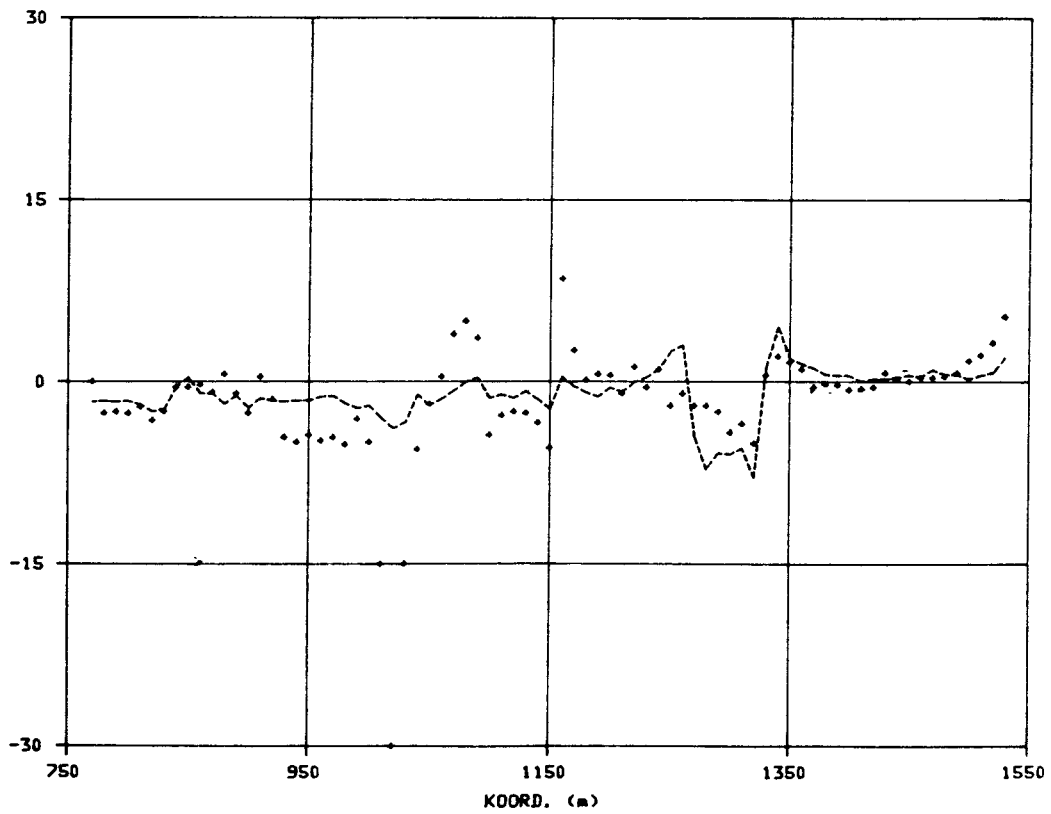


Figure 4.5 Slingram measurements at profiles parallel to the Zone 1 (Brändan).

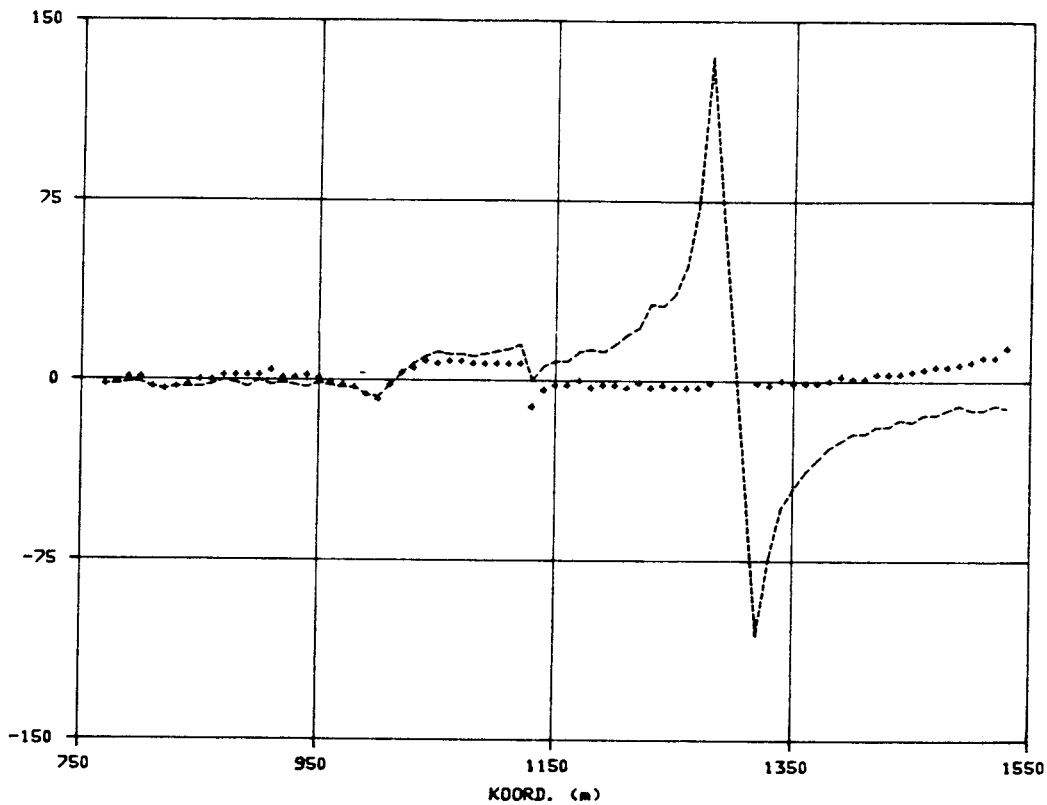
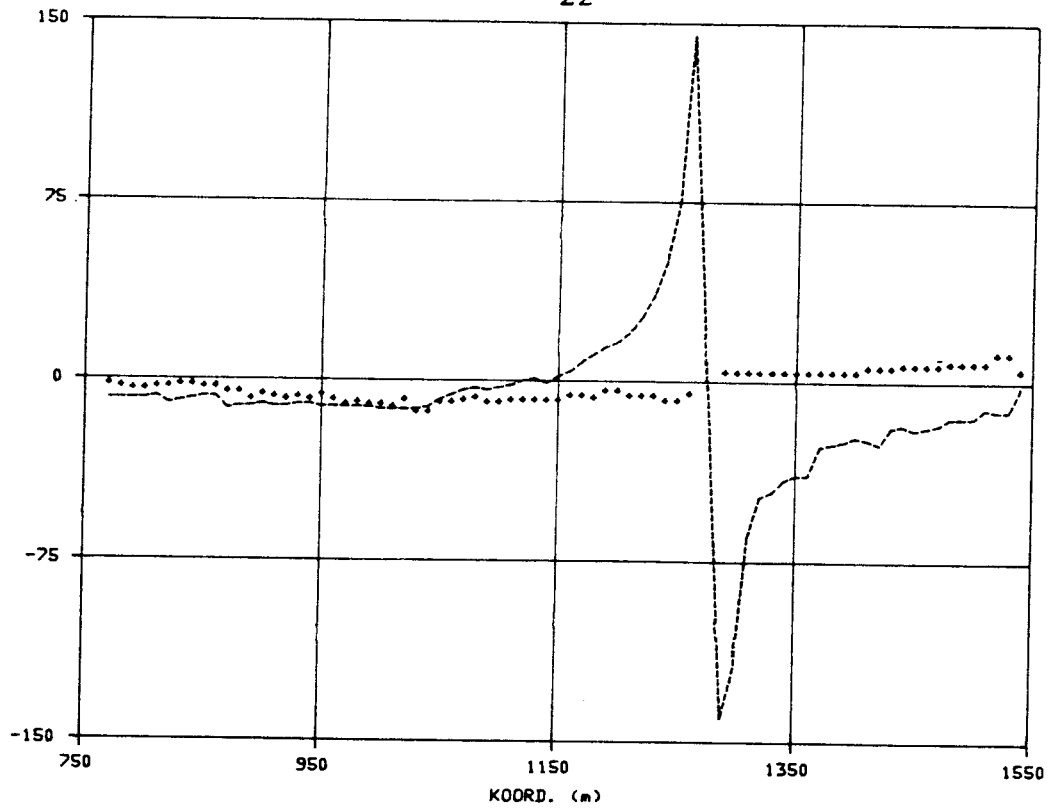


Figure 4.6 VLF imaginary (GBR) measurements at profiles parallel to the Zone 1 (Brändan).

5. LITHOLOGY AND FRACTURE LOGS

Within the central part of the Brändan area four deep cored boreholes are located, figures 2.1 and 2.2. The boreholes F1 5 and F1 6 were drilled and mapped during 1978-1979, Olkiewicz et. al. (1979). Some sections of these boreholes have been remapped within this project. New boreholes are F1 9 and F1 10. For all core mapping within this project a computer based core mapping system (Almén et. al., 1983) has been used. Detailed logs of rock types and fractures are presented in an internal SKB report from 1985: "Fracture zone project, core logging and technical data for boreholes F1 5, F1 6, F1 9 and F1 10" (see page 2).

The major rock type in the cores is a fine - medium grained, grey, pink or red granodiorite with a weak foliation. The colour is a function of the fracture frequency and degree of tectonization of the rock. Thus, where the core is red, there is always a high fracture frequency and/or a tectonized section. The term tectonite is here used by the core mapping geologist for a core strongly affected by cataclastic to mylonitic transitional deformation.

Other mapped rock types are xenolites of leptite and basic rock types and dikes of aplite, late-orogenic granite (young granite) and metabasite. The location of the different rock types are shown in the complot diagrams, figures 6.1 - 6.4.

Table 5.1 below shows the content of different rock types in the boreholes. The content of red granodiorite, tectonite and mylonite is overestimated, since only the tectonized parts of the boreholes F1 5 and F1 6 have been remapped.

Table 5.1 Content of different rock types in the boreholes F1 9 and F1 10 and in the remapped parts of F1 5 and F1 6.

Rock type	% of total borehole length
Grey granodiorite	25.6
Pink granodiorite	33.6
Red granodiorite	29.2
Tectonite	7.2
Mylonite	0.5
Late-orogenic (young) granite	0.2
Pegmatite	1.7
Aplite	0.3
Xenolites	1.7

Both coated and sealed fractures have been mapped in the drill core. Coated fractures are here defined as discontinuities with fracture infillings, along which the core is parted. The figures 5.1 and 5.2 show the frequency of coated and sealed fractures, the frequency of coated fractures with hematite and laumontite (excluding crushed and highly fractured sections in the core log) and the hydraulic conductivity.

Fracture infillings are dominated by calcite and dark coloured sheet minerals, e.g. chlorites. These minerals occur in all sections along the boreholes. In the fracture zones other common minerals are hematite, laumontite, asphaltite and clay minerals.

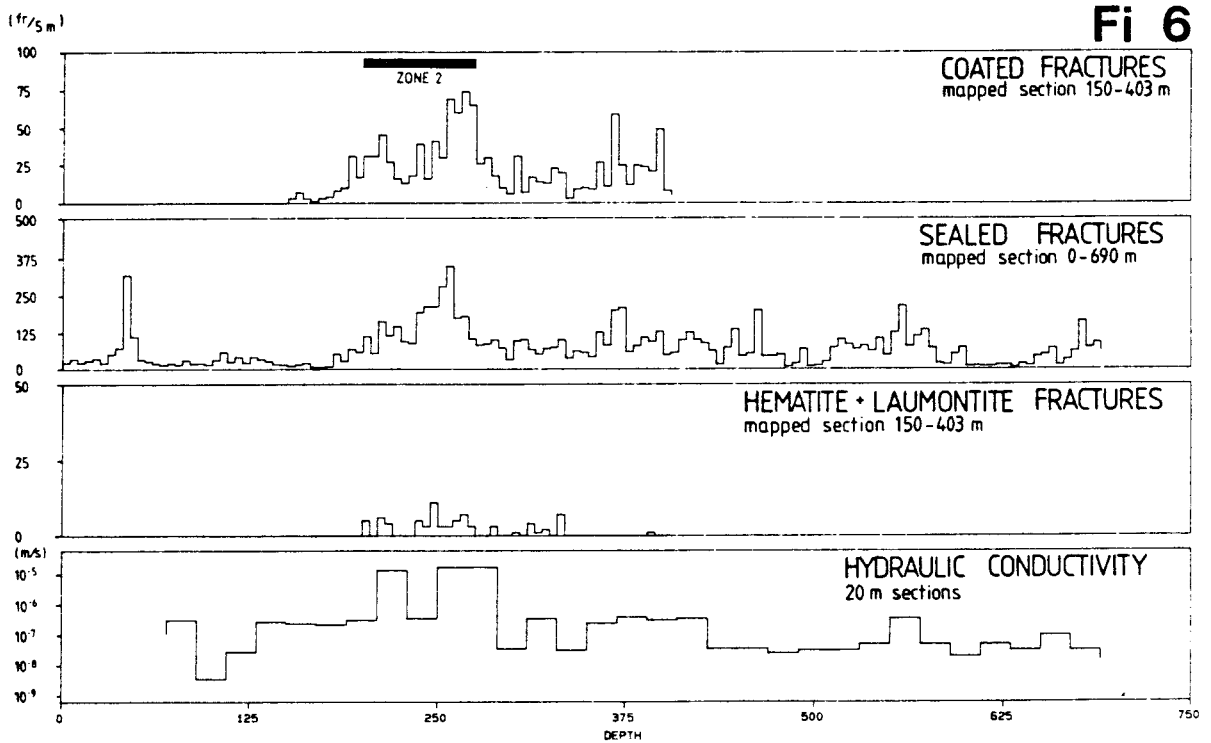
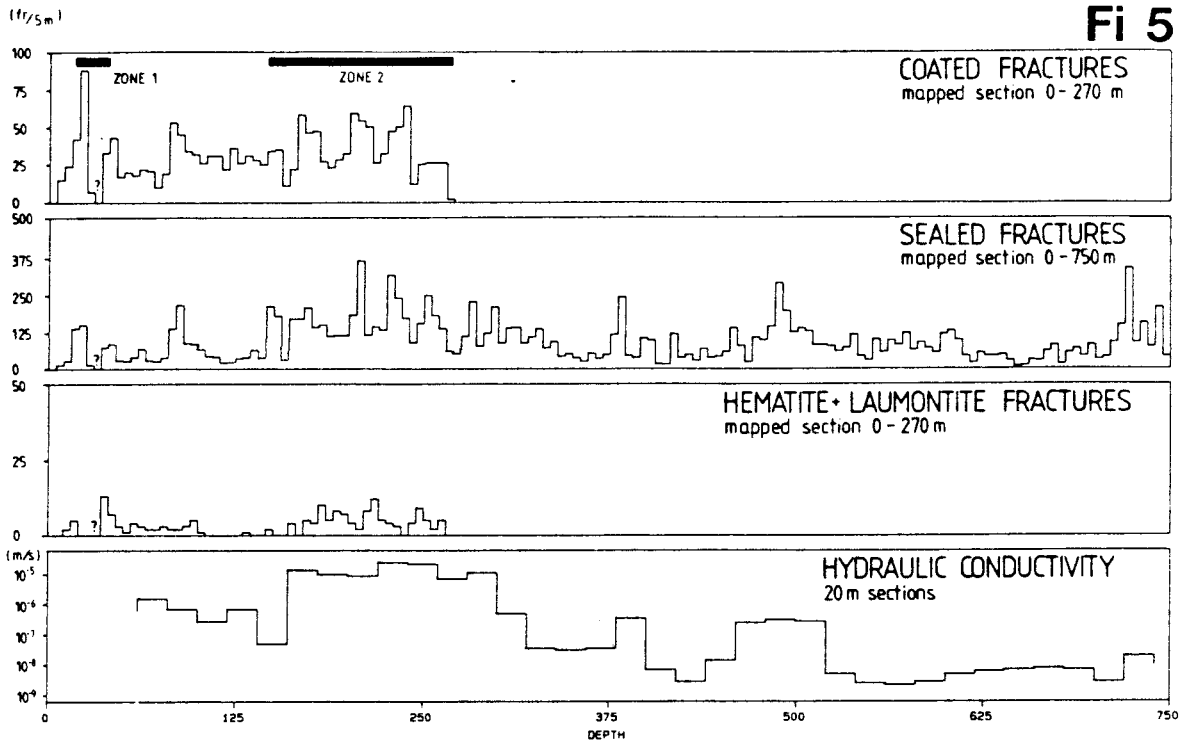


Figure 5.1 Fi 5 (751 m) and Fi 6 (691 m). Frequency of different types of fractures per 5 m of core and hydraulic conductivity measured in 5 or 20 m sections.

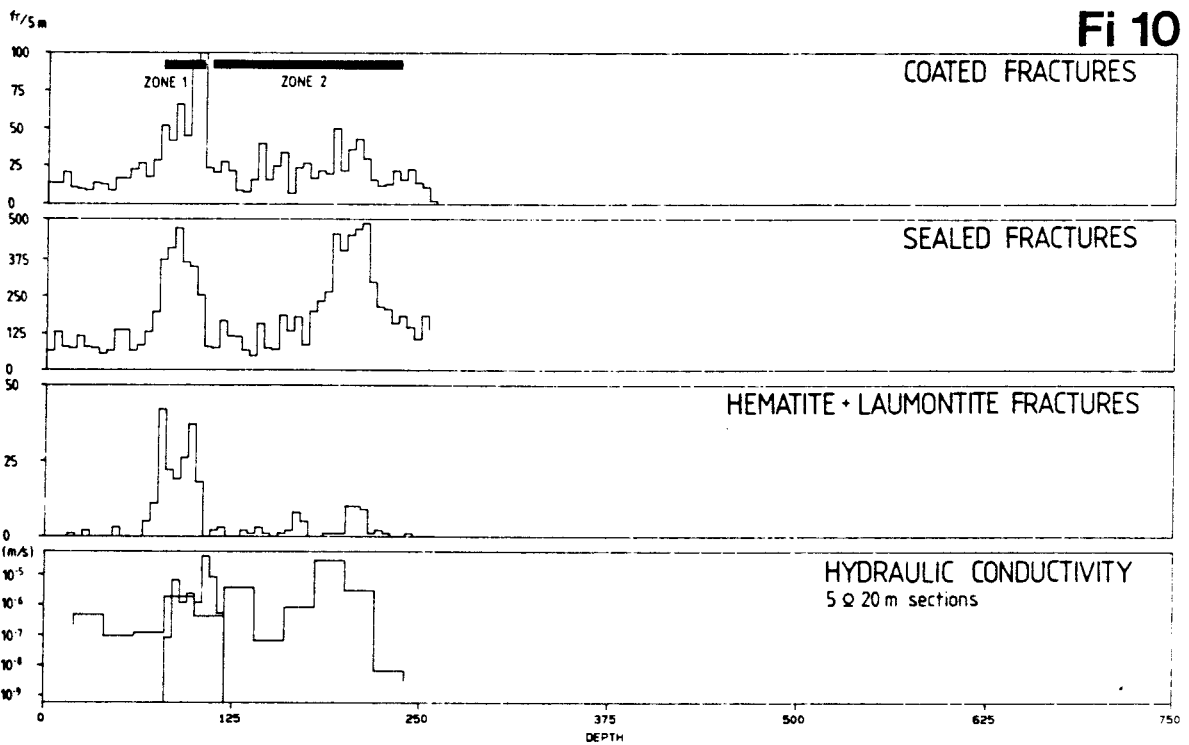
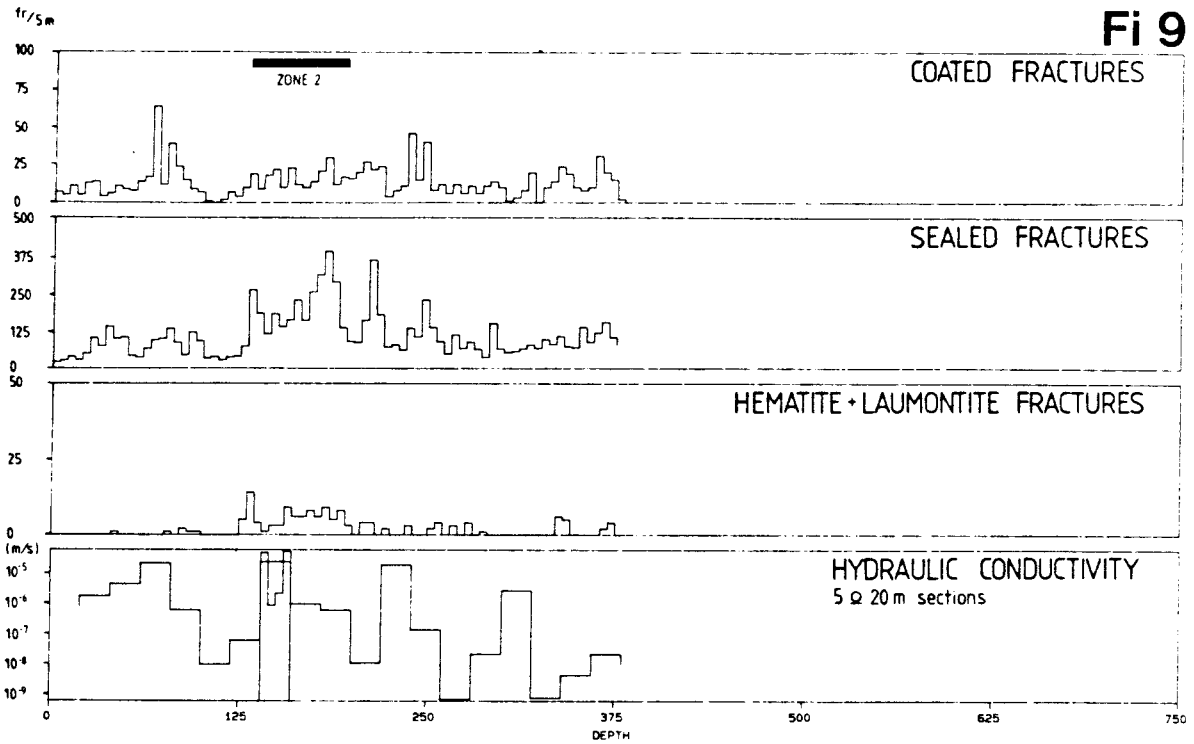


Figure 5.2 F1 9 (375 m) and F1 10 (256 m). Frequency of different types of fractures per 5 m of core and hydraulic conductivity measured in 5 or 20 m sections.

5.1 Core mapping of Fi 5

The cores of Fi 5 have been remapped in the sections 7-26 m and 37-266 m. The cores in the section 26-37 m have not been available. There are many sections with red granodiorite and tectonite down to the depth of 255 m. From this depth and downwards the frequency and width of tectonized sections decreases. Of major interest for this project are sections in the cores, where tectonized bedrock and high frequency of coated fractures occur. In the table below these sections are noted.

The borehole is interpreted to intersect Zone 1 at 18-46 m and Zone 2 at 167-255 m.

Table 5.2 Sections in Fi 5 with tectonized bedrock and/or high fracture frequency. Remapped sections 7-26 m and 37-266 m. Data from other sections of the borehole are taken from Olkiewicz et al. (1979).

18-46 m	red granodiorite with high frequency of coated fractures with hematite and asphaltite.
83-86 m	tectonized section with breccias, cavities, high fracture frequency and strongly weathered bedrock. 0.2 m core loss and 0.4 m crushed core.
167-170 m	red granodiorite, weathered fractures and idiomorphic quartz crystals.
204-215 m	tectonized section, strongly weathered, high fracture frequency, 0.5 m crushed core and 1.7 m core loss.
227-230 m	tectonized section with mylonites, cavities, idiomorphic quartz crystals and high fracture frequency.

Table 5.2 continued

233-239 m	red granodiorite with high fracture frequency.
249-255 m	tectonized section.
382-384 m	crushed section in metabasite.
472-473 m	crushed section in metabasite.
485-501 m	tectonized section with high fracture frequency and partly crushed core.
540-542 m	young granite with high fracture frequency.
553-554 m	metabasite with high fracture frequency.
592-606 m	tectonized section with high fracture frequency.
712-716 m	young granite with high fracture frequency.

5.2 Core mapping of Fi 6

The cores of Fi 6 have been remapped within the interval 150 - 403 m. Above and below this interval only minor sections with tectonized core are found. Within the remapped interval the core is highly fractured and breccias and mylonites are common.

The borehole is interpreted to intersect Zone 2 at 201-287 m.

Table 5.3 Sections in Fi 6 with tectonized bedrock and/or high fracture frequency. Remapped section 150-403 m. Data from other sections of the borehole are taken from Olkiewicz et. al. (1979).

40-47 m	tectonized section with crushed rock.
47-49 m	metabasite with high fracture frequency.
115-116 m	metabasite with high fracture frequency.
201-203 m	tectonized rock with high fracture frequency.
213-216 m	tectonized rock with high fracture frequency and weathered crushed parts.
235-237 m	tectonized section with high fracture frequency.
245-287 m	several tectonized sections with breccia and mylonite. High fracture frequency and partly crushed core.
302-303 m	red granodiorite with 0.2 m crushed core.
330-331 m	tectonized section, more than 10 mm clay.
369-371 m	tectonized section, 0.3 m crushed core.
394-395 m	tectonized section with normal fracture frequency.
554-557 m	tectonized section, red stained, strongly weathered and crushed core.
674-691 m	grey granodiorite with high fracture frequency and partly crushed core. The borehole ends within a crushed section.

5.3 Core mapping of Fi 9

The cores from Fi 9 display only one section of highly fractured and tectonized core down to 134 m. This is a section around 67 m, where the core is fractured and weathered within a red and tectonized granodiorite. Between 134-217 m several sections with tectonized and brecciated granodiorite alternate with grey granodiorite. The fracture frequency is high, but no sections of crushed core occur. The fracture surfaces are often coated with hematite and laumontite. Below 217 m and to the end of the borehole (376 m) only minor sections with tectonized rock are found.

The borehole is interpreted to intersect Zone 2 at 134-205 m.

Table 5.4 Sections in Fi 9 with tectonized bedrock and/or high fracture frequency.

65-69 m	red granodiorite with 1.4 m of tectonized, strongly weathered rock. 0.2 m of the core is altered to clay.
74-77 m	red granodiorite with high fracture frequency and 0.2 m crushed core.
134-137 m	red granodiorite with 0.02 m of microbreccia. Slightly increased fracture frequency.
146-147 m	red granodiorite with a 0.02 m microbreccia at 60 degrees to the core axis. High fracture frequency.
154-182 m	red granodiorite, high fracture frequency.

Table 5.4 continued

182-184 m	strongly tectonized section with a 12 mm clay filled fracture at 65-75 degrees to the core. Only slightly increased fracture frequency.
204-205 m	tectonized section with high fracture frequency.
215-216 m	red granodiorite with high frequency of hematite coated fractures.
245-250 m	section with red granodiorite and pegmatites. High fracture frequency in pegmatites.

5.4 Core mapping of F1 10

During the drilling the core was marked in the borehole with a falling weight. This made it possible to orientate a breccia at 211 m.

High fracture frequency and tectonization occur within two intervals, 77-104 m and 157-232 m. The characters of these two fractured intervals are different. Within the upper interval the granodiorite is red, the frequencies of both coated and sealed fractures are high and characteristic minerals are hematite and asphaltite. This interval is interpreted to represent Zone 1 (Brändan).

The lower interval, 157-232 m, is characterized by several sections of tectonized core, including breccias and mylonites, interchanging with sections of grey granodiorite. This interval is interpreted to represent Zone 2. The frequency of coated fractures within the tectonized part of the core is only slightly increased. However, the frequency of sealed fractures is high. At 211 m a 25 mm breccia has an orientation of N 20 E/ 25 W. The breccia is shown in figure 5.6.

Table 5.5 Sections in Fi 10 with tectonized bedrock and/or high fracture frequency.

77-104 m	the interval consists of red and tectonized granodiorite. The frequency of coated fractures is high throughout the interval. Characteristic fracture minerals are hematite and asphaltite. Hematite is most common at the upper and lower boundaries of the fracture zone. Asphaltite is concentrated to the lower boundary of it. The core is partly weathered and clay altered.
157-159 m	red and tectonized granodiorite, partly clay altered. Slightly increased fracture frequency.
189-191 m	red and tectonized granodiorite, partly clay altered. Breccia in a 0.05 m section. High frequency of fractures.
191-207 m	red granodiorite with slightly increased fracture frequency.
207-215 m	tectonized section with mylonite and breccia. The breccia, figure 5.6, is oriented in N 20 E/ 25 W. The tectonized section contains clay altered rock, cavities and idiomorphic quartz crystals. Only a slightly increased frequency of coated fractures is observed in the tectonized section.

5.5 Drilling characteristics of and sampling of drilling debris from the percussion borehole HFi 1

During the drilling of HFi 1 sampling of drilling debris was made in 3 m intervals. Since highly fractured rock and/or tectonized granodiorite is characterized by a change from grey to red colour, the colour of the cuttings was recorded. In table 5.6 below these colour changes and the size of the drilling debris are tabulated.

Table 5.6 Colour and size of cuttings from borehole HFi 1.

0-3 m grey clay	63-66 m red gravel
3-6 "-	66-69 "-
6-9 "-	69-72 "-
9-12 dark grey sand	72-75 "-
12-15 grey silt	75-78 "-
15-18 "-	78-81 red clay-sand
18-21 "-	81-84 "-
21-24 "-	84-87 red sand
24-27 "-	87-90 "-
27-30 "-	90-93 "-
30-33 redish grey clay-sand	93-96 red sand-gravel
33-36 "-	96-99 "-
36-39 grey gravel	99-102 red sand-gravel-stones
39-42 dark red sand	102-105 red sand
42-45 "-	105-108 red sand-gravel
45-48 red gravel	108-111 "-
48-51 red sand	111-114 greyish red gravel-stones
51-54 red gravel	114-117 no sample
54-57 red sand	117-120 greyish red gravel-stones
57-60 red gravel	120-123 red sand
60-63 "-	123-126 no sample
	126-129 red sand

There is a major change from grey to red drilling debris at the interval 30-33 m. This is in accordance with a 10 m wide fracture zone starting at 34 m borehole depth, interpreted from the geophysical logs (figure 6.5). At 99 m and at 111-120 m inter-

vals the size of the drilling debris is larger. This is probably due to high frequency of fractures in Zone 2 (starting at 100 m) together with a fast sinking of the percussion hammer which made it difficult to crush the rock into clay, silt or sand sizes. At 99.2 m the drilling debris contained two larger stones. A thin section has been made from one of these stones.

A drillers log is presented in figure 5.3. The right column represents the sinking velocity (the time it takes for the percussion hammer to drill 0.2 m). The left column shows the well recovery (the time for the water level to rise a certain distance from an empty borehole).

High sinking velocity (possible fracture zone) was recorded in the intervals 35-45 m and 105-115 m. At the upper interval a water inflow of 1800 l/h was recorded. A very high inflow of water, 15 000 l/h, was recorded for the interval 99-115 m. The low sinking velocity below the lower interval is probably caused by the high amount of inflowing ground water.

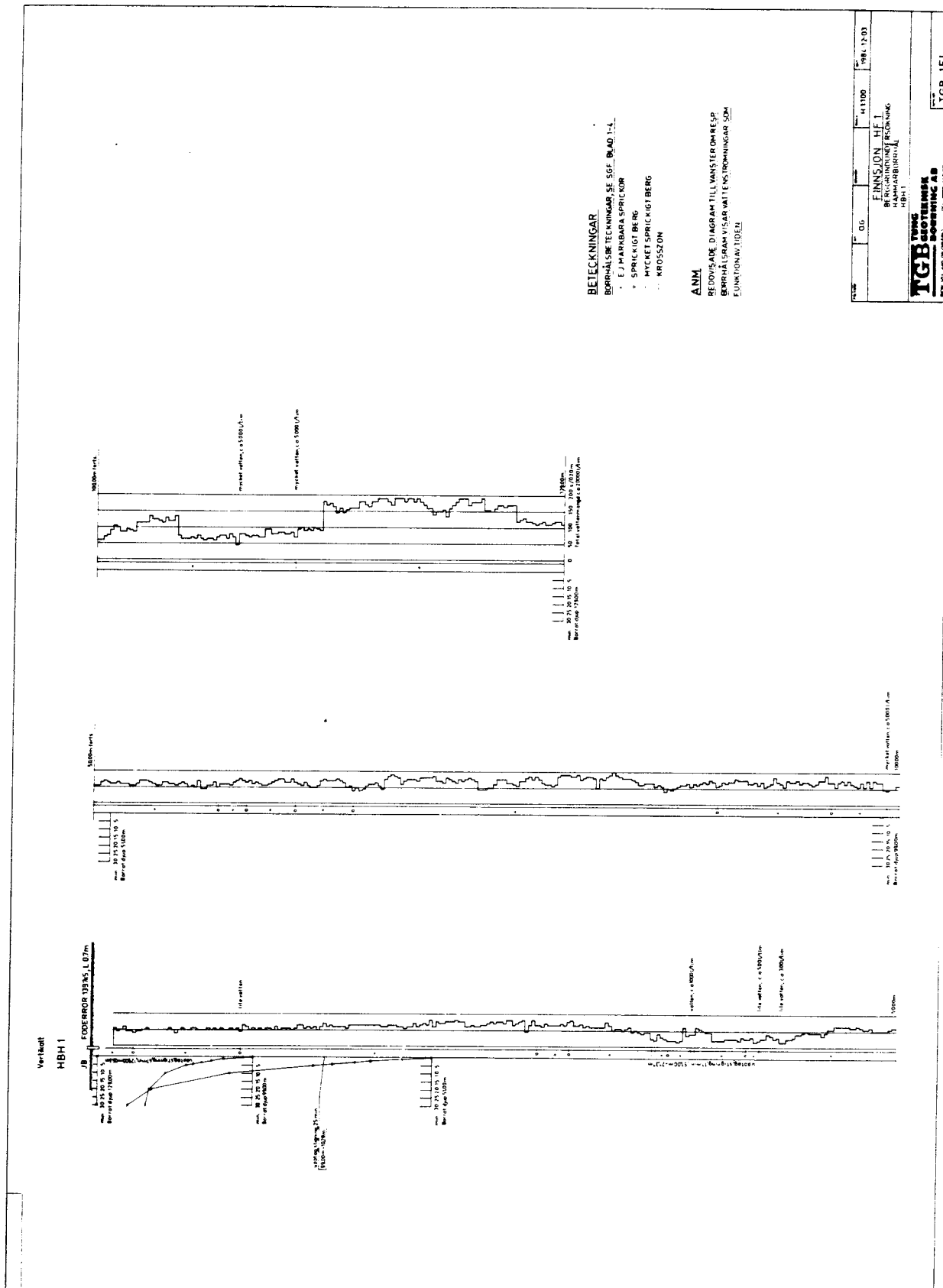


Figure 5.3 Drillers log for the percussion borehole HFi 1.

5.6 Core samples obtained by the Borros sampler.

A profile of 19 short boreholes was drilled across the small gully north of and close to borehole Fi 5 (figure 3.3 and figure 5.4). Zone 1 (Brändan) is interpreted to be located in the gully. The purpose was to obtain data of the soil composition and soil depth and to take core samples from the bedrock.

The sampler used was a Borros soil and core sampler. This is a light weighted, portable machine, with which about 5 short boreholes per day can be drilled. The diameter of the obtained cores was 32 mm.

The soil in the profile consists mostly of clayey-silty to sandy till. A thin layer (about 0.1 m) of clay and peat was found in the uppermost part of some boreholes. The maximum soil depth is 3.4 m (figure 5.5).

Most boreholes were drilled one metre into the bedrock. In order to make dip calculations of the fracture zone, some boreholes were drilled deeper, down to 13 m into the bedrock.

The core samples were mapped with regard to rock types and fracture characteristics (figure 5.5). The main rock type is grey, pink or red granodiorite. Tectonite is found in four boreholes and leptite in two. Common fracture minerals are calcite, chlorite, hematite, "rust" minerals and clay minerals. The frequency of hematite coated fractures is high within the zone, 20-98 % of the total number of coated fractures for each borehole. The maximum frequency of hematite fractures occurs in the boreholes B1-B4 and B9 - B12, i.e at the boundaries of the fracture zone. In the boreholes drilled in the country rock west of the fracture zone (B14, B15, B18) hematite fractures are almost lacking.

There is also an increase in the frequency of sealed fractures within the fracture zone (figure 5.5). The increase is strongest at the lower boundary of the zone.

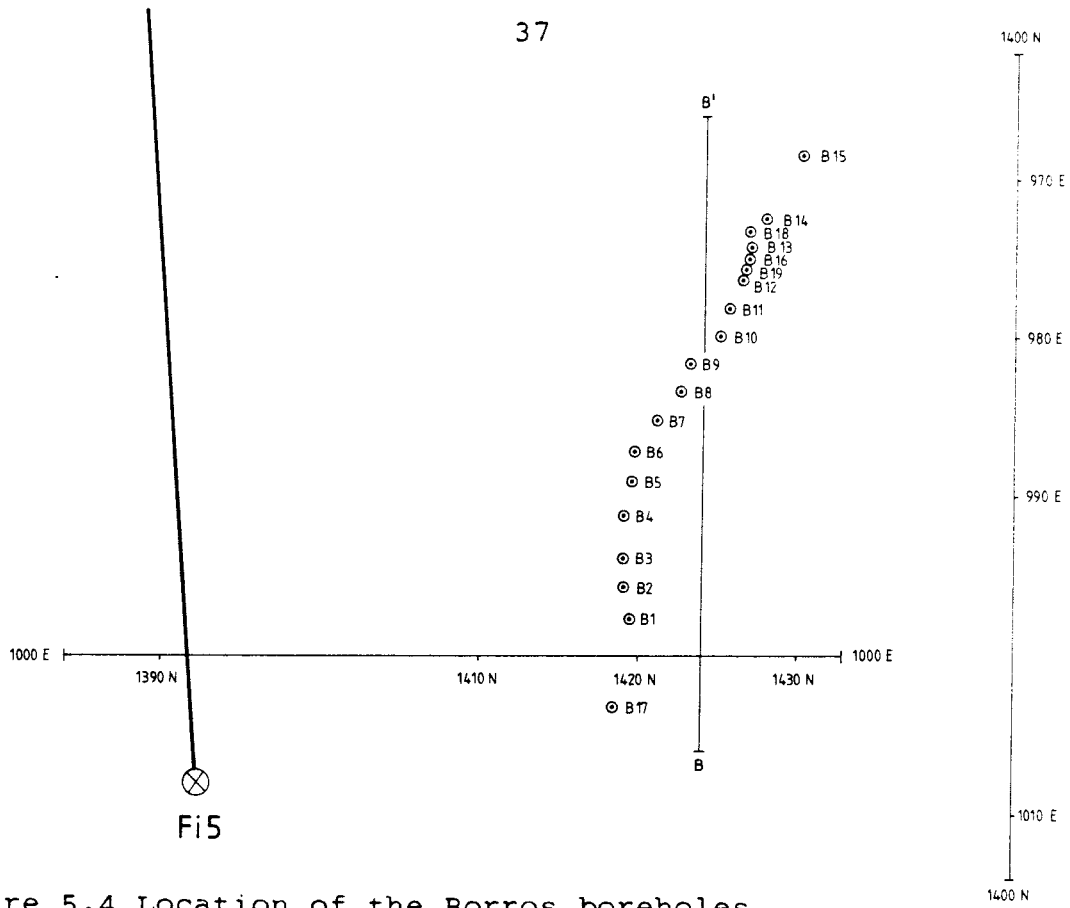


Figure 5.4 Location of the Borros boreholes.

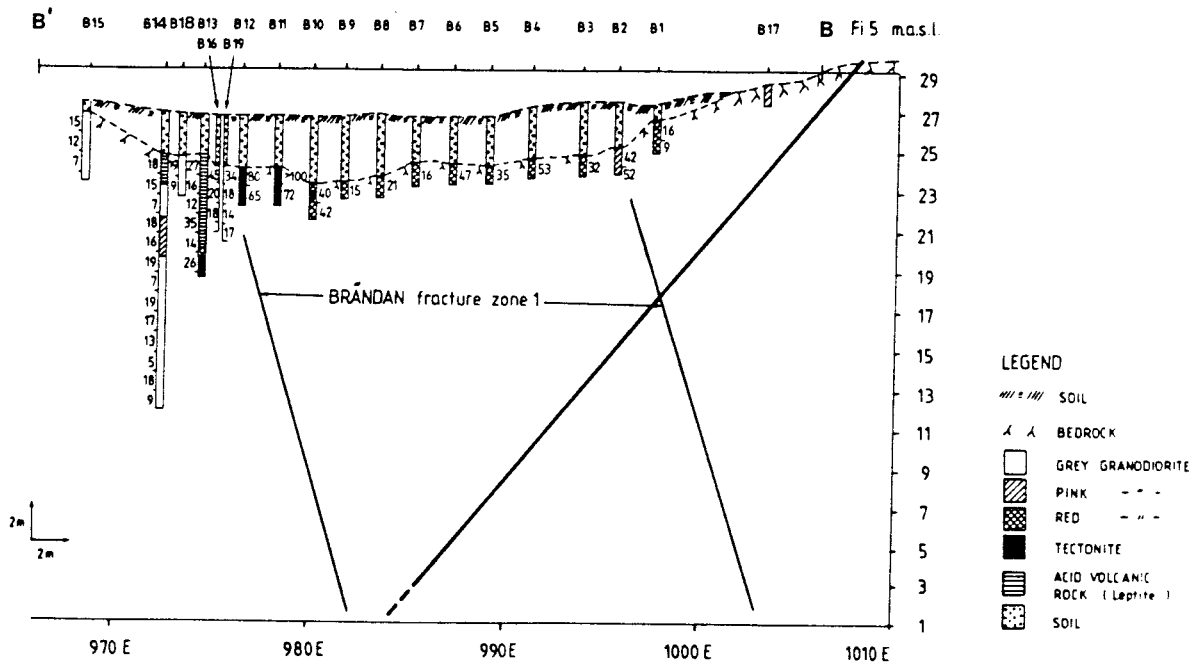


Figure 5.5 Core mapping of the Borros boreholes. Numbers at the boreholes refer to the number of sealed fractures per metre.



Figure 5.6 Brecciated section at 211 m in borehole Fi 10. The breccia is oriented N 20 E/25 W and is interpreted to represent a part of the Zone 2 (the subhorizontal zone).

5.7 Thin section microscopy

In order to study weathering and alteration in the granodiorite, samples were collected from every ten metres in borehole Fi 9 and from selected fractured and tectonized sections in the boreholes Fi 9, Fi 5 and Fi 6.

Various degree of alteration has been observed in the studied samples. The colour of the cores varies from grey to red due to hematization. The red colour is especially distinct within and close to the fracture zones. Fresh, grey samples of the granodiorite contain quartz, K-feldspar and sericitic plagioclase. Femic minerals present are biotite and hornblende (normally green but some bluegreen varieties also exist). These samples are only poorly hematized. In the altered, red samples plagioclase

clase is red-stained by hematite and the biotite and hornblende are decomposed to form epidote and chlorite. Prehnite and pumpellyite have also been observed. Mineral paragenesis indicates a "low-temperature hydrothermal" alteration at oxidizing conditions.

5.7.1 Fracture infillings

The fracture infillings studied are mostly hydrothermal minerals like prehnite, laumontite, pyrite, quartz and calcite. The fracture filling history fits to the sequence described in Wiman (1930) and Tullborg and Larson (1982).

From oldest to youngest:

- 1) Epidote (associated with mylonite)
- 2) Prehnite and prismatic calcite +/- quartz
- 3) Hematite, laumontite +/- calcite and quartz
- 4) Chlorite and calcite

Most of the fractures are considered to be initiated early in the geologic history and reactivated several times. Rb-Sr and K-Ar dating of epidote and prehnite veins in central Sweden have yielded ages of 1600-1500 Ma for epidote and 1250-1100 Ma for prehnite veins (Wickman et.al, 1983).

Both prismatic and granular calcite occur indicating different stress conditions during growth. Prismatic calcite is suggested to be grown in a stress field (Kamb, 1959). Also, some of the prehnite sealed fractures are crosscut by hematite and laumontite sealed fractures. This also indicates different stress conditions during the two hydrothermal events. Potentially young fractures, lacking hydrothermal minerals and reactivation, are rare.

Most of the hematite observed in the fractures is suggested to be of hydrothermal origin. Nevertheless, small amounts of young hematite may occur in the fracture zones. A maximum of hematite in the thin sections corresponds to the Zone 2 at 150 to 215 m

in borehole Fi 9.

Somewhat surprising, pyrite can be found in samples containing hematite. The reason for this could be a later formation of the pyrite.

5.7.2 Fracture minerals within Zone 2

The cores at 150-215 m (Zone 2) in Fi 9 consist of several fractured sections. They contain fine-grained epidote, quartz and feldspar and are intersected by fractures sealed by prehnite, laumontite, hematite and at least two generations of calcite.

One sample at the 204 m level shows a prehnite bearing mylonite in the contact zone between granodiorite and amphibolite (parallel to the core axis) intersected by a fracture sealed by laumontite, calcite and hematite (40° angle to the core axis).

The mineral assemblages described above for Zone 2 in borehole Fi 9 have also been found in Fi 5 at 220-240 m and in Fi 6 at 260-275 m. Thus, the location of Zone 2 in the boreholes Fi 5, Fi 6 and Fi 9 is supported from a mineralogical point of view.

5.7.3 Fracture minerals within other fracture zones

Studies of a minor fracture zone in borehole Fi 5, section 80-90 m, show that this zone is hematized and mineralized with calcite (mostly not prismatic) and probably lawsonite (a mineral indicating high pressure conditions). These minerals also occur in a minor fracture zone in borehole Fi 6 at 555 m. No studies of fracture minerals were made for Zone 1.

6. GEOPHYSICAL LOGGING

Geophysical logging has been carried out in all five boreholes within the Brändan area. The following methods were used: borehole deviation, normal resistivity and single point resistance, borehole fluid resistivity (salinity) and temperature, natural gamma radiation and borehole radar. The borehole radar measurements are treated separately in chapter 7. Other boreholes within the Finnsjön study site but outside the Brändan area, have been measured with the methods: borehole deviation, normal resistivity, borehole fluid resistivity and temperature. The location of the boreholes is shown in figure 2.1.

6.1 Geophysical logging of boreholes in the Brändan area.

The boreholes measured in the Brändan area are F1 5, F1 6, F1 9, F1 10 and HF1 1. Results from these boreholes are presented in the complot diagrams, figures 6.1 - 6.5. The complot diagrams for the cored borholes also contain data regarding rock types, frequency of coated and sealed fractures and hydraulic conductivity.

6.1.1 Logging of borehole F1 5

Figure 6.1 presents data from borehole F1 5. This cored borehole was drilled, core logged and hydraulically tested during 1978-1979. The section 7-266 m has been remapped within this project. The borehole is inclined about 50 degrees from the horizontal and is cased down to 50 m. The borele length is 751 m. Thus, results regarding the physical and hydraulic conditions of the bedrock are available only below 50 m.

Resistance and resistivity logs indicate Zone 2 between 160-240 m. This is also supported by the core log and the high fracture frequency. There is a high hydraulic conductivity within the zone. A strong increase in salinity occurs at the upper boundary of the fracture zone. There is also an anomaly in the temperature curve at 168 m borehole length, i.e. 129 m

vertical depth. (Unfortunately the temperature gradient curves are missing in the complot logs from Fi 5 and Fi 6.) Since the piezometric measurements (chapter 9) show a piezometric low value at this depth, the temperature anomaly is caused by continuous flow of ground water from the borehole and into the fracture zone.

Minor fracture zones are indicated at 80-90 m, 280-300 m, 360-380 m, 480-500 m and 710-725 m borehole length. A slight increase in the natural radiation is in most cases associated with the fracture zones. There is a good correlation between high fracture frequency, high hydraulic conductivity and low resistivity.

6.1.2 Logging of borehole Fi 6

Figure 6.2 shows data from the vertical borehole Fi 6. The borehole length is 691 m. This borehole was drilled, core logged and hydraulically tested during 1978-1979. The cores from section 150-400 m have been remapped within this project. The borehole is cased down to 56 m.

The resistivity measurements indicate Zone 2 at 200-285 m. Within the zone two temperature anomalies occur at 212 and 256 m. The anomalies are similar as in borehole Fi 5. Since the anomalies occur at sections with piezometric low values (chapter 9), the water is constantly flowing from the borehole and into to the fracture zone.

Minor fracture zones are found at 375-400 m and at 550-560 m. At the lower fracture zone a similar temperature anomaly as described above is found indicating continuous water flow from the borehole into the fracture zone.

The salinity log shows a non-saline water down to 150 m. The salinity gradually increases from this depth to the fracture zone and the temperature anomaly at 212 m. Another increase of salinity occurs at the temperature anomaly at 256 m. From this depth and downwards the salinity stays constantly high, (>6000

mg/l of equivalent chloride).

The natural radiation log shows a change in the background level at 110 m indicating a different rock type. However, no indication of change in rock type is found in the core. There is a good correlation between fracture frequency, hydraulic conductivity and geophysical logs.

6.1.3 Logging of borehole Fi 9

This cored borehole was drilled during Nov-Dec 1984. It is inclined 60 degrees from the horizontal. The borehole length is 376 m. The resistance and resistivity logs, figure 6.3, indicate Zone 2 between 130-180 m. This zone might possibly extend down to 215 m. The zone has a high frequency of sealed fractures but only a minor increase of open, coated fractures. Minor fracture zones, as indicated by the resistance and resistivity logs, occur at 65-70 m and 240-250 m. The low resistivity zone at 200-215 m could either be regarded as a part of the major fracture zone or be interpreted as a separate minor fracture zone.

This borehole was logged shortly after the drilling. The salinity and temperature logs are therefore unreliable. However, the temperature log have two anomalies, at 70 m and 180-205 m, indicating continuous flow of groundwater between the borehole and the surrounding bedrock. The salinity log shows a non-saline water down to 70 m and a high saline water below 215 m. Between these two depths there is a mixture of waters with low and high salinity which is probably caused by mixing of waters during drilling.

6.1.4 Logging of Fi 10

This cored borehole was drilled during april 1985. It is inclined 50 degrees from the horizontal. The borehole length is 256 m. The resistance and resistivity logs, figure 6.4, show two major fracture zones, at 75-105 m and 140-215 m. The upper zone (Zone 1) has a high amount of both coated and sealed

fractures, while the lower zone (Zone 2) is recognized by a high frequency of sealed fractures but only a slight increase of coated fractures. A minor zone occurs at 230-245 m.

This hole was logged shortly after the drilling. The temperature log therefore shows numerous anomalies. Most of these are caused by fractures that have been injected with water of a higher temperature during the drilling. However, a pronounced anomaly occurs at 100 m indicating flow of water from the borehole into the lower part of the fracture zone. The salinity log shows a low saline water down to about 100 m and a high saline water below 180 m. Between these depths there is a mixture of water with different salinity. An increase in natural radiation is found at Zone 1, 70-100 m.

6.1.5 Logging of the percussion borehole HFi 1

This vertical borehole was drilled during september 1984 to provide circulating water for the drilling of the cored boreholes. The logging was made shortly after drilling. The resistance and resistivity logs, figure 6.5, reveal two fracture zones, at 34-43 m and at 105-129 m (end of borehole). The upper zone has a pronounced radiation anomaly. The temperature and salinity logs are very disturbed and not possible to interpret.

6.2 Geophysical logging of boreholes outside the Brändan area but within the Finnsjön study site

To obtain information of major fracture zones and changes in the ground water salinity outside the Brändan area all other cored boreholes at the Finnsjön site were geophysically logged. Unfortunately, many of the boreholes were plugged with instruments, that were stuck in the boreholes during earlier investigations.

6.2.1 Logging of F1 1

This cored borehole is vertical and 500 m deep. The hole is open down to about 340 m to which depth measurements have been performed (figure 6.6). The total length of the borehole has been measured earlier, although without a temperature probe (Hult et.al., 1978). The interpretation below is made from all available geophysical logs.

Several minor fracture zones are identified. These are located at 227-236 m, 335-350 m, and 425-435 m. The section 335-435 m might possibly be regarded as one major fracture zone.

The salinity of the borehole water is low down to 340 m, where the resistivity of borehole fluid drops from 55 to 30 ohm m, showing slightly higher saline water. The temperature log shows only a minor anomaly at 150 m, which indicates water flow. No information of fluid temperature is available below 340 m.

6.2.2 Logging of F1 2

The cored borehole F1 2 has a length of 699 m and is inclined 50 degrees from the horizontal. No earlier geophysical logging was made in this borehole. The logging that was made in 1985 reached only 100 m, where the borehole was plugged. Figure 6.6 shows the results of the geophysical logging. Neither the resistivity log nor the temperature or salinity logs have indications of major fracture zones or water movements down to 100 m.

6.2.3 Logging of F1 3

This cored borehole has a length of 731 m and is drilled inclined, 50 degrees from the horizontal. A point resistance log made in 1978 is the only available geophysical log for this borehole. All of the borehole is now plugged with an instrument. The point-resistance log indicates a major fracture zone

between 180-260 m or possibly 180-360 m borehole length. Minor fracture zones occur at 50-60 m, 140-160 m, 340-360 m, 610-640 m and 670-700 m (end of logged section).

6.2.4 Logging of F1 4

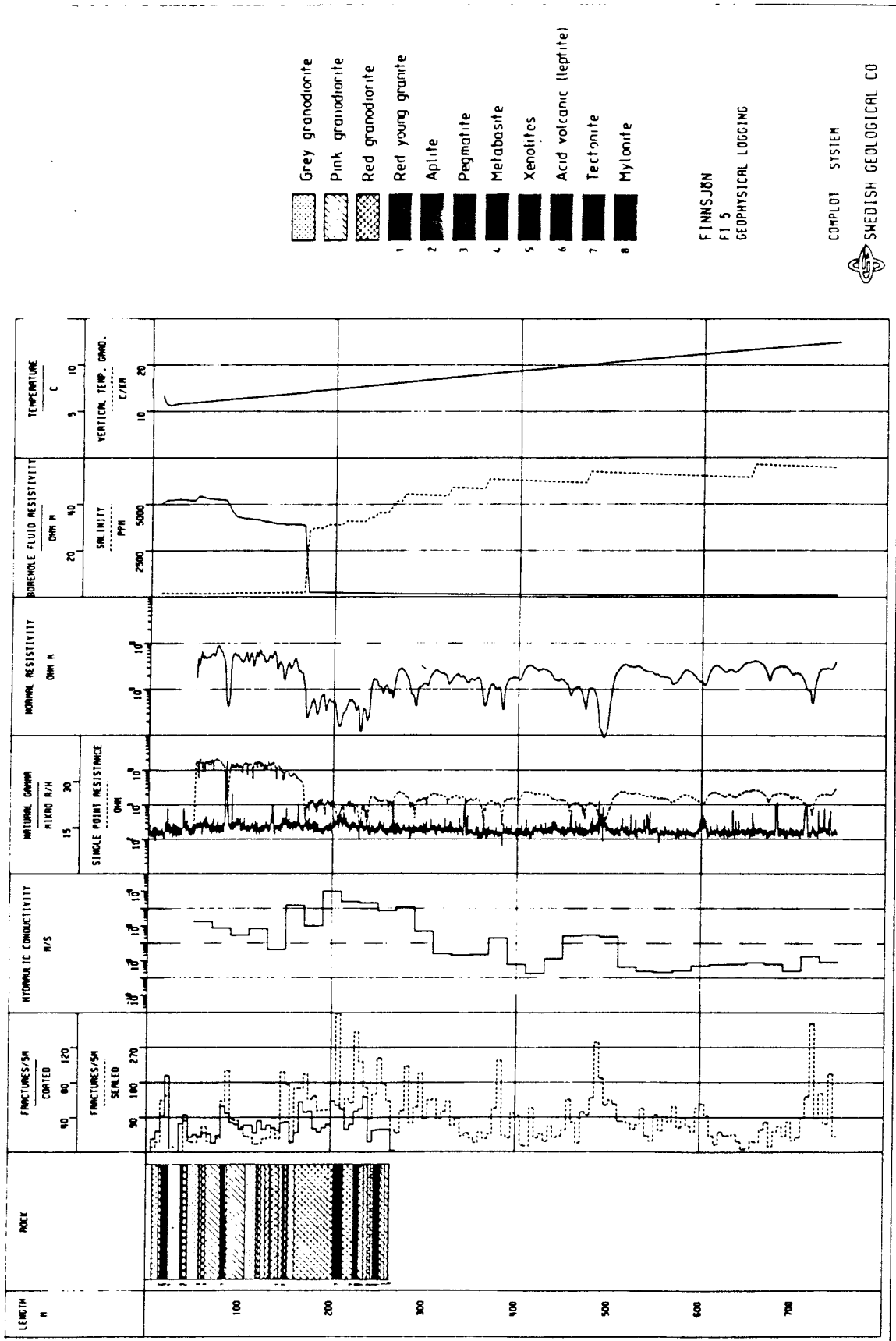
This cored borehole has a length of 603 m and is drilled slightly inclined, 80 degrees from the horizontal. No geophysical log was earlier available. Due to plugging of the borehole, geophysical logging during 1985 was possible only down to 70 m. The borehole is cased down to 50 m. The resistivity, temperature or salinity logs show no anomalies between 50-70 m.

6.2.5 Logging of F1 7

Borehole F1 7 has a length of 553 m and is almost vertical, 85 degrees from the horizontal. The geophysical logs, figure 6.7, show a major fracture zone at 300-380 m. At the upper part of this fracture zone the salinity increases to more than 4000 mg/l equivalent chlorine. At 505 m to the end of the measured section 515 m there is a strong decrease in resistivity indicating a fracture zone. Minor fracture zones are indicated between 195-235 m. The temperature log shows minor anomalies at 185 and 300 m.

6.2.5 Logging of F1 8

This cored borehole has a length of 464 m and is drilled inclined, 60 degrees from the horizontal. The geophysical logs, figure 6.7, indicate a major fracture zone from 0-150 m borehole length. At the lower part of this section an increase in salinity to more than 5000 mg/l equivalent chlorine occurs. Minor fracture zones are indicated at 200-215 m, 315-335 m, and 410-430 m borehole length. The temperature log shows numerous anomalies down to 200 m indicating continuous water flow out or/and into the borehole. Only minor temperature anomalies occur below this borehole length.

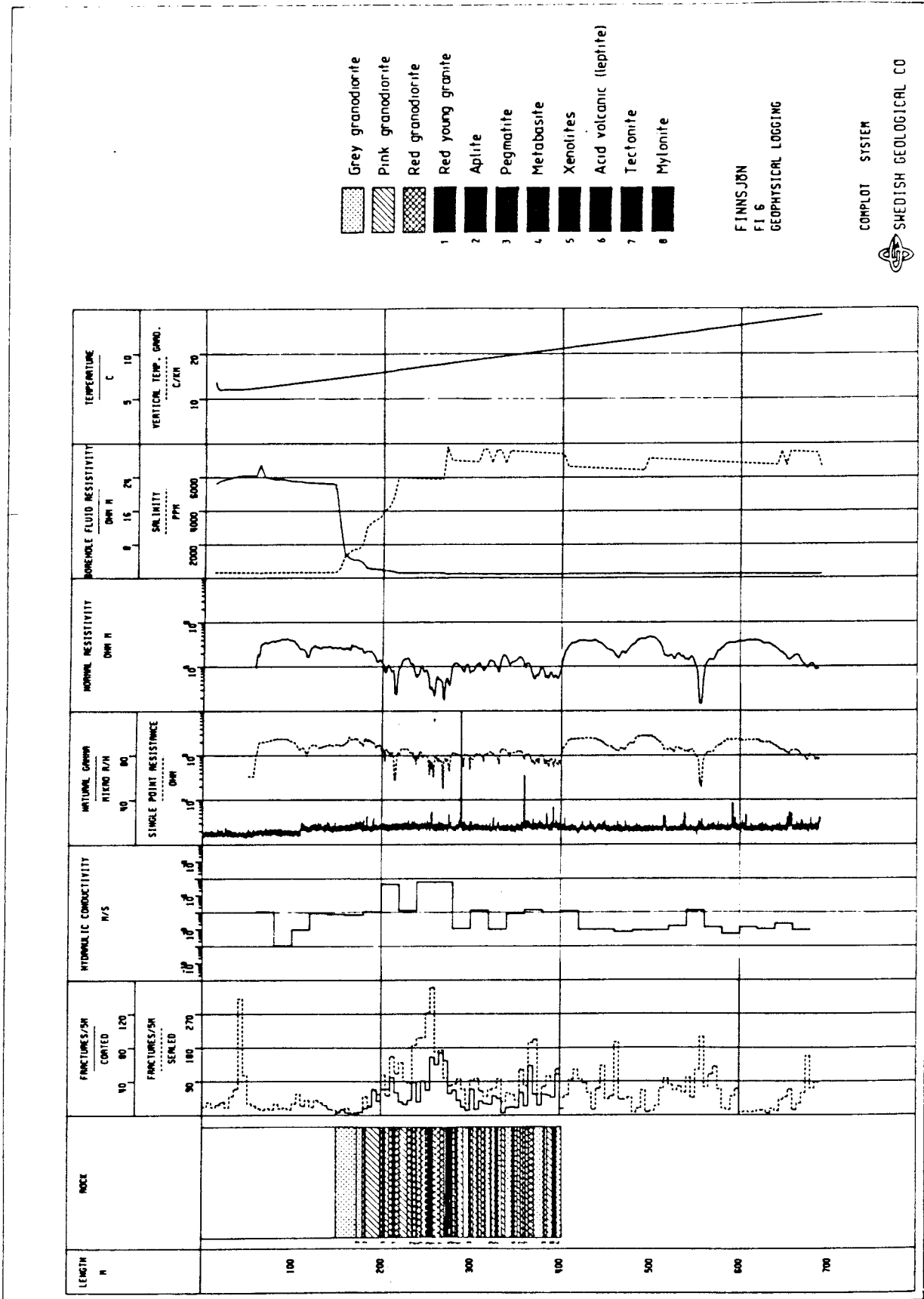


- Grey granodiorite
- Pink granodiorite
- Red granodiorite
- Red young granite
- Aplite
- Pegmatite
- Metabasite
- Xenolites
- Acid volcanic (lephite)
- Tectonite
- Mylonite

FINNSJÖN
FI 5
GEOPHYSICAL LOGGING

COMPLIT SYSTEM
SWEDISH GEOLOGICAL CO

Figure 6.1 Complot diagram of borehole measurements in Fi 5.



- Grey granodiorite
- Pink granodiorite
- Red granodiorite
- Red young granite
- Aplite
- Pegmatite
- Metabasite
- Xenolites
- Acid volcanic (lephite)
- Tectonite
- Mylonite

FINNSJÖN
FI 6
GEOPHYSICAL LOGGING

COMPLIT SYSTEM
SWEDISH GEOLOGICAL CO

Figure 6.2 Complot diagram of borehole measurements in Fi 6.

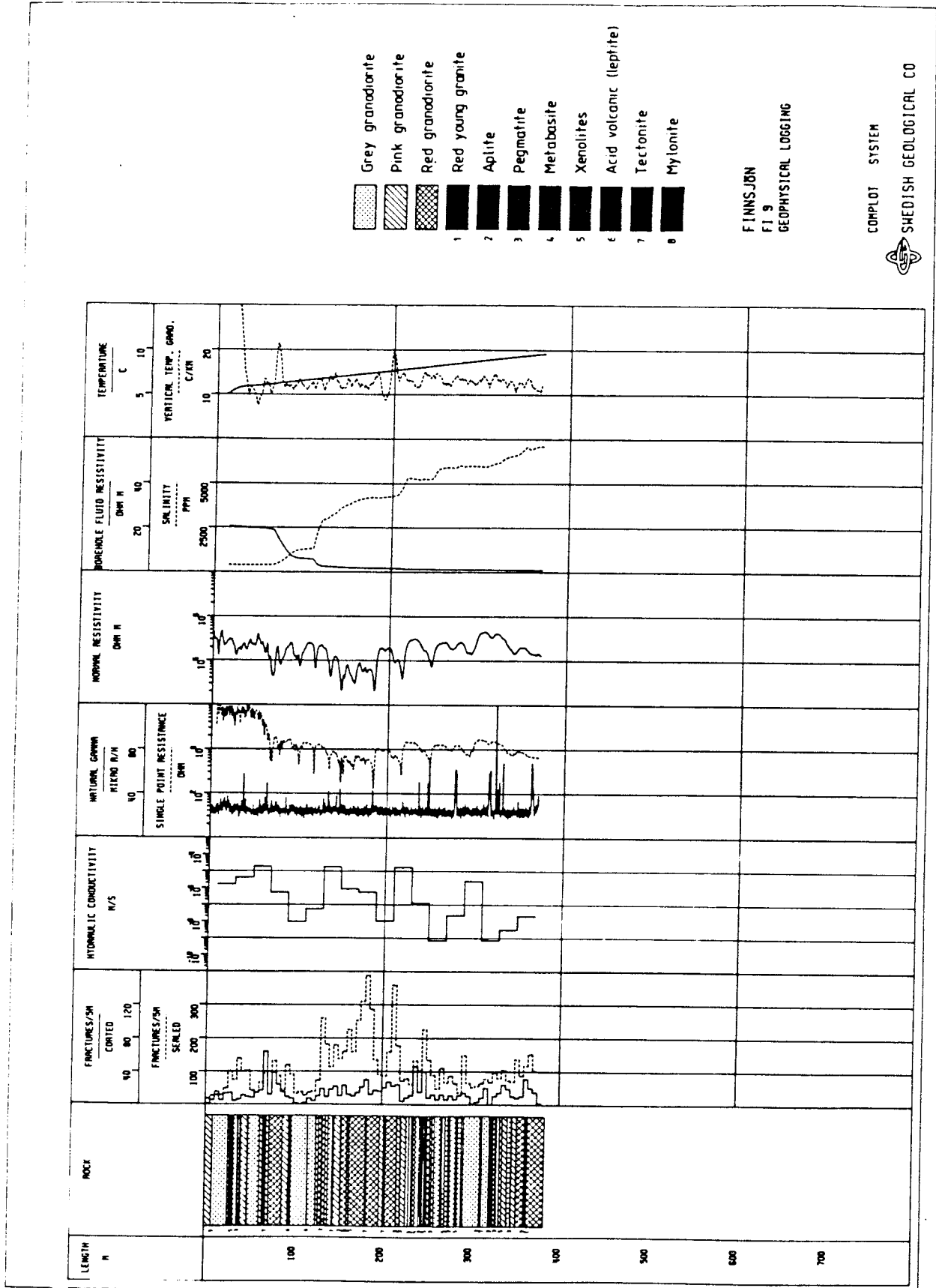


Figure 6.3 Complot diagram of borehole measurements in Fi 9.

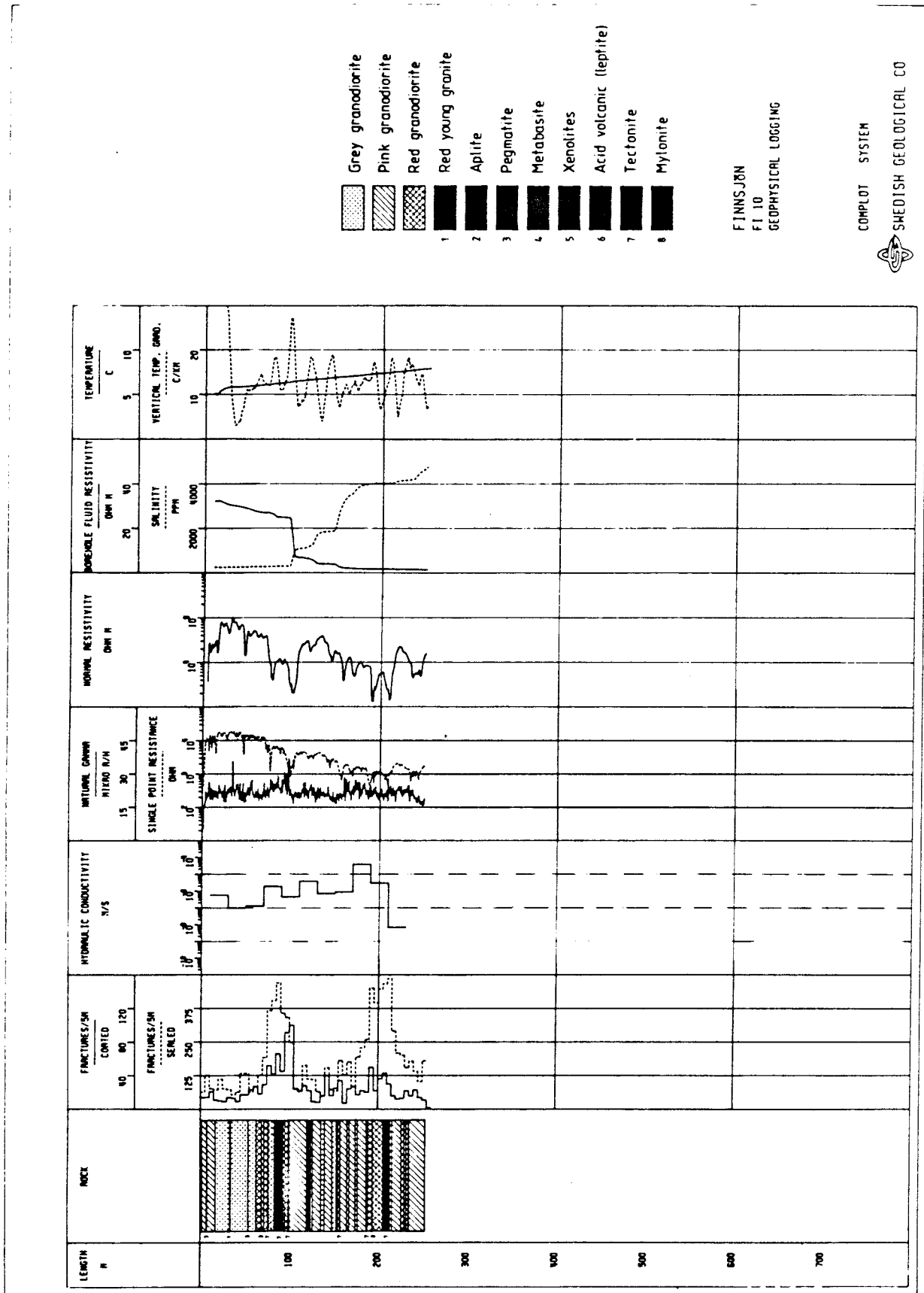
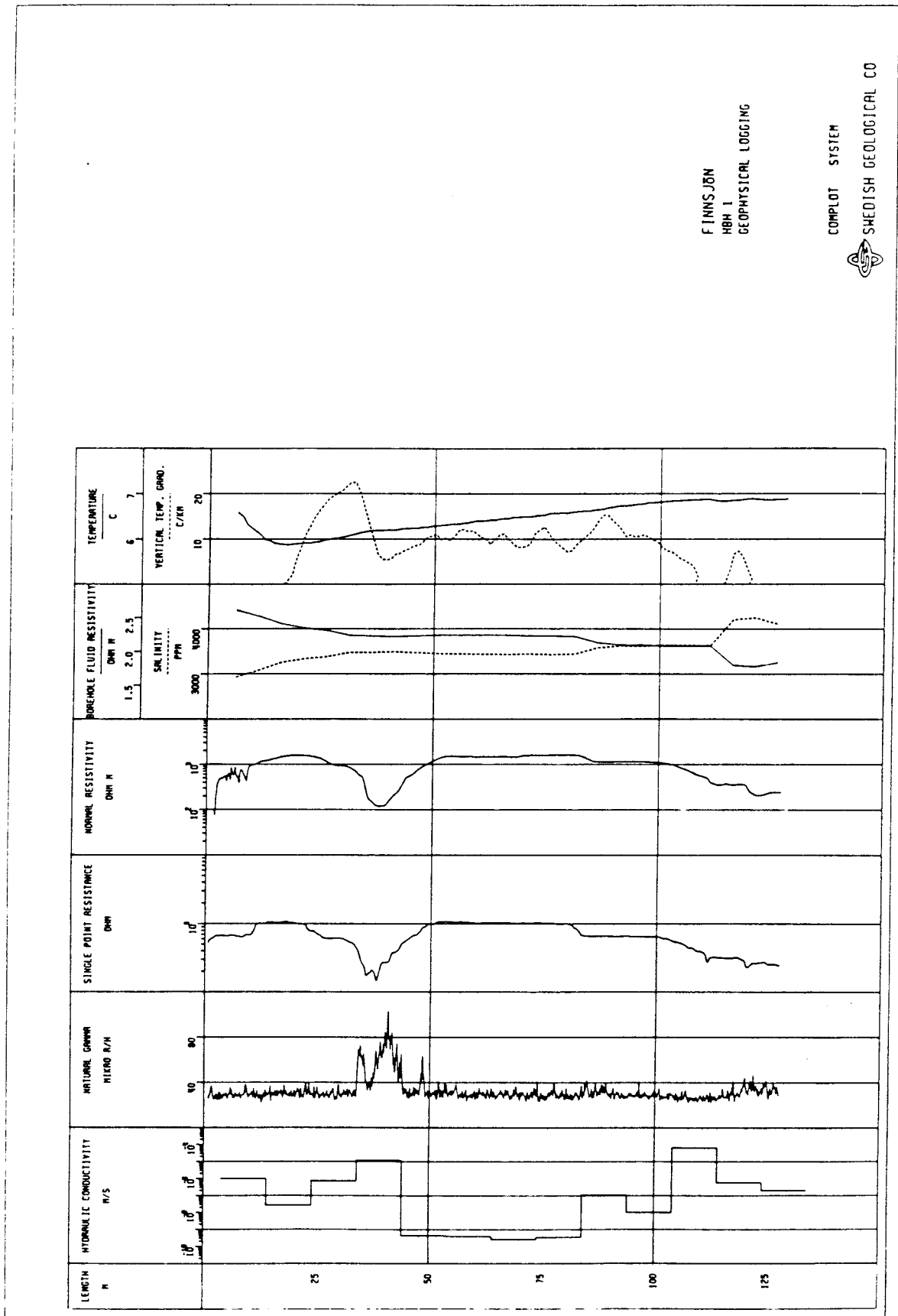


Figure 6.4 Complot diagram of borehole measurements in Fi 10.



F INNSJÖN
 HBI 1
 GEOPHYSICAL LOGGING


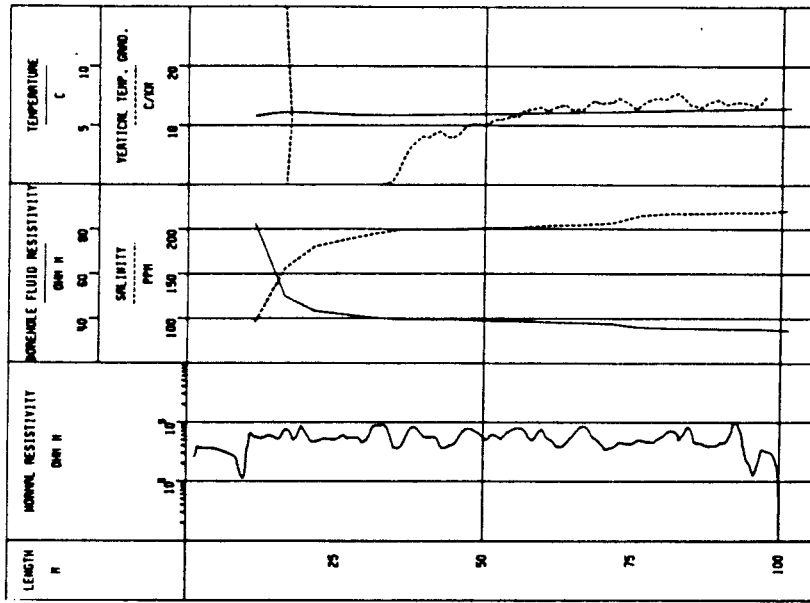

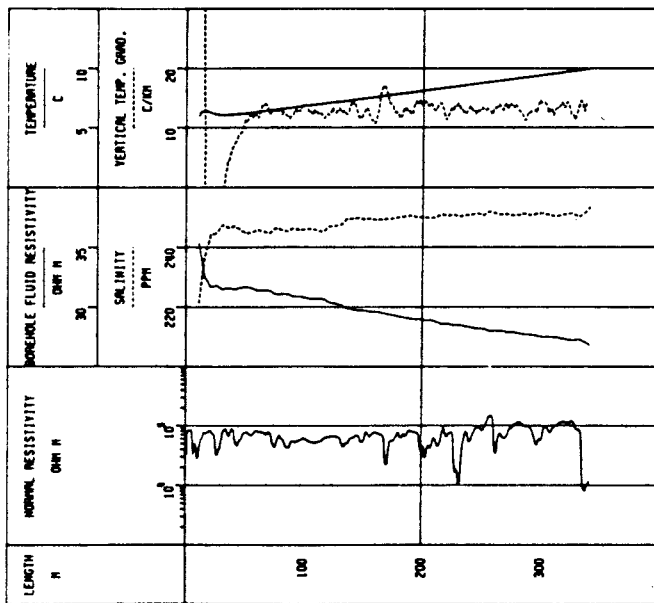
COMPLIT SYSTEM
 SWEDISH GEOLOGICAL CO

Figure 6.5 Complot diagram of borehole measurements in HFi 1.



FINNSJÖN
FI 2
GEOPHYSICAL LOGGING

COMPLIT SYSTEM
 SWEDISH GEOLOGICAL CO



FINNSJÖN
FI 1
GEOPHYSICAL LOGGING


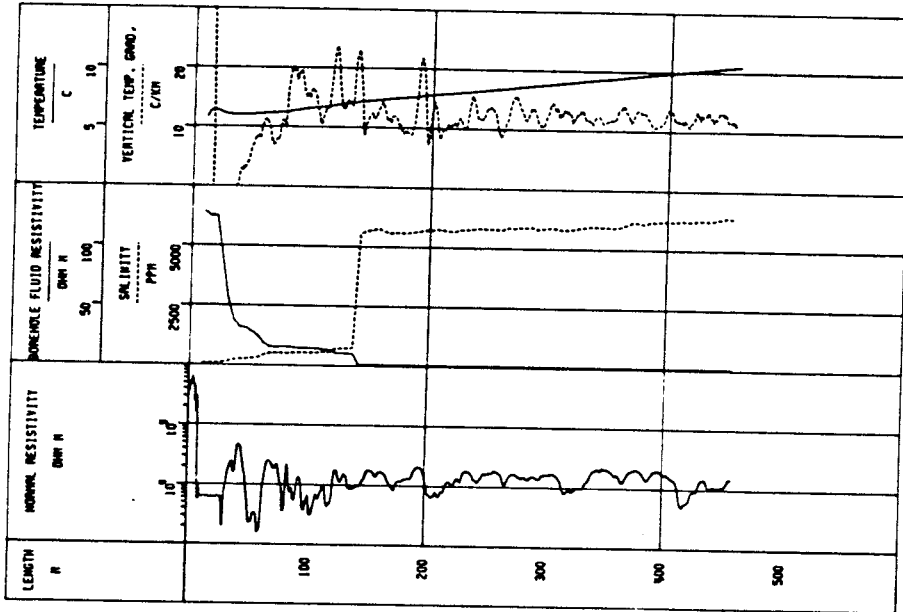
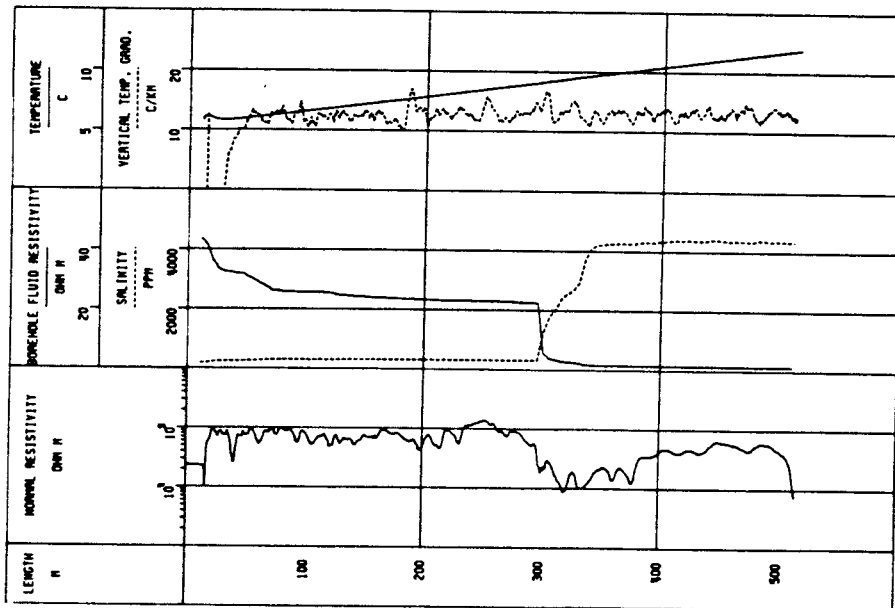
COMPLIT SYSTEM
 SWEDISH GEOLOGICAL CO

Figure 6.6 Complot diagrams of borehole measurements in boreholes Fi 1 and Fi 2.



FINNSJÖN
FI 8
GEOPHYSICAL LOGGING

COMPLIT SYSTEM
SWEDISH GEOLOGICAL CO



FINNSJÖN
FI 7
GEOPHYSICAL LOGGING

COMPLIT SYSTEM
SWEDISH GEOLOGICAL CO

Figure 6.7 Complot diagrams of borehole measurements in boreholes Fi 7 and Fi 8.

7. BOREHOLE RADAR MEASUREMENTS

7.1 General

All boreholes within the Brändan area have been measured using a borehole radar built by the Swedish Geological Co on commission from SKB. A detailed description of the borehole radar is given in Olsson et.al., (1985). The purpose was to study the extension of the fracture zones and to obtain the orientation of the fracture zones relative to the borehole axis. The 3-D orientation of fracture zones and other discontinuities may be achieved by using stereographic analyse of angular intersections in several boreholes of a fracture zone. In this case the direction of the normal to a reflector is plotted in a plane using the Wulff projection. The points where the curves intersect are candidates for the correct orientation of the plane. The result could then be compared with the structural framework based on other type of information. The principle of the radar system is shown in figure 7.1. The distance to a reflecting object is determined by measuring the difference in arrival time between the direct and the reflected pulse. The two basic patterns are point reflectors and plane reflectors as shown by figure 7.1. Fracture zones and lithological contacts are often characterized by planar patterns.

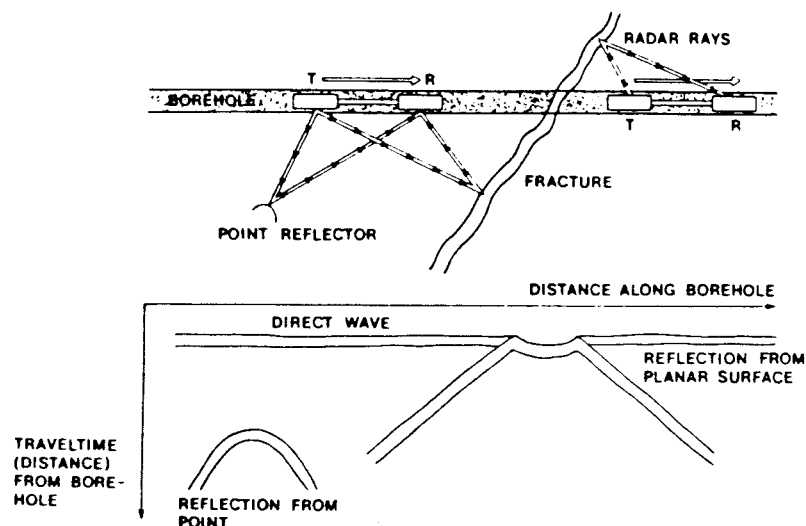


Figure 7.1 Principle of the borehole reflection radar and the patterns generated by plane and point reflectors.

The angle of intersection between a reflecting plane and a borehole is determined using a nomogram. Angles from 60 degrees to 90 degrees are so close to each other in the nomogram that they are difficult to determine with precision. Good precision is possible when the angles are less than 50 degrees. Also the amplitude of the reflecting signal varies with the angle of intersection. Fracture zones perpendicular to a borehole give small reflections, while the opposite applies to zones parallel to the borehole.

For the boreholes at the Finnsjön site, radar measurements have been performed in 1 m intervals for a maximum borehole length of 590 m.

7.2 Radar measurements of boreholes in the Brändan area

7.2.1 Borehole Fi 5

Radar measurements from borehole Fi 5, figure 7.2 and 7.3, show a loss of penetration between 168-234 m. This is caused by Zone 2. There is a decrease in velocity of the direct wave indicating high porosity. Weak reflections at both sides of the zone indicate an angular intersection between the zone and the borehole of 31-35 degrees. The most pronounced minor fracture zones are located at 83-90 m (30-35 degrees) and 475-500 m (25-40 degrees). There is also a strong reflection parallel to the borehole between 250-400 m at a distance of 26 m from the hole.

7.2.2 Borehole Fi 6

Zone 2 is geologically interpreted to intersect borehole Fi 6 between 201-287 m. There is also a loss of penetration and a decrease in direct wave velocity at this depth, figures 7.3 and 7.4. Reflections within this interval range from 35-70 degrees, the strongest being 60-70 degrees. Since the borehole is vertical, 60-70 degrees corresponds to a fracture zone dipping 20-30

degrees from the horizontal. There is also some loss in penetration of the radar waves between 300-400 m. A pronounced minor fracture zone occurs at 550-570 m. Two possible angular intersections (radar angles) have been interpreted from the radar picture, 50 and 17 degrees.

7.2.3 Borehole Fi 9

Radar pictures from the borehole are presented in the figures 7.5 and 7.6. The section 0-115 m was measured twice because of an instrumental error. Core logging indicates that Zone 2 intersects the borehole at 134-205 m, while geophysical logging indicates an intersection at 130-215 m. There is a loss of penetration for the radar waves at 130-215 m. Reflexions within the section indicate angles ranging from 13 to 60 degrees. The angular intersection between the earlier interpreted Zone 2 and the borehole is 70-80 degrees. Thus, if the penetration loss is mainly caused by the Zone 2, then this zone must, at this location, be intersected by discontinuities with other orientations.

7.2.4 Borehole Fi 10

Figure 7.6 shows the borehole radar picture of borehole Fi 10. Reflections from the upper and the lower walls of Zone 1 (Brändan) are possible to distinguish, 44 and 46 degrees respectively to the borehole axis. The angle of the fracture zone to the borehole Fi 10 axis has earlier been calculated from borehole and surface information to about 55 degrees.

A strong radar reflection of 30 degrees was produced from the fault breccia of Zone 2 at 214 m borehole length (see photo, figure 5.6). This is in accordance with the angle of intersection of the breccia to the borehole axis. Figure 7.6 also shows a strong radar reflex at 14-79 m borehole length. The angle to the borehole is 8 degrees. This reflex is probably caused by a dyke or a small fracture zone.

7.2.5 Percussion borehole HF1 1

Radar measurements in the vertical borehole HF1 1 show a pronounced minor fracture zone at 37-48 m, figure 7.7. The radar angles are 55 and 47 degrees respectively. Another fracture zone appears in the lower part of the borehole. Two radar angles have been measured at this zone, 10 and 55 degrees (or 80 and 35 degrees from the horizontal). The lower zone is from other data interpreted to represent the upper part of Zone 2, dipping 17 degrees from the horizontal. The discrepancy in angle might be caused by the earlier mentioned inaccuracy in the nomogram when determining angles of fracture zones intersecting a borehole at steep angles. Another explanation might be that the radar reflex is caused by other discontinuities, e.g. dykes.

7.3 Wulff net plots

Radar measurements carried out in the four cored boreholes give an opportunity to test the earlier interpreted orientations of the fracture zones 1 and 2 calculated from core and geophysical logging. A Wulff plot of the radar angle obtained from Zone 1 in borehole Fi 10 and the earlier interpreted orientation of Zone 1, Brändan, is shown in figure 7.8. The radar angles correspond reasonably well to the interpreted orientation of Zone 1.

Figure 7.9 shows the radar angles generated from fracture Zone 2 plotted on the Wulff net for all cored boreholes except Fi 9. In this borehole no radar reflection was obtained for Zone 2. Instead, the angle of a fault breccia to the borehole axis was used. This figure also shows a plot of the normal to the Zone 2, interpreted from core and geophysical logs, striking 151 degrees and dipping 17 degrees (local grid system). The radar angles strongly confirm the orientation of the fracture zone.

7.4 Conclusions of the radar measurements

At the major fracture zones the direct radar wave between the transmitter and receiver shows a decrease in velocity caused by increased porosity in the fractured bedrock. These sections also show a loss of penetration due to attenuation of the radar waves. The width of the borehole section with penetration loss along the borehole coincides in general with the increased frequency of sealed fractures.

Relatively small reflexions occur from the major fracture zones while minor fracture zones and lithological contacts often show stronger reflections. This is probably due to a more gradual change in the bedrock resistivity in connection to major fracture zones compared to minor fracture zones and lithological contacts. Another cause for small reflections is the steep angle of intersection between the boreholes and the Zone 2.

Wulff net plots of the radar angles for Zone 1 and Zone 2 confirm the earlier calculated orientations of the fracture zones.

Reflexions from minor fracture zones and lithological contacts occur with a frequency of 3-4 reflections/100 m.

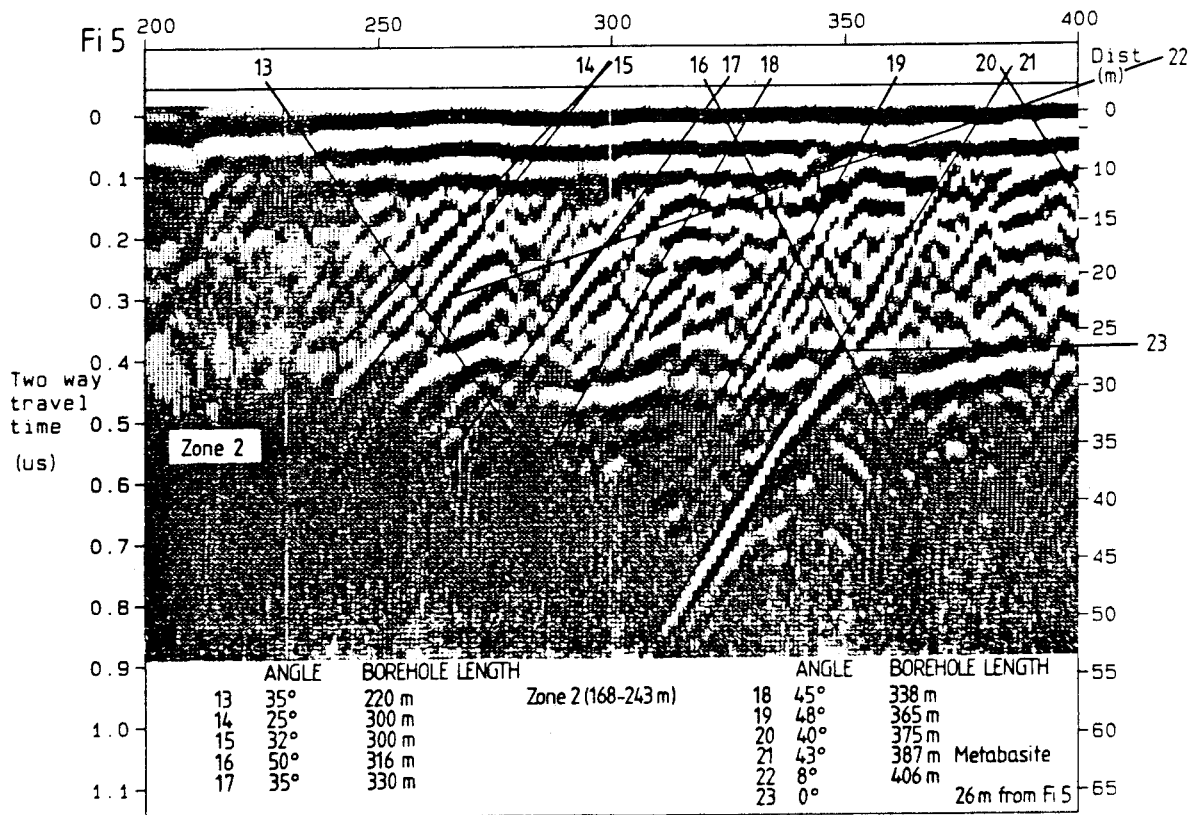
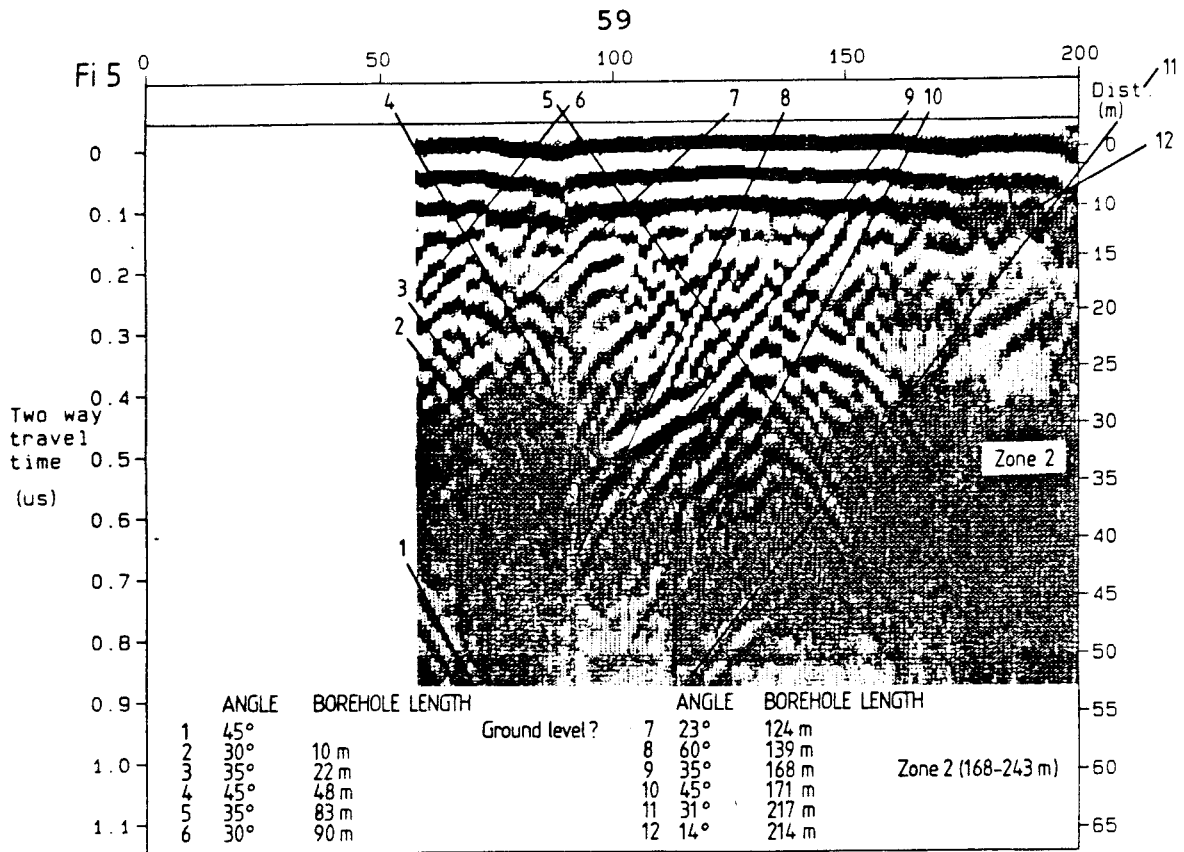


Figure 7.2 Radar pictures for borehole Fi 5.

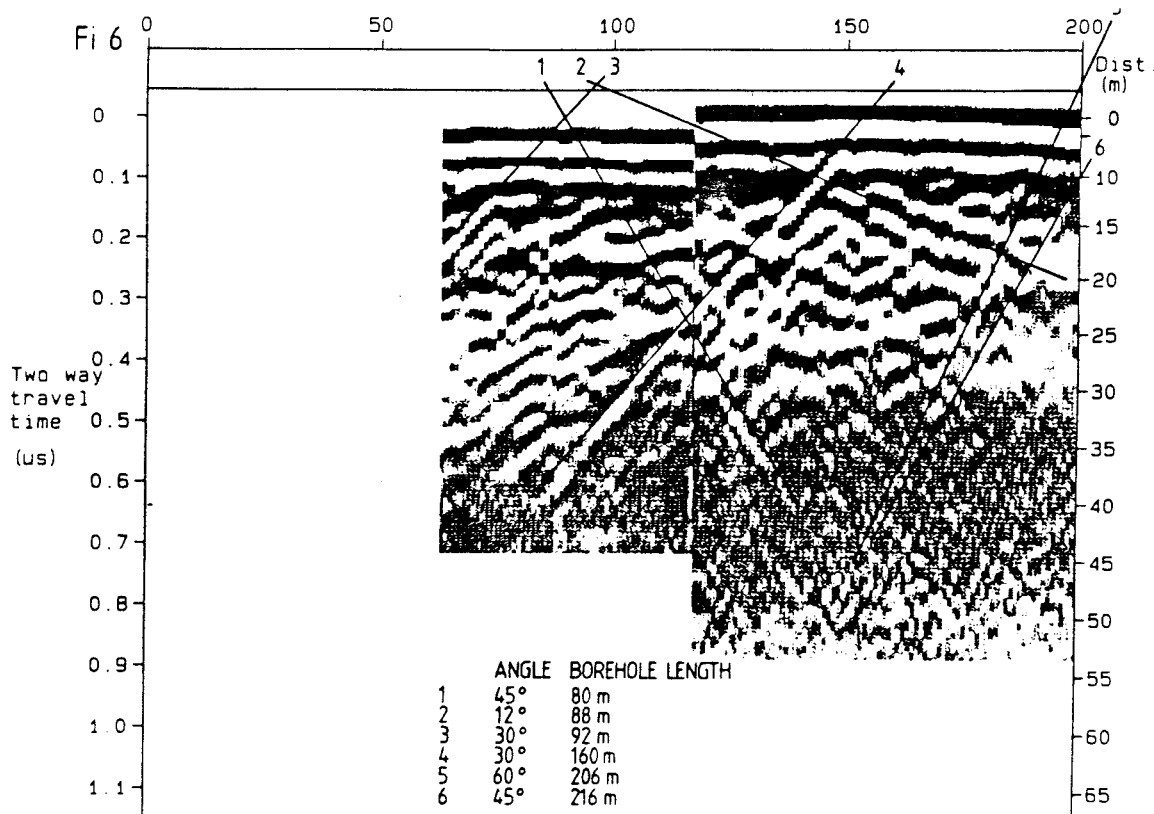
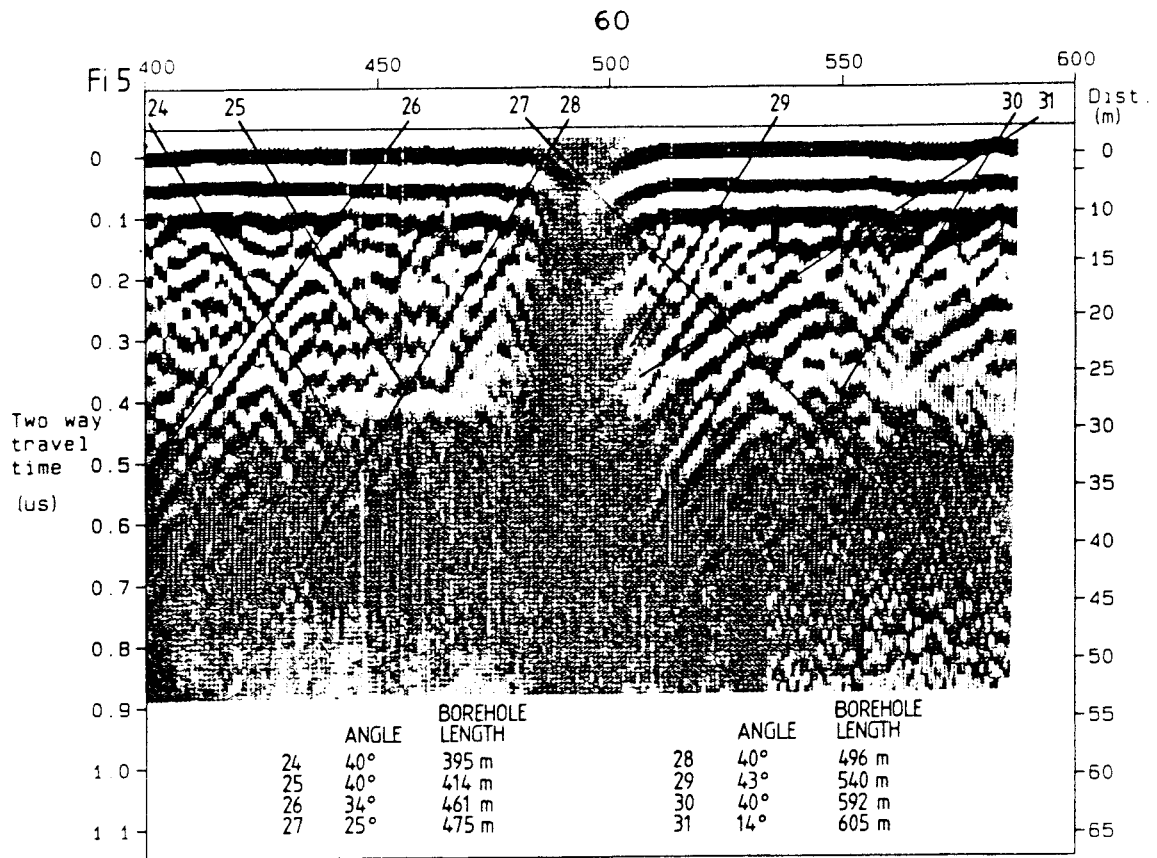


Figure 7.3 Radar pictures for boreholes Fi 5 and Fi 6.

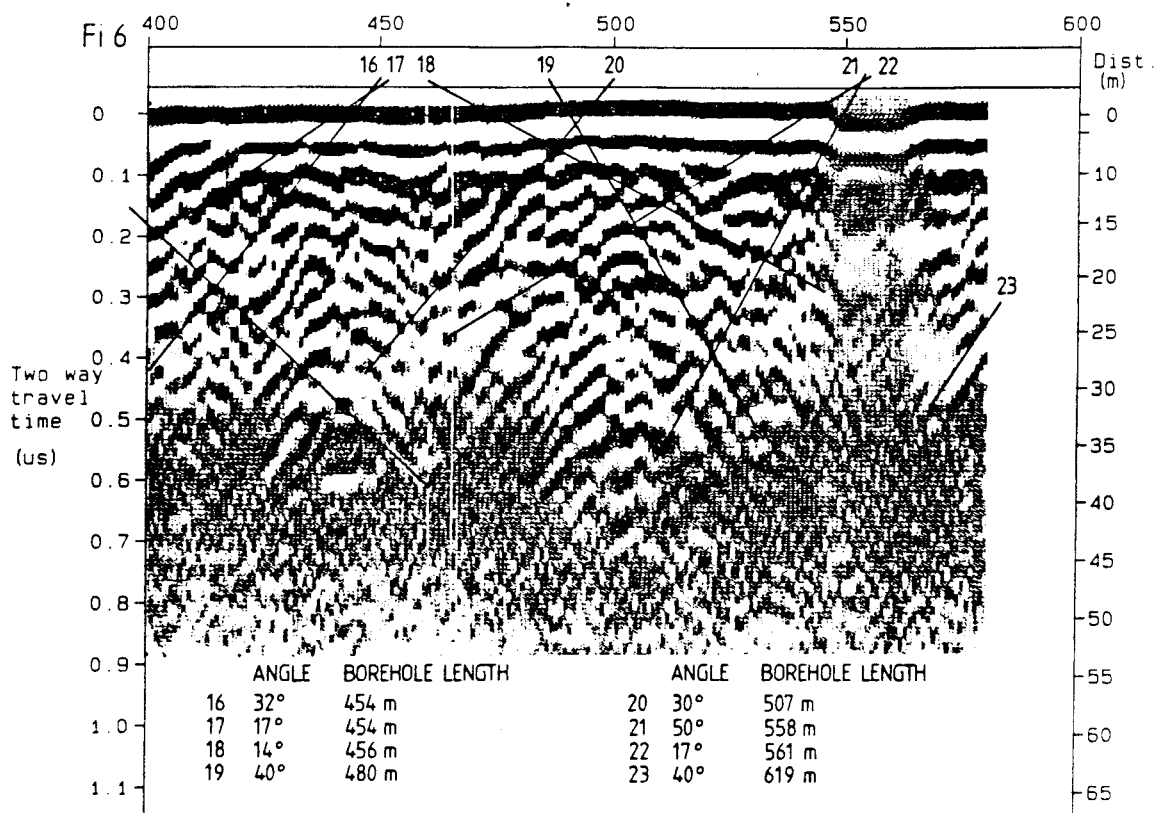
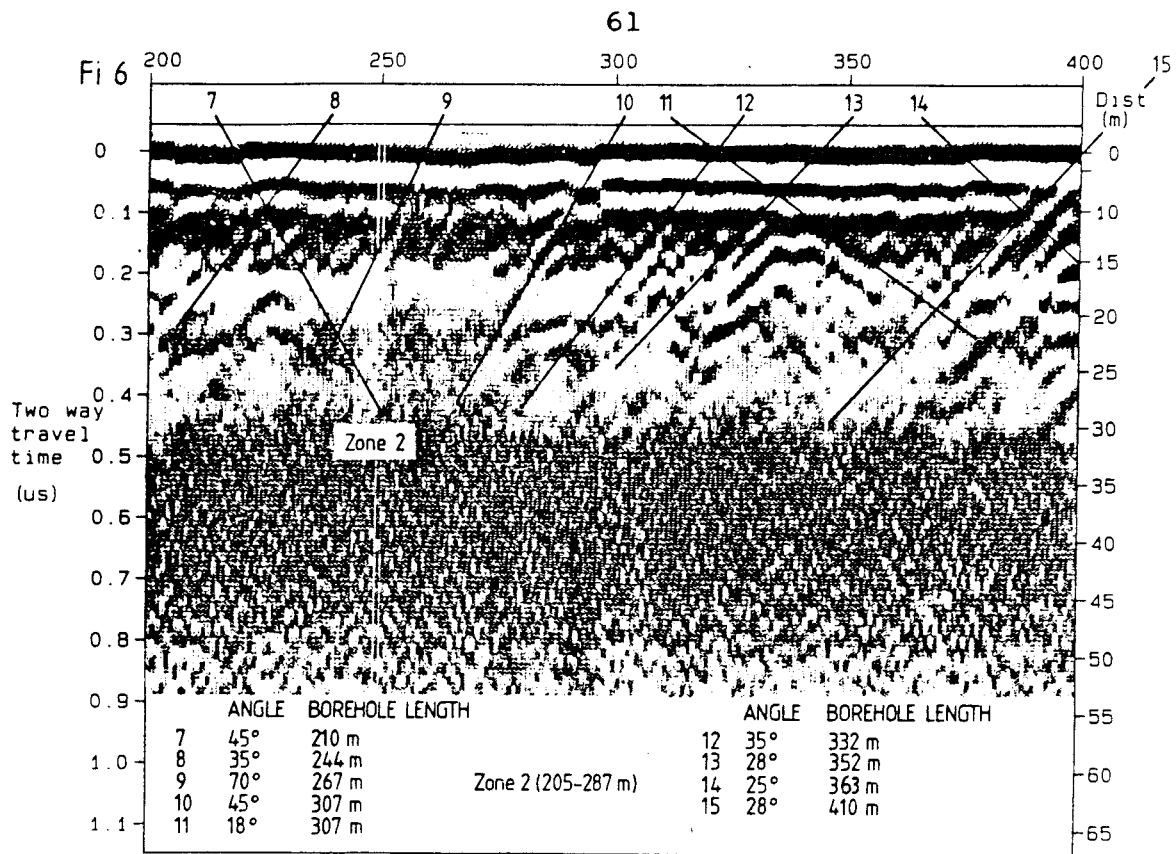


Figure 7.4 Radar pictures for borehole Fi 6.

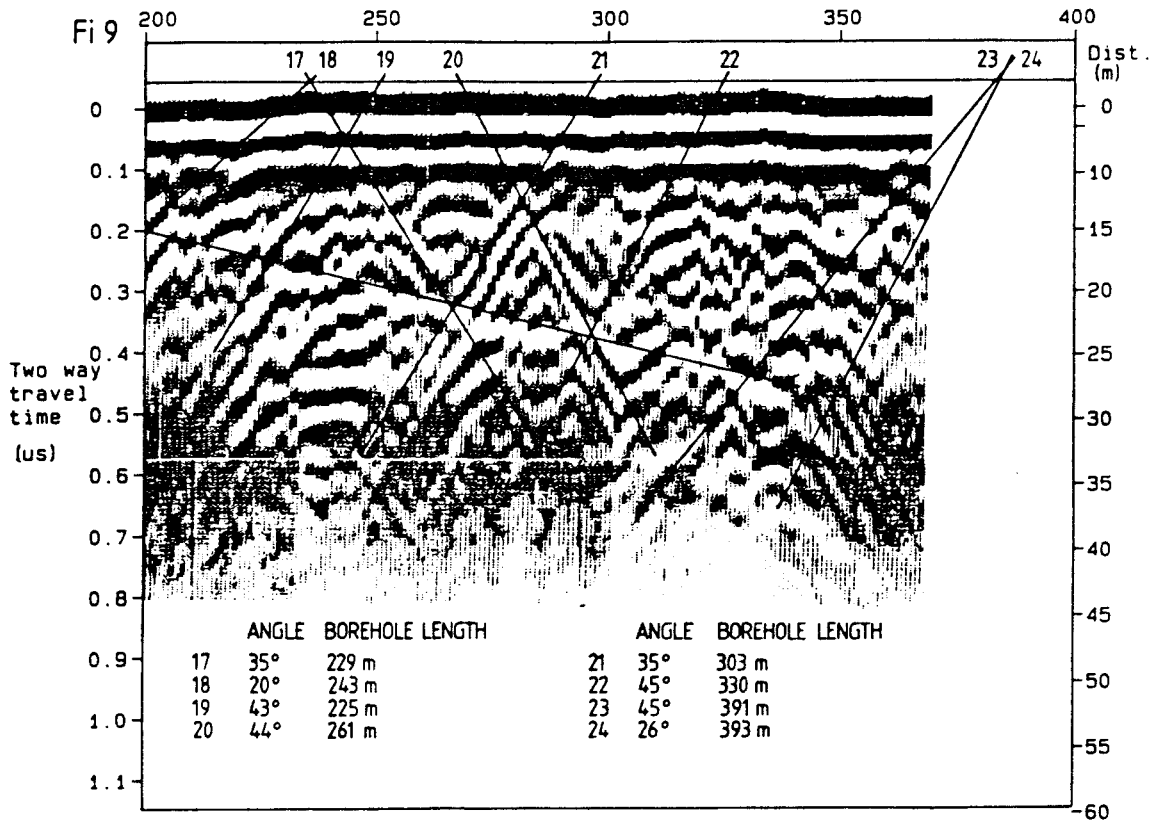
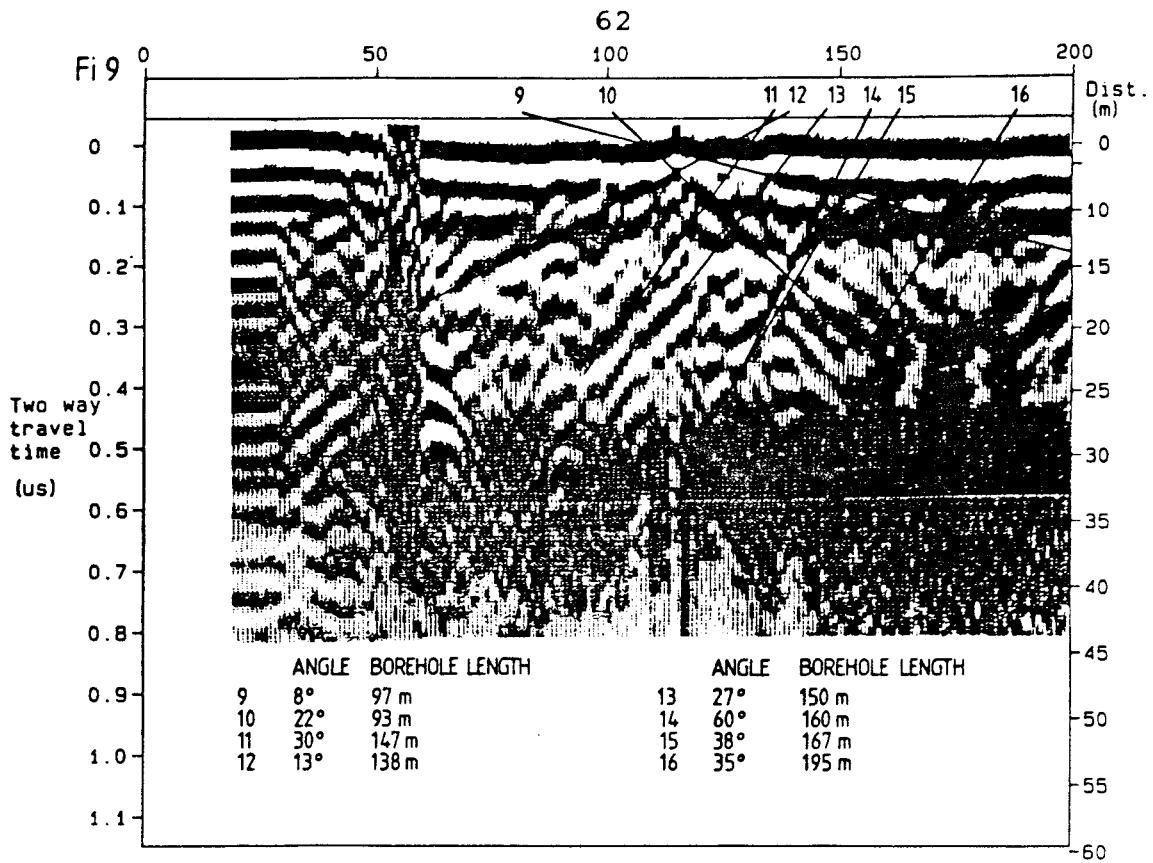


Figure 7.5 Radar pictures for borehole Fi 9.

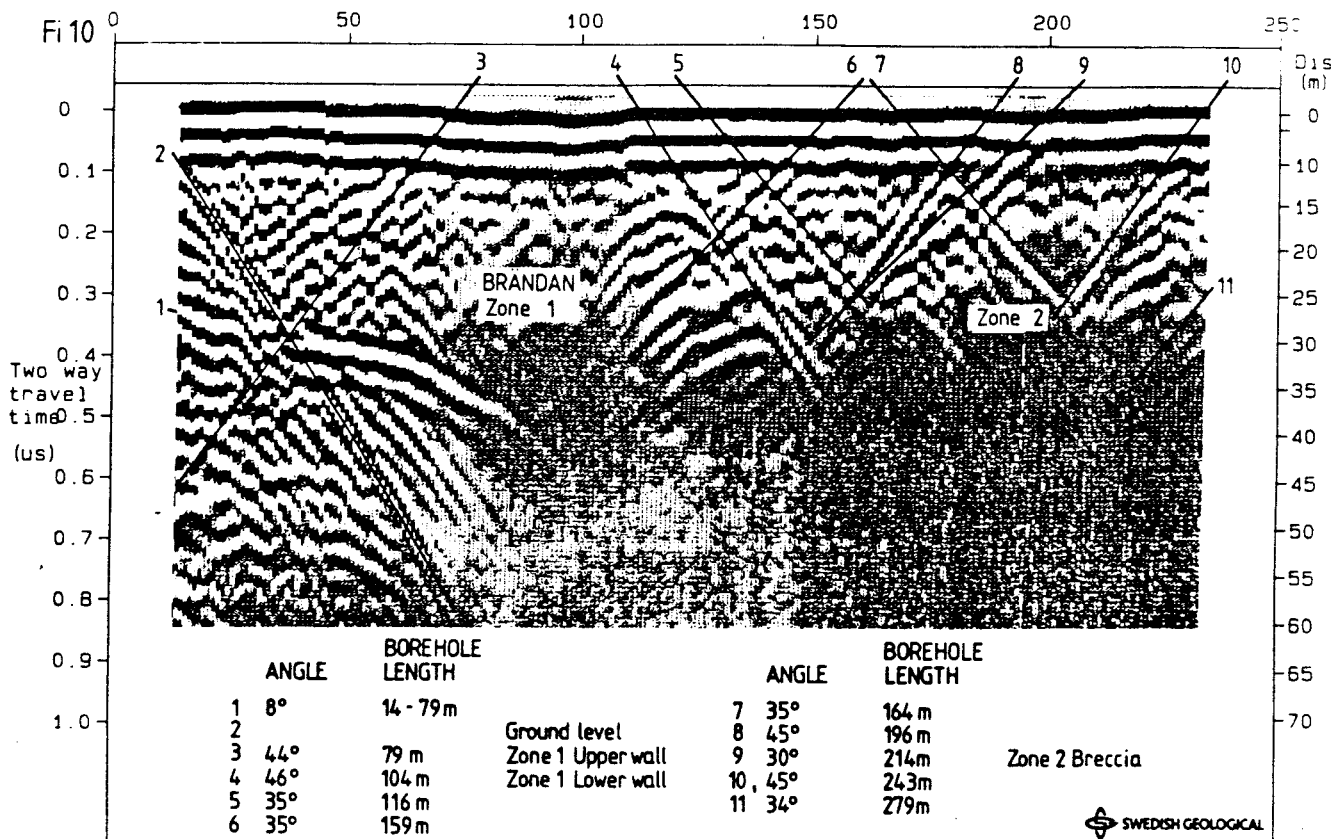
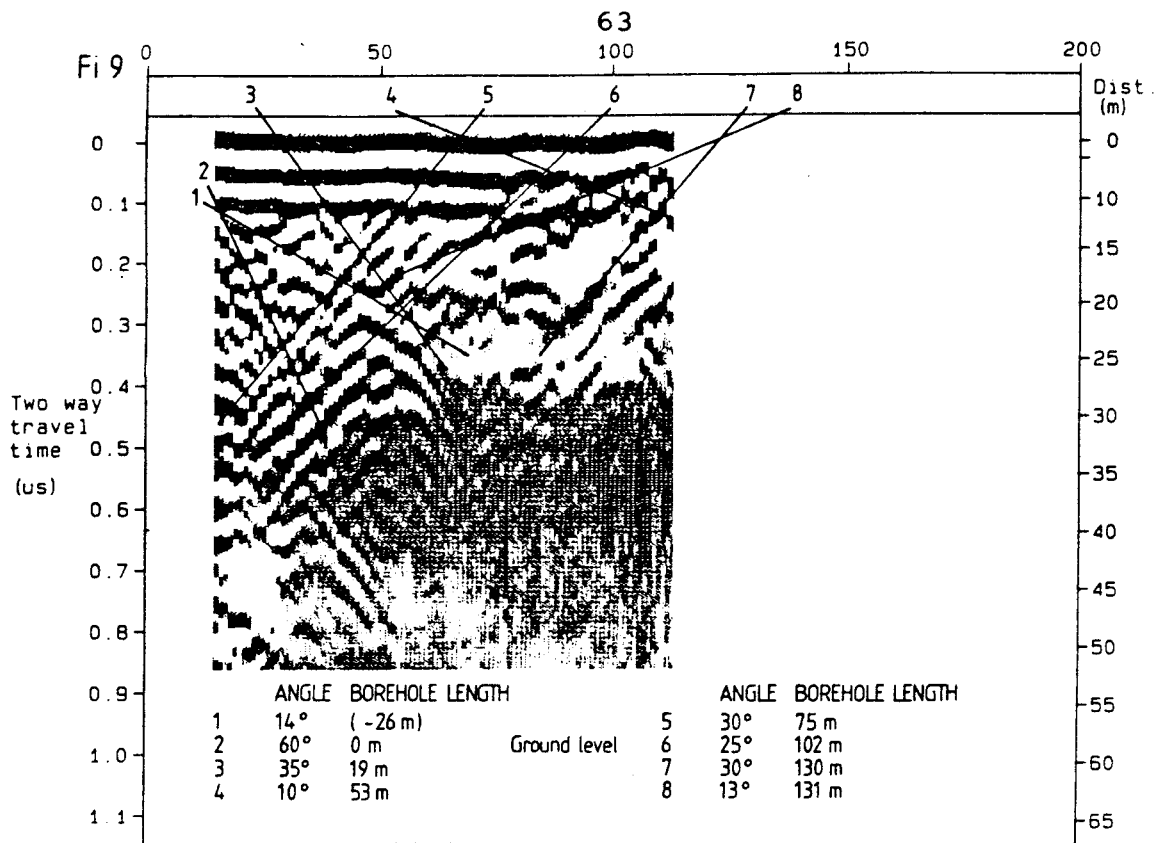


Figure 7.6 Radar pictures for boreholes Fi 9 and Fi 10.

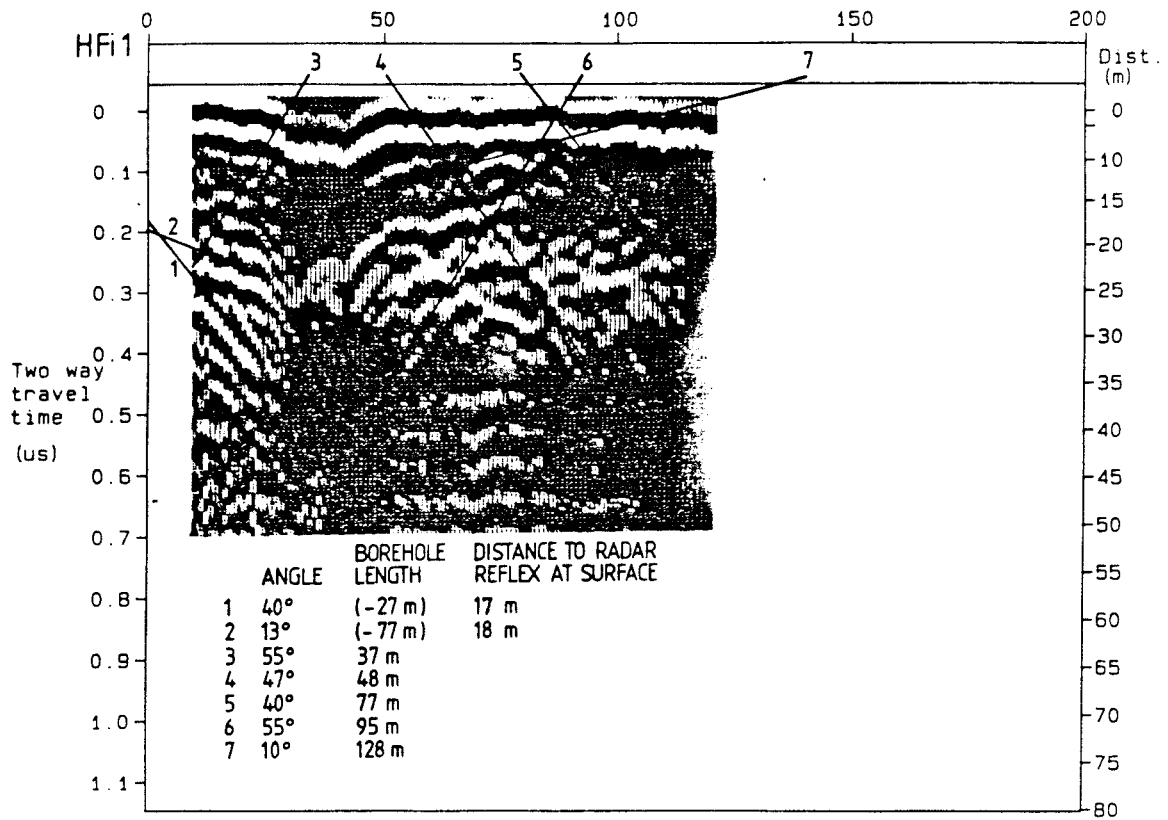


Figure 7.7 Radar picture for borehole HFi 1.

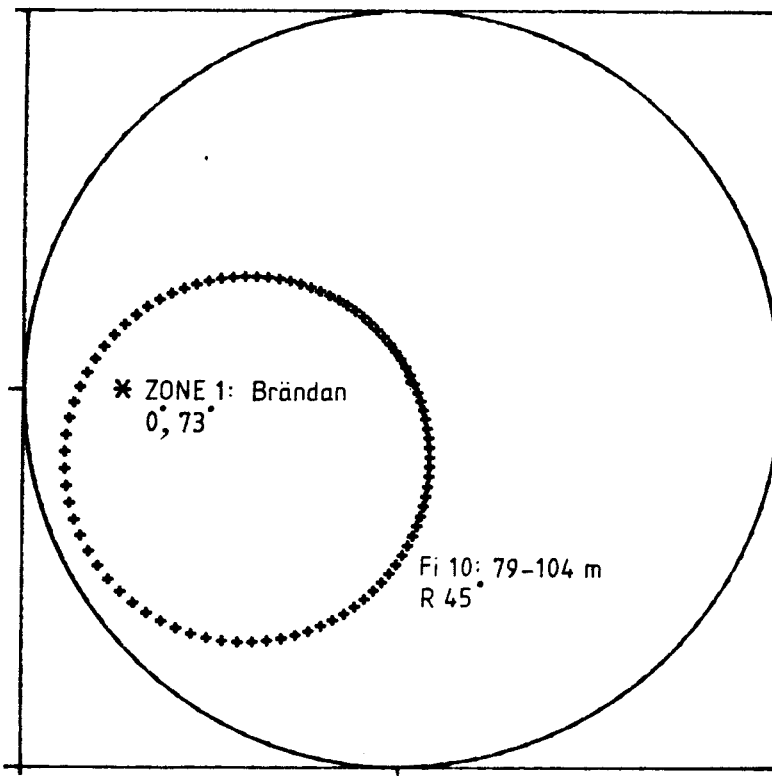


Figure 7.8 Wulff plot, orientation of Zone 1.

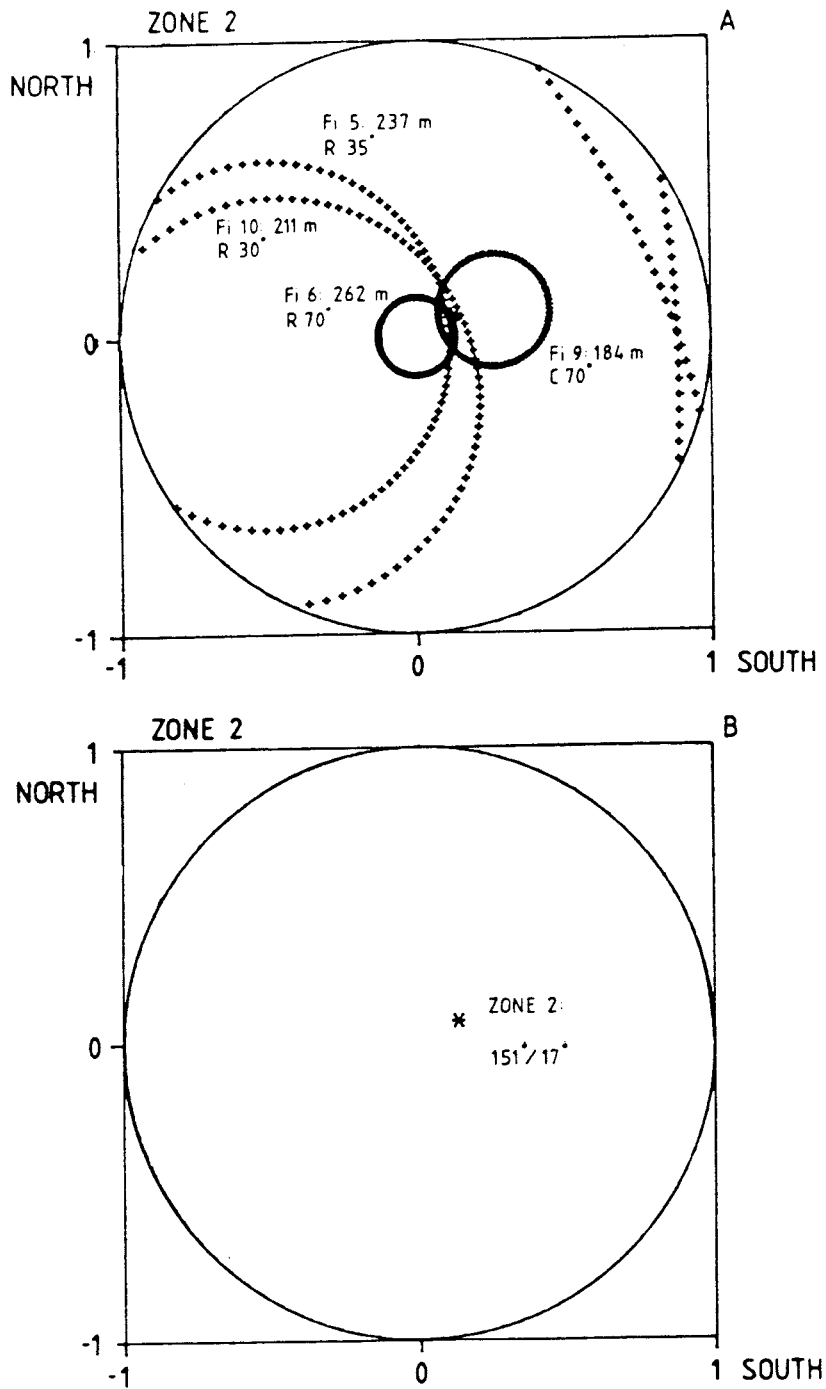


Figure 7.9 Wulff plot, orientation of Zone 2. Upper part of the figure, show plot of radar angles (R) and core angle (C), lower part show orientation of fracture zone 2 calculated from intersections in boreholes.

8. MEASUREMENTS OF HYDRAULIC CONDUCTIVITY AND ESTIMATES OF STORATIVITY

Hydraulic tests performed within this project comprise measurements of hydraulic conductivity, estimates of the specific storage coefficient and measurements of hydraulic head (piezometric measurements). Hydraulic conductivity and storativity are described in this chapter, hydraulic head conditions in chapter 9.

8.1 Measurements of hydraulic conductivity by single-hole injection tests and interference tests

8.1.1 Different tests applied

The hydraulic conductivity of the bedrock has been determined by means of single-hole water injection tests and interference tests. For the water injection tests, three different equipments and two injection methods have been used. The lengths of the tested sections varied between the different boreholes. However, in the current report the conductivity values have been normalized to the same section length, 20 m, in order to simplify a comparison between different boreholes. In specific parts of the boreholes also shorter sections lengths (detailed measurements) are shown.

The interference tests were performed as gas-lift pumpings in the cored borehole F1 9 with piezometric registration in F1 5, F1 6 and HFi 1 and, during two of the tests, also in the test-well, i.e. F1 9 (section 8.1.5 - 8.1.10).

8.1.2 Water injection tests. Methods

The two cored boreholes drilled in 1978, F1 5 and F1 6, were tested in 1978-79. The equipment and the results available at that time are described by (among others) Carlsson et al. (1980). The tests in F1 5 and F1 6 were performed and evaluated as steady-state tests. The injection time was about 15

minutes. The length of the tested sections during the double packer measurements was 3 m. Also single packer measurements were performed. The length of the test sections was in this case sometimes several hundred metres. The packers used had the length of 0.3 m.

The measurements in HF1 1 were made in 1984 with an improved equipment described by Almén et al. (1983). The packer length was one metre. The injection method used was steady-state with about 15 min injection time. The section length was 10 m. Also 2 m sections (altogether 10) were measured in selected parts of the borehole. In order to minimize leakage around the packers, two packers on each side of the test section were used.

The tests in F1 9 and F1 10, finally, were made in 1984 and 1985 with the "umbilical hose system" equipment, which is described in detail by Almén et al. (1983). In this equipment, the water to the test section is conducted through a hydraulic tube. This tube and other tubes and electrical cables for the regulation of packers, valves, pressure transducers etc. are put together in a 52 mm "umbilical hose". The water pressure in the test section during a test is regulated automatically by a valve system and a computer. The whole equipment is built into two trailers.

F1 9 and F1 10 were tested with 20 m long sections. Parts of the boreholes were tested in detail with 5 m section tests (totally 4 sections in F1 9 and 8 in F1 10). The injection method chosen in this case was transient tests with two hours injection time and two hours pressure recovery. The hydraulic conductivity was calculated from the injection phase and, if possible, from the recovery. The values of hydraulic conductivity in the diagrams (figure 8.2) refer to the injection phase. Theory and methodology for transient tests are described in an internal SKB-report (83-02): "Almén, K-E., Andersson, J-E., Carlsson, L., Hansson, K., 1982: Hydrauliska tester, Del 4: Jämförande studier av olika hydrauliska metoder."

In table 8.1 an overview is given of the equipments and sec-

tion lengths used for the different water injection tests.

Table 8.1 Water injection tests. Equipments and section lengths.

Borehole	Equipment	Section length
Fi 5	Steel pipes for conducting water to test section. Packer length 0.3 m	3 m
Fi 6	"-	3 m
HF1 1	Aluminium pipes for conducting water. Automatic data collecting system. Packer length 1 m. Two packers on each side of test section.	10 m, 2 m
Fi 9	Umbilical hose system: hydraulic tube for conducting water. Automatic pressure regulation in test section. Automatic data collecting system. Packer length 1 m.	20 m, 5 m
Fi 10	"-	20 m, 5 m

8.1.3 Water injection tests. Results

Only Fi 9 and Fi 10 were tested in 20 m long sections. However, the measurements of Fi 5, Fi 6 and HF1 1 with 3 and 10 m sections respectively were recalculated to 20 m sections according to the formulas:

$$K_{20} = (K_1 \cdot 3 + K_2 \cdot 3 + \dots + K_6 \cdot 3 + K_7 \cdot 2) / 20 \quad (3-1)$$

$$K_{20} = (K_1 \cdot 10 + K_2 \cdot 10) / 20. \quad (3-2)$$

The results are accounted for in figure 8.1 and 8.2. All diagrams show 20 m long sections. Measurements made with 2,3 or 5 m section lengths are indicated as shaded parts of the diagrams (for Fi 5 and Fi 6 this applies only to measurements within the Zone 2). The geological interpretation of Zone 1 and Zone 2 is marked in the diagrams.

Borehole Fi 5

In Fi 5 the hydraulic conductivity is high down to 300 m borehole length. The maximum value for the 20 m sections, $2.5 \cdot 10^{-5}$ m/s, occurs in the lower part of Zone 2. The 3-m measurements in the zone clearly illustrate, that there are three conductivity maxima. One peak-value is observed in the section 167-170 m (no measurable pressure increase could be reached, which means $K > 2.0 \cdot 10^{-4}$ m/s) and another in 227-230 m ($K = 1.2 \cdot 10^{-4}$ m/s). The third peak occurs in the section 263-266 m ($K = 3.2 \cdot 10^{-5}$ m/s). If the conductivity diagram alone was used to define the width of Zone 2, it would be extended downwards to about 290 m. That would give the zone a vertical width of about 107 m. Due to the casing, Zone 1 could not be measured in Fi 5.

Borehole Fi 6

In Fi 6 the hydraulic conductivity has a maximum for the 20 m sections at 240-280 m ($6.3 \cdot 10^{-6}$ m/s), which is the lower part of Zone 2. The rest of the hole varies approximately between 10^{-7} to 10^{-8} m/s except for a few values. The 3 m sections show two conductivity maxima within Zone 2: 214-217 m ($3.0 \cdot 10^{-5}$ m/s) and 253-271 m (four values with $K > 10^{-4}$ m/s). The vertical width of Zone 2, considering the conductivity values alone, is about 80 m.

Borehole HFi 1

HFi 1 is a short hole, which penetrates only the upper part of Zone 2 (figure 2.1 and 8.2). The detailed measurements reveal a high value, $1.9 \cdot 10^{-4}$ m/s, in the test section 112-114 m. At the length 38-40 m there is a superficial, highly conducti-

ve zone, with a peak value of $7.2 \cdot 10^{-5}$ m/s.

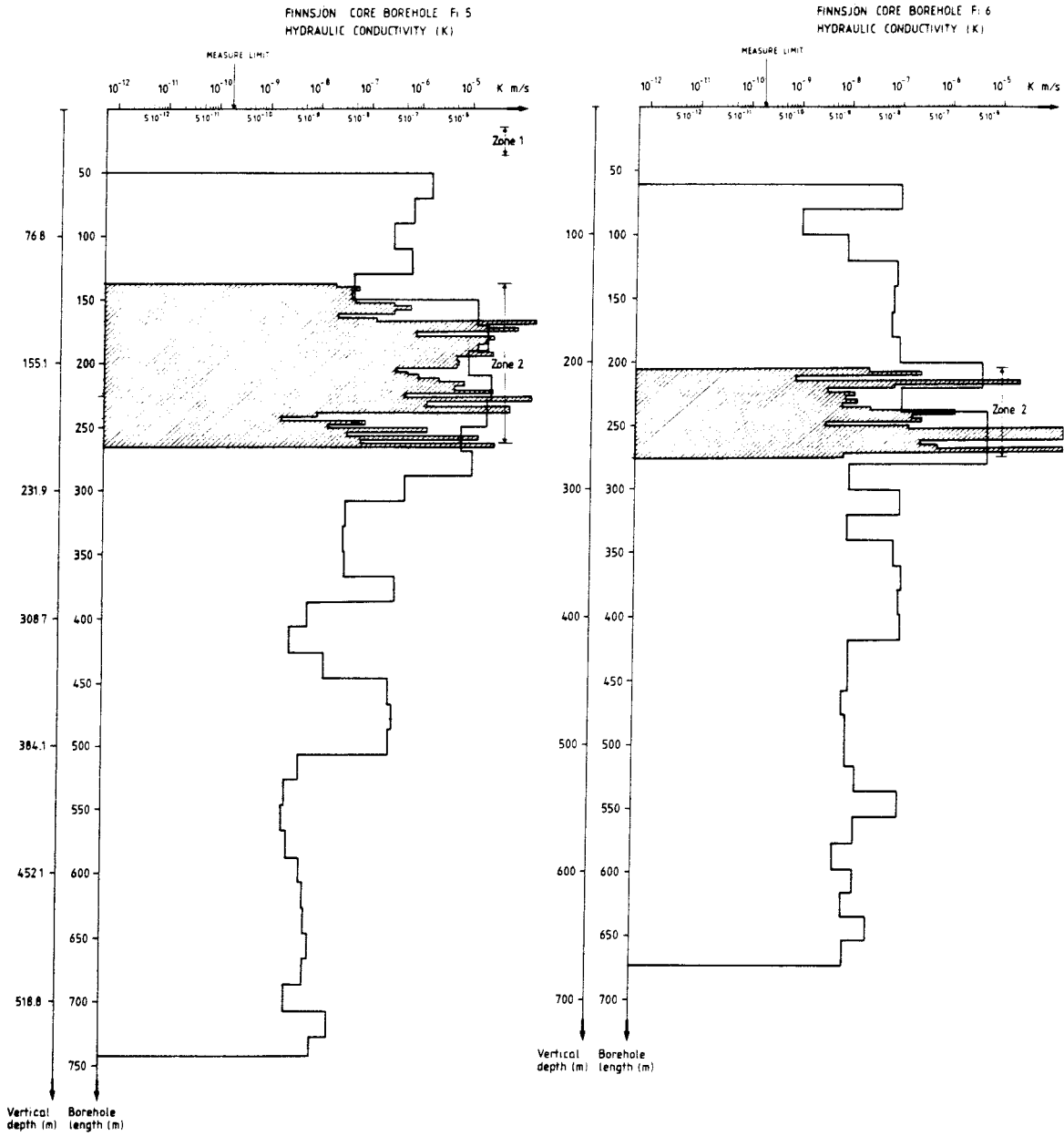


Figure 8.1 Hydraulic conductivity in the cored boreholes F: 5 and F: 6. The results are normalized from 3 m sections to 20 m sections.

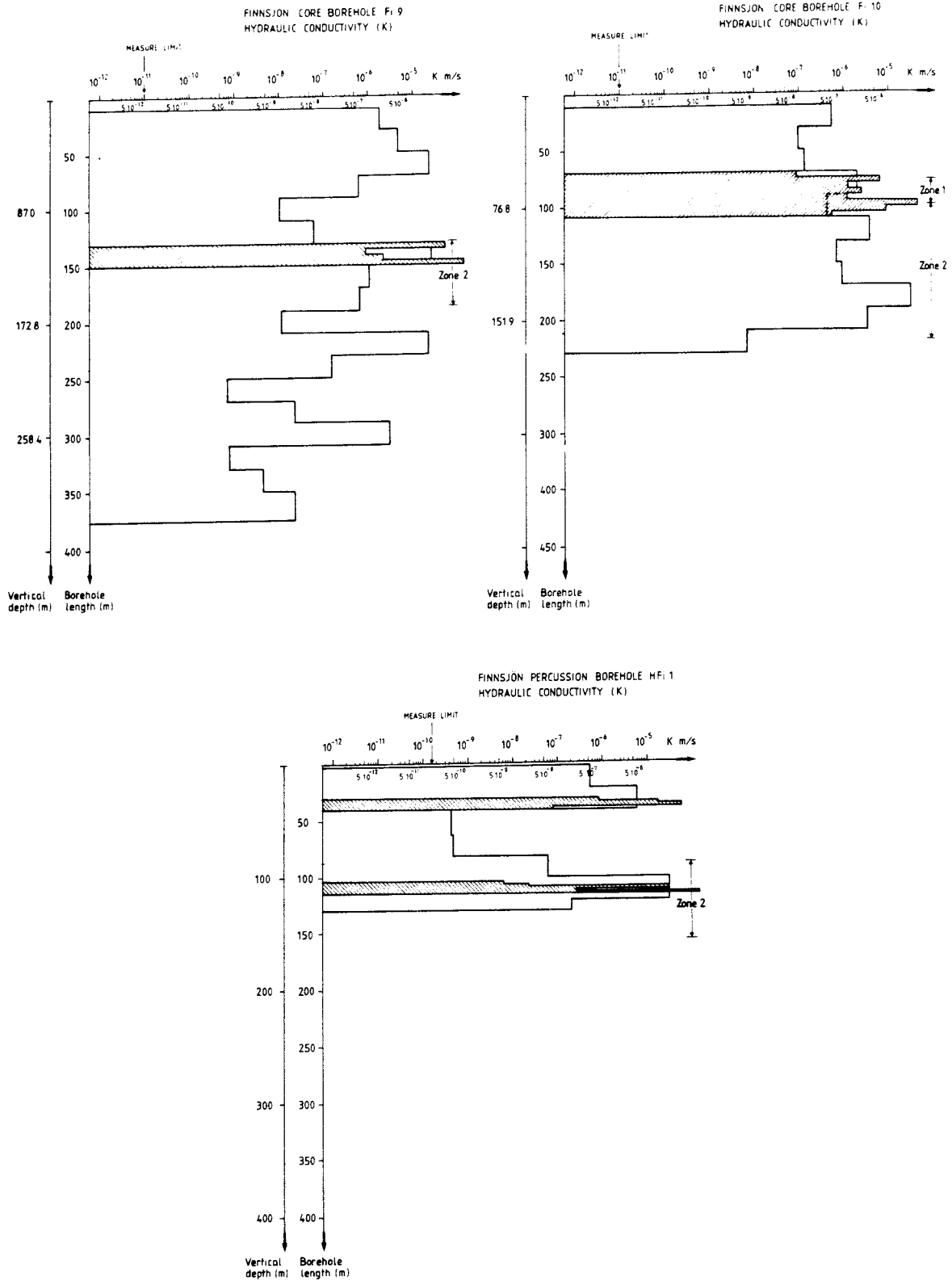


Figure 8.2 Hydraulic conductivity of the cored boreholes Fi 9 and Fi 10 and the percussion borehole HFi 1. The results from the percussion borehole is normalized from 10 m sections to 20 m sections.

Borehole Fi 9

The highest value of hydraulic conductivity in borehole Fi 9 occurs at 145-150 m ($1.3 \cdot 10^{-4}$ m/s), which is the upper part of Zone 2. Just below the bottom of Zone 2, as it is defined in figure 2.1, there is another conductivity maximum, $1.7 \cdot 10^{-5}$ m/s in the section 210-230 m. This might indicate, that a better definition of Zone 2 is to include section 210-230 m. That would give the zone a "two peaks" appearance similar to the earlier described conductivity distribution in Fi 6. The vertical width would in this case be about 86 m. Also superficially, between 70 and 90 m, there is a high conductive zone. The maximum value is $2.1 \cdot 10^{-5}$ m/s. Below Zone 2 there are two other conductivity maxima, separated by a low conductive interval. The highest value (at 290-310 m) reaches $2.6 \cdot 10^{-6}$ m/s .

Borehole Fi 10

Fi 10 penetrates Zone 1 as well as Zone 2 (figure 2.1). In fact, the major part of the borehole passes close to the intersection of the two fracture zones. This explains the appearance of the conductivity diagram with high conductivities from the top almost to the bottom. Zone 1 reaches a maximum value of $4.8 \cdot 10^{-5}$ m/s in the 5 m-section 95-100 m. The lower part of Zone 2, section 170-190 m, has a similar value, $3.8 \cdot 10^{-5}$ m/s. Another conductivity maximum occurs in the upper part of Zone 2. The vertical width of Zone 2 can be estimated to about 86 m.

8.1.4 Water injection tests. Conclusions

The Zones 1 and 2 are hydrologically important. The hydraulic conductivity for Zone 1 varies between $1.2 \cdot 10^{-6}$ and $4.8 \cdot 10^{-5}$ m/s measured at vertical depths between 57 and 76 m (only few data exist). This, together with the width of about 20 m and the steep inclination, makes the Zone 1 a locally important pathway for groundwater in an almost vertical direction. Since there are no piezometric data from the zone, the discharge - recharge pattern is unknown.

Zone 2 has a still greater water transportation capacity than Zone 1 but in the subhorizontal direction. The zone width is geologically interpreted to almost 70 m, but the water injection tests indicate, that the width might be still greater. The conductivity values (in this case data is abundant) are high, sometimes very high, although the zone is not homogeneous concerning conductivity distribution. The highest values, 10^{-5} - 10^{-4} m/s (in detailed sections), tend to occur at the upper and lower border of the zone, while there is a more low-conductive section in between, about $3 \cdot 10^{-9}$ - $7 \cdot 10^{-7}$ m/s. In table 8.2 the hydraulic transmissivity of Zone 2 (the width is defined hydraulically) calculated from four different boreholes can be studied. Also the "hydraulic" width and the vertical depth of the upper surface of the zone from the ground surface is calculated.

Table 8.2 Transmissivity (m^2/s), "hydraulic" width (m) and vertical depth (m below ground surface) of fracture Zone 2 in different boreholes.

Borehole	Transm.	Width	Depth
F1 5	$1.5 \cdot 10^{-3}$	107	115
F1 6	$3.5 \cdot 10^{-4}$	80	200
F1 9	$9.5 \cdot 10^{-4}$	86	113
F1 10	$9.8 \cdot 10^{-4}$	92	76
HFi 1	$6.6 \cdot 10^{-4}$ *	25	104

* HFi 1 only partly penetrates zone 2.

As can be seen from the table, the transportation capacity defined in this way, is very similar in most boreholes, close to 10^{-3} . (If the same width of the zone is assumed in

HFi 1 as in Fi 9, the transmissivity would probably be slightly higher than the corresponding value in Fi 9). Fi 6, however, deviates somewhat towards a lower transmissivity. This might be an effect of the greater depth of the zone in Fi 6. Since the test sections used for the definition of the zone are as long as 20 m, the zone thickness might be somewhat overestimated. However, since detailed measurements all over Zone 2 are not available in all boreholes, comparison can be made only by using the 20-m sections.

One interesting aspect of the hydrogeological character of the fracture zones is the conductivity contrast to the surrounding bedrock. This parameter is of importance when determining the water exchange between fracture zones and rock matrix. The less contrast, the greater the water exchange might be. The conductivity contrast between Zone 1 and the bedrock SE of the zone has been determined only at one point (in Fi 10) to the factor 75. In other words, the contrast is below two orders of magnitude, a rather low value. However, it should be noticed, that the contrast applies to measurements at a vertical depth of only 57 m. The contrast to NW is not known. The corresponding figures for Zone 2 are somewhat safer, since there are more data. They are accounted for in table 8.3. The contrast values are based on the hydraulic definition of the zone. The contrast is higher than for Zone 1 in most boreholes, about two-three orders of magnitude.

Table 8.3 The conductivity contrast (dimensionless) between zone 2 and the rock mass.

Borehole	Conductivity contrast zone 2/overlying rock	Conductivity contrast zone 2/underlying rock
Fi 5	350	240
Fi 6	43	570
HFi 1	6500	-
Fi 9	390	130
Fi 10	-	-

The water injection tests support the interpretation of the fracture zone geometry presented in chapter 2. However, the width of Zone 2, defined exclusively from hydraulic data, ranges between 80 and 107 m, whereas core logging and geophysical data indicate a width of about 70 m.

Figure 8.3 attempts to illustrate the distribution of high conductivity values for the section A-Å in the Brändan area (figure 2.1). The conductivity values in the different boreholes are connected to each other with guidance from geology and geophysics. This means, that the hydraulic interpretation of the fracture zone geometry in this figure is not completely independent of the other methods. All rock with a hydraulic conductivity less than $1.0 \cdot 10^{-6}$ m/s is coloured dark, whereas higher conductivity is given brighter nuances. If this figure is superimposed upon fig. 2.2, which represents the geologically interpreted fracture zone geometry of the area, a good concordance can be noticed for the inclination of the zones. The width of Zone 2, however, diverges as described above. Besides Zone 1 and 2, there are two other high conductive areas, one superficial and one below Zone 2 (only in F1 9). They represent minor fracture zones of unknown orientation.

Fig. 8.4 illustrates the conductivity variations in the rock outside the major fracture zones. A striped pattern can be seen. However, the conductivity data alone are not sufficient to determine the direction of all "conductivity layers". Therefore the information of the figure just represents one possible alternative. Some of the layers with increased conductivity represent minor fracture zones, as can be concluded from the borehole radar measurements. A thorough analysis of the borehole radar data, combined with the hydraulic conductivity and other results, might give a more detailed interpretation of the rock mass outside the major fracture zones. However, this is beyond the scope of this study.

SE

NW

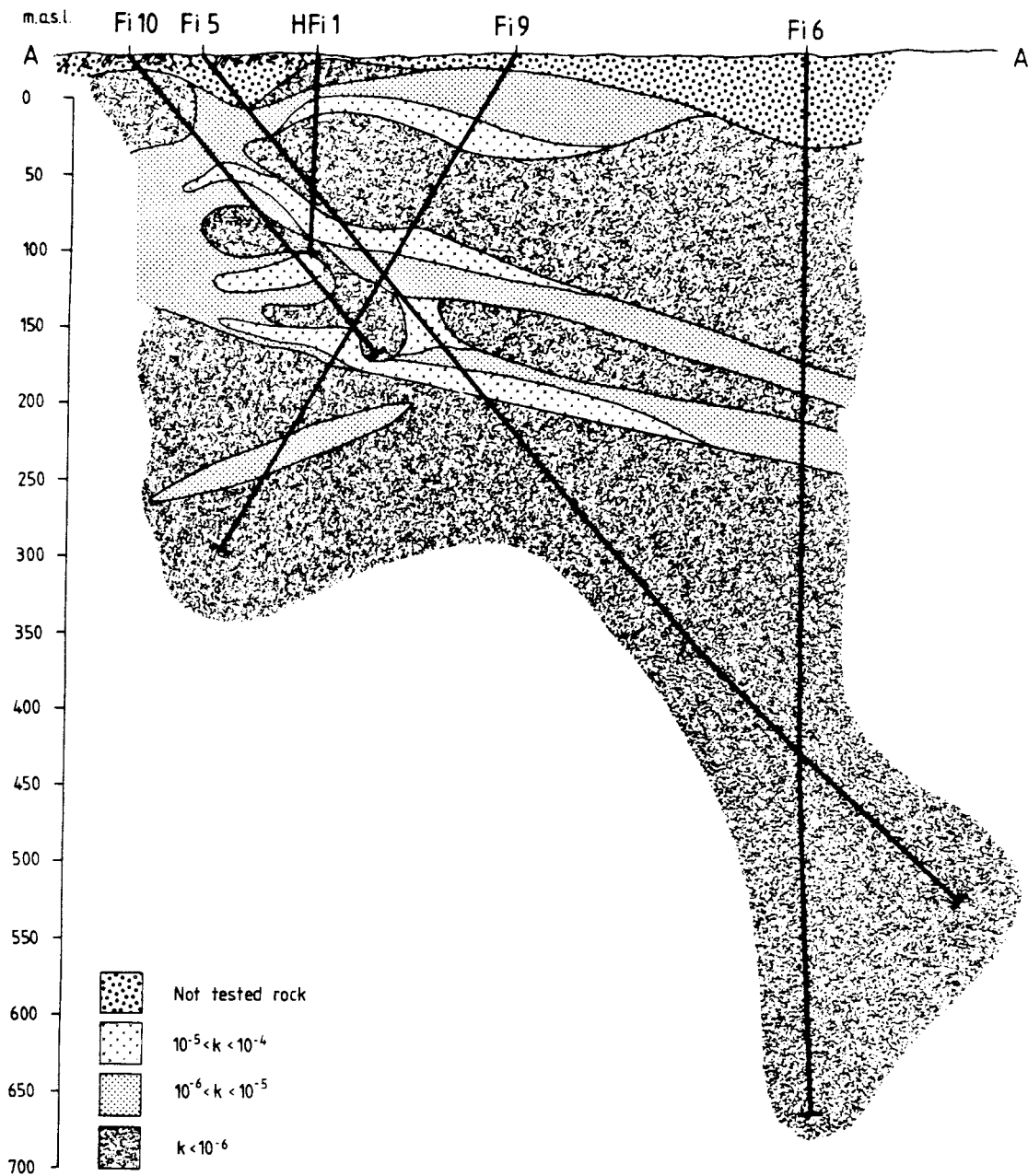


Figure 8.3 The hydraulic conductivity distribution in the fracture zones for section A-A' in the Brändan area.

SE

NW

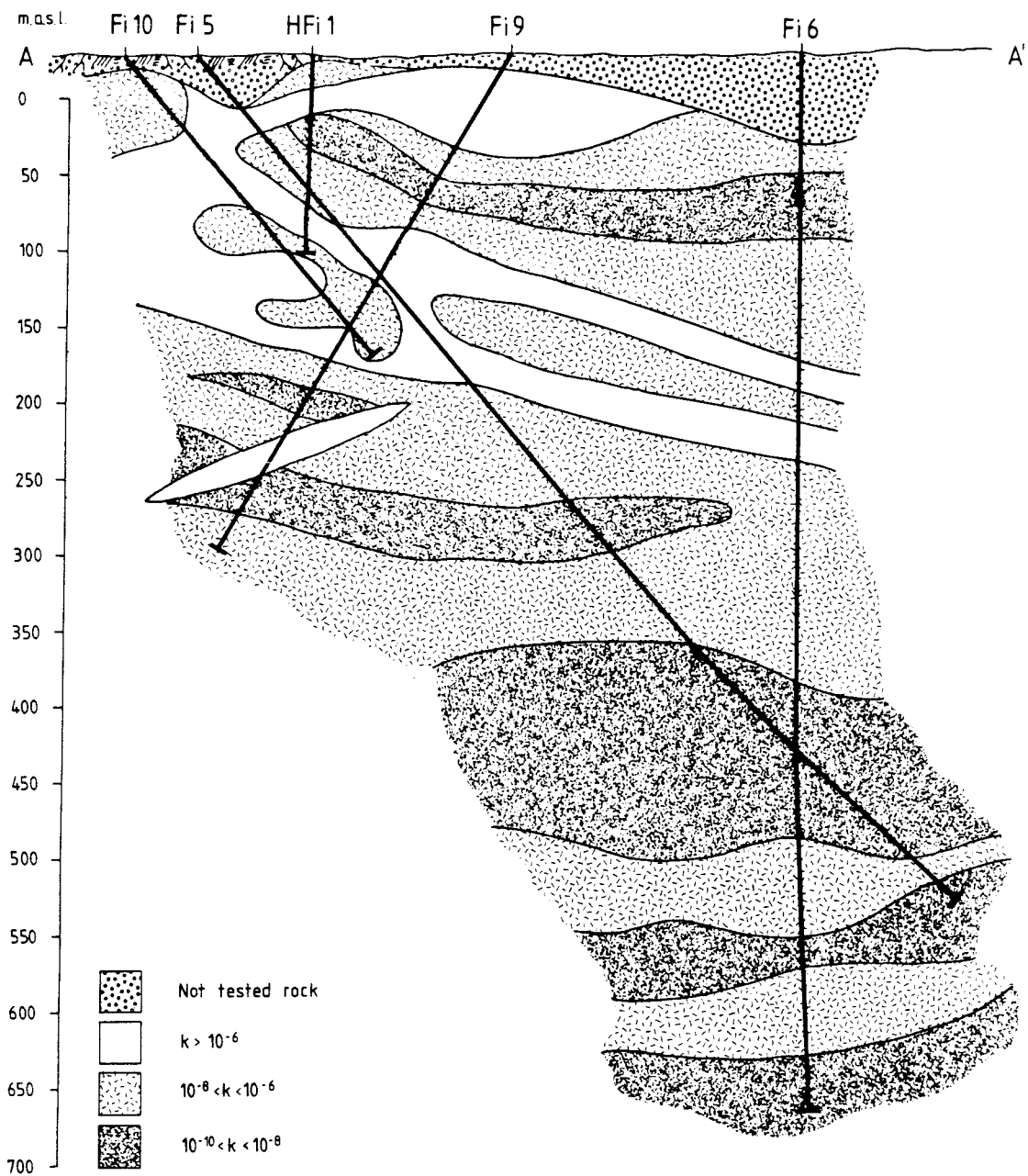


Figure 8.4 The hydraulic conductivity distribution in the rock mass outside the major fracture zones for section A-A' in the Brändan area.

8.1.5 Hydraulic interference tests by gas-lift pumping in F1 9

Gas-lift pumping is a method of flushing a borehole in order to clean it from drilling fluid and drilling debris. In the SKB site investigations, gas-lift pumping is used as a standard procedure, which follows immediately after drilling of a cored borehole. Nitrogen is used as the flushing gas in order to minimize contamination of the groundwater. Flushing a borehole is a way of pumping it. The capacity is considerable, but since the flow is pulsating, the method has not been much considered for making pump tests, where constant flow is essential. However, in this project gas-lift pumping with a modified equipment was tried as a method for interference tests with borehole F1 9 used as the pumping well. The tests were performed at three different occasions. One pumping test was made without packers in the pumping well and two tests were made within a specific borehole-section isolated between packers. Especially the tests with packers were successful. Methods and results from these tests are described below. It should be noticed, that when the concepts gas-lift pumping "with packers" and "without packers" are used in the text below, "packers" refers only to the pumping well. All observation boreholes were instrumented with packers during all three gas-lift pumpings.

8.1.6 Gas-lift pumping without packers in the pump-hole.

Methods

The equipment used for gas-lift pumping without packers is illustrated in figure 8.5. The performance of the test method is described below. A sink weight is lowered down to about 5 m above the bottom of the borehole, where a sedimented layer of drilling debris is accumulated. The debris can be rather compact, but the thickness of it seldom exceeds 5 m in a 700 m borehole. The water pressure at the level of the sink weight is calculated from the borehole length, borehole inclination, groundwater level and water density. A gas pressure exceeding the groundwater pressure at the lower part of the sink weight with about 800 kPa is produced with the gas regulator in the

gastube system. This means that gas with a certain overpressure is injected into the borehole at the bottom of the sink weight. This creates a flow of water upwards in the hole. The water flow is mostly pulsating. Especially in low-conductive boreholes, where the flow-rate of water is limited during pumping, the flow can be very intermittent. The time needed to empty two series of N_2 -gas bottles is about 10-12 hours.

A gas-lift pumping of F1 9 in January 1985 (85 01 18) was made according to this method. Because F1 9 is only 375 m long, only one series of N_2 -gas bottles was regarded necessary. The gas pressure needed to create an overpressure of 800 kPa was about 4 000 kPa. The pumping lasted for six hours. The outflow from the hole seemed to be somewhat pulsating, but repeated

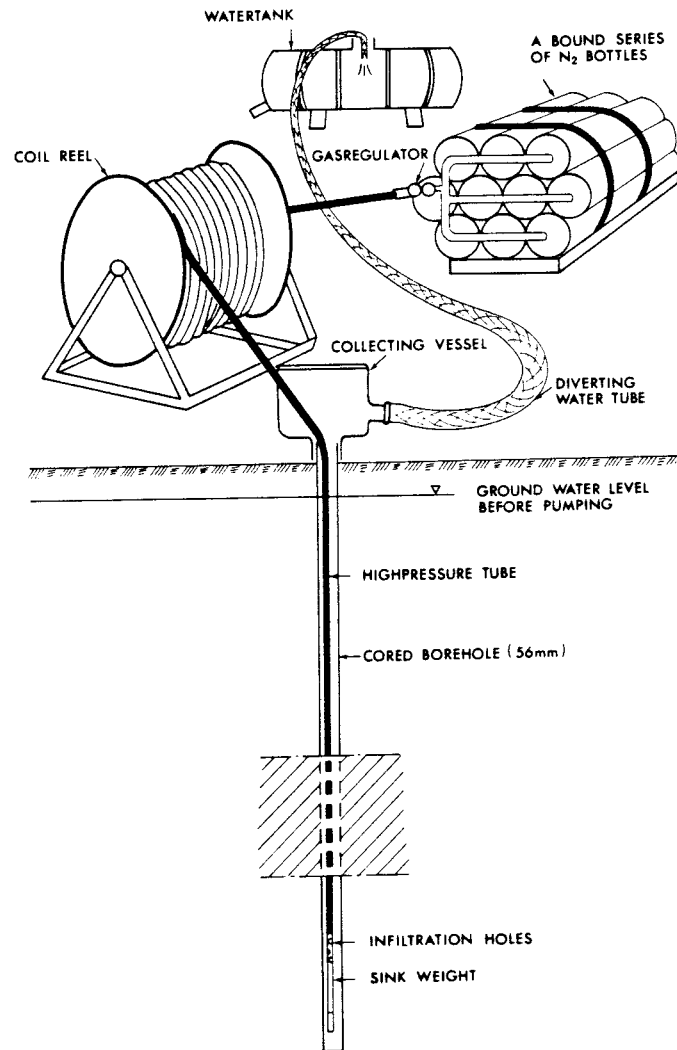


Figure 8.5 Equipment for gas-lift pumping without packers.

flow measurements gave approximately the same result, between about 94 to 100 l/min (1.57-1.67 l/sec). The flow measurements were made with a 20 l vessel and a stop watch. Between 34 and 36 m³ of water were pumped out during the six hours. Unfortunately a heavy and nonreparable leak arose on the casing vessel. Only a minor part of the water was therefore collected in the water tank. The rest infiltrated in the gravel around the casing. Because of the winter conditions with frozen ground it is difficult to estimate how much of the leaking water reached the groundwater table.

During the gas-lift pumping 10 water samples were taken for water chemical analysis and analysis of the amount of recovered drilling debris (chapters 10 and 11).

Piezometric registrations in five test sections in Fi 5 (chapter 9) and manual measurements of the drawdown in three sections in HFi 1 were made during the gas-lift pumping. No piezometric registration was obtained from Fi 6 due to instrument failure.

8.1.7 Gas-lift pumping without packers. Results

The change of piezometric head versus time for each observation section was plotted in a lin-log graph and the hydraulic conductivity was calculated according to a straight line approximation of the data curve (Jacob's method, Cooper and Jacob, 1946). The conductivity values of the sections in Fi 5 were also calculated from the recovery graph, where head change is plotted versus the expression $t/(t_p + t)$ in a lin-log graph. "t" represents time after pump stop and "t_p" the pumping time. These evaluation methods are built on the assumption, that the aquifer is homogeneous and isotropic. For interference tests in a fractured crystalline rock there are reasons to believe that the homogeneous-isotropic approach may not always be applicable. Therefore, also evaluation from log head change versus log time graphs according to a double porosity model (Streltsova, 1983 and Streltsova, 1984) was made for each tested section. This model takes into consideration the heterogeneity of the rock. A double porosity medium is

composed of two media with distinctly different hydraulic properties, the fracture system and the rock matrix. The pressure responses in these two media are illustrated in figure 8.6(1) and 8.6(2) respectively for an assumed storage ratio of 100 between matrix and fracture system (Streltsova, 1983 and Streltsova, 1984). As can be seen from the figure the curves have similar shapes, particularly the matrix curves. To obtain a unique match with field data, thus a rather long test time would be required. When the straight line method is used for interpretation in a double porosity medium, the hydraulic conductivity will be overestimated, if the analysis is made on data from the intermediate-time region (Streltsova, 1984). In the Brändan area, the double porosity model should be more applicable than the homogeneous-isotropic approach. However, when the instrumentation was made for the current tests, the fracture zone structure was not known in detail. Therefore the packer configuration was not ideal in the sense that the fracture zones were not properly isolated from the rock matrix. The packer configuration in the boreholes during the pumping tests is illustrated in figure 8.7. Several packers were placed within Zone 2 causing a similar reaction in many sections due to interconnection.

With the hydraulic conditions prevailing at the site, gas-lift pumping showed to be a suitable method for pumping tests. The flow rate was high enough to achieve a drawdown at a distance of at least 210 m. It was also sufficiently constant to permit evaluation according to the methods mentioned above. The results are, in spite of this, somewhat uncertain. The reasons for this are the reinfiltration into the pumped aquifer and the fact that the packer configuration not was perfect.

The graphs from the interference test 85 01 18 are presented in figures 8.8 - 8.10.

Pressure responses in HF1 1

Figure 8.8(1) shows the piezometric head change versus time, plotted in a log scale, for the three sections 0-35 m, 36-90 m and 91-129 m in the borehole HF1 1. Figure 8.8(2) illustrates

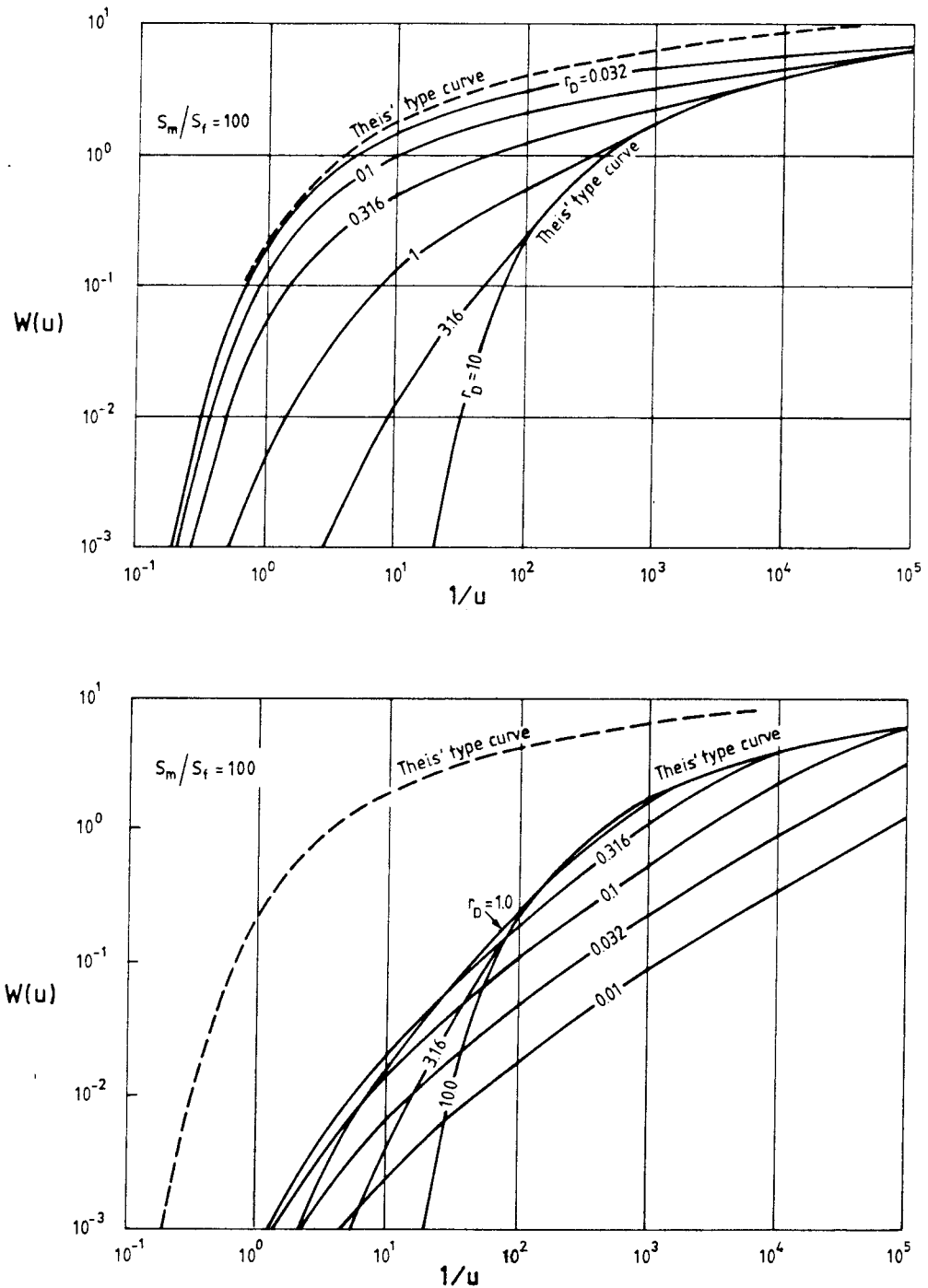


Figure 8.6 Type curves for fracture zones (1, above) and matrix (2, below) according to the double porosity model (after Streltsova, 1983 and Streltsova, 1984). $W(u)$ = Theis' well function, S = storage coeff. for matrix (m) and fracture zones (f) respectively, $r_D = r/E \cdot \sqrt{K_m/K_f}$, where r = distance from pump well to obs. hole, E = half distance between fracture zones and K = hydr. cond. for matrix (m) and fracture zones (f).

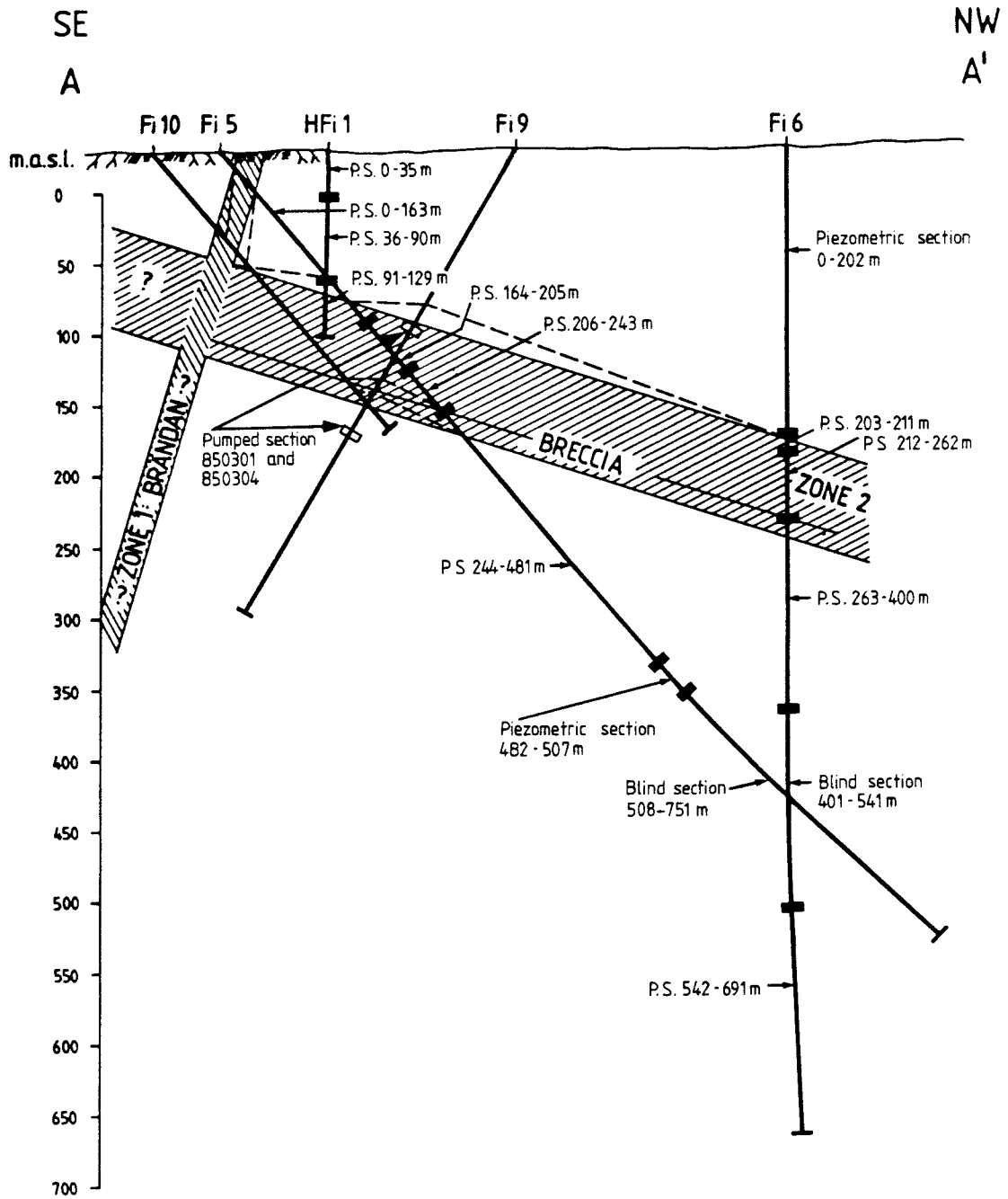


Figure 8.7 The packer configuration during the gas lift pumpings of Fi 9.

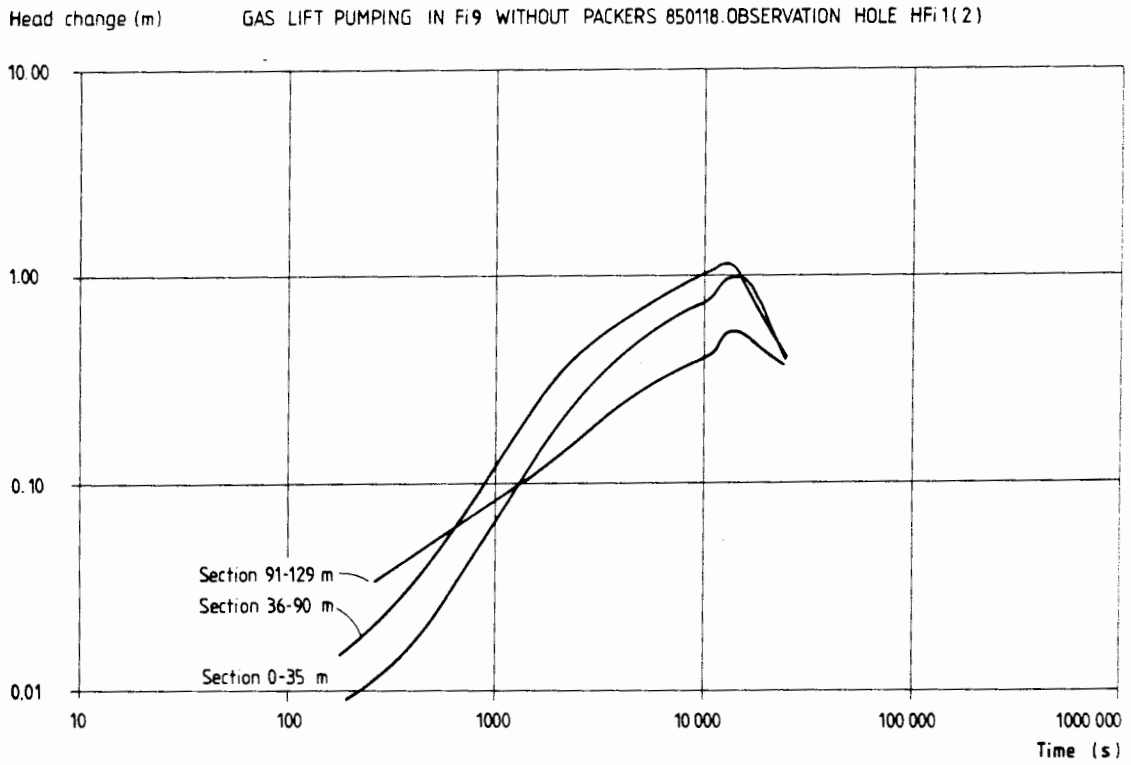
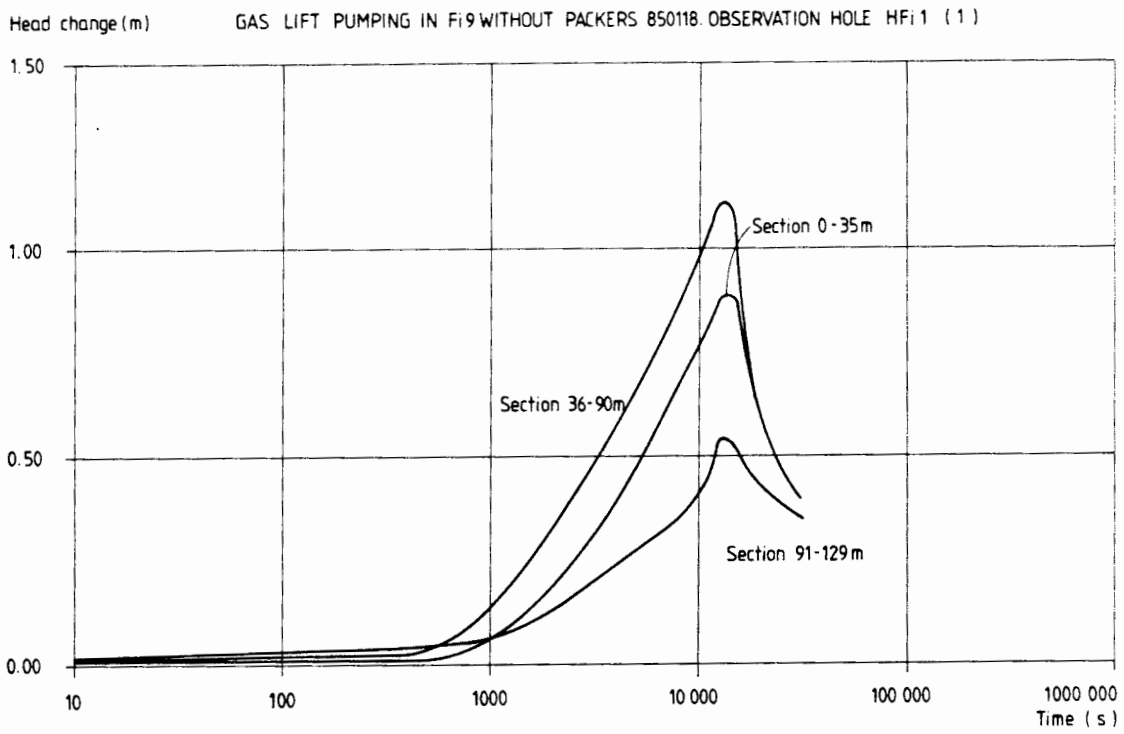


Figure 8.8 Interference test without packers 85 01 18.
Head change graphs from HFi 1.

head change versus time for the same sections in a double-logarithmic graph. The groundwater head starts slowly to decrease (the head change increases) in all sections at the beginning of the pump test. The rate of the drawdown increases after about 5 min in section 36-90 m, after 25 min in section 0-35 m and a few minutes later in section 91-129 m. After about 3 hours and 20 min the groundwater head increases again in all sections, although the pumping continues. This is probably an effect of the reinfiltration described above.

The conductivity values calculated from the gas-lift pumping tests are compared with the single-hole injection test values in table 8.4. It should be emphasized that the interference test values represent a larger volume of rock around the pumped well than the injection test values do.

Table 8.4 Hydraulic conductivity (m/s) in HF1 1 according to different test methods and evaluation models.

Section	Injection	Pumping-H	Pumping-D
0- 35	$5.9 \cdot 10^{-7}$	$9.7 \cdot 10^{-6}$	$5.3 \cdot 10^{-6}$
36- 90	$1.8 \cdot 10^{-6}$	$6.2 \cdot 10^{-6}$	$4.1 \cdot 10^{-6}$
91-129	$1.7 \cdot 10^{-5}$	$2.2 \cdot 10^{-5}$	$1.6 \cdot 10^{-5}$

H Homogeneous-isotropic evaluation model

D Double porosity evaluation model

It can be noticed, that values from the double porosity evaluation (based on the type curves shown in figure 8.6) are closest to the injection test values. The interference test evaluations result in similar values for the upper two sections, whereas the injection test values show a clear separation between all three sections.

Pressure responses in borehole Fi 5

The head change graphs from Fi 5 are shown in figures 8.9 and 8.10. A similar break in the curve as of HFi 1 occurs in the section 0-163 m after about 3 hours and 20 min from the start of pumping. The explanation is probably, as above, the reinfiltration. The calculated values of hydraulic conductivity in the five test sections according to the pumping phase and the recovery phase are compared to the conductivity calculated from the single-hole injection tests in table 8.5. For the pumping phase the two evaluation models described above have been used. In this case there is a good agreement between the injection test and the pumping phase values evaluated according to the homogeneous-isotropic model except for the lowest section. The conductivity values from the pumping phase (homogeneous approach) are slightly higher than the values from the recovery phase in all but the uppermost section.

In the log-log graph, figure 8.9(2), each section, except the uppermost, has a straight line appearance. This may indicate, that the response in these sections represents the head change in the rock matrix outside the fracture zones, cf. the type curves in fig. 8.6(2). Theoretically, the hydraulic conductivity of the matrix should be possible to calculate according to the double porosity model. Due to the relatively short test time a unique interpretation is, however, not possible in this case (the curves have no characteristic shape). If, on the other hand, the responses in the sections 164-205 m, 206-243 m and 244-481 m are assumed to represent the fracture zone, the conductivity values are possible to calculate. These values are presented in table 8.5. The evaluated K-values in these three sections are significantly lower than the injection test values. The response in section 482-507 m is interpreted as a matrix response with corresponding type curves due to the long distance from Zone 2. The hydraulic conductivity can be estimated to about $1.6 \cdot 10^{-8}$ m/s. However, this value is uncertain.

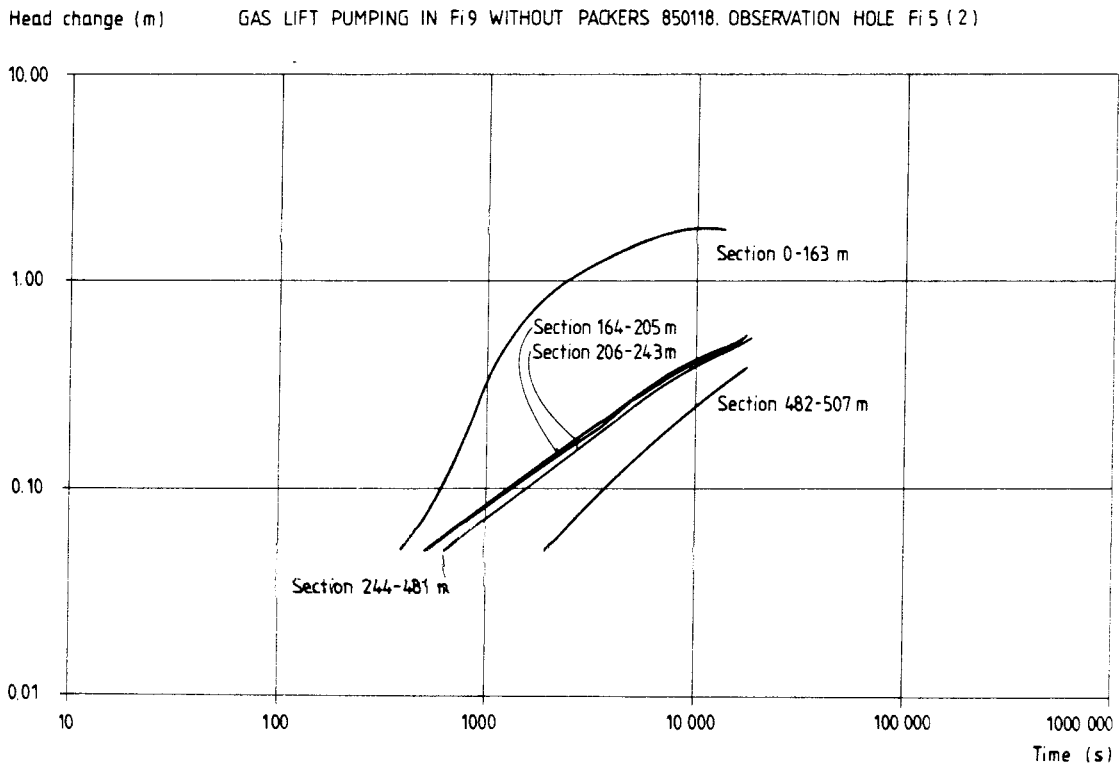
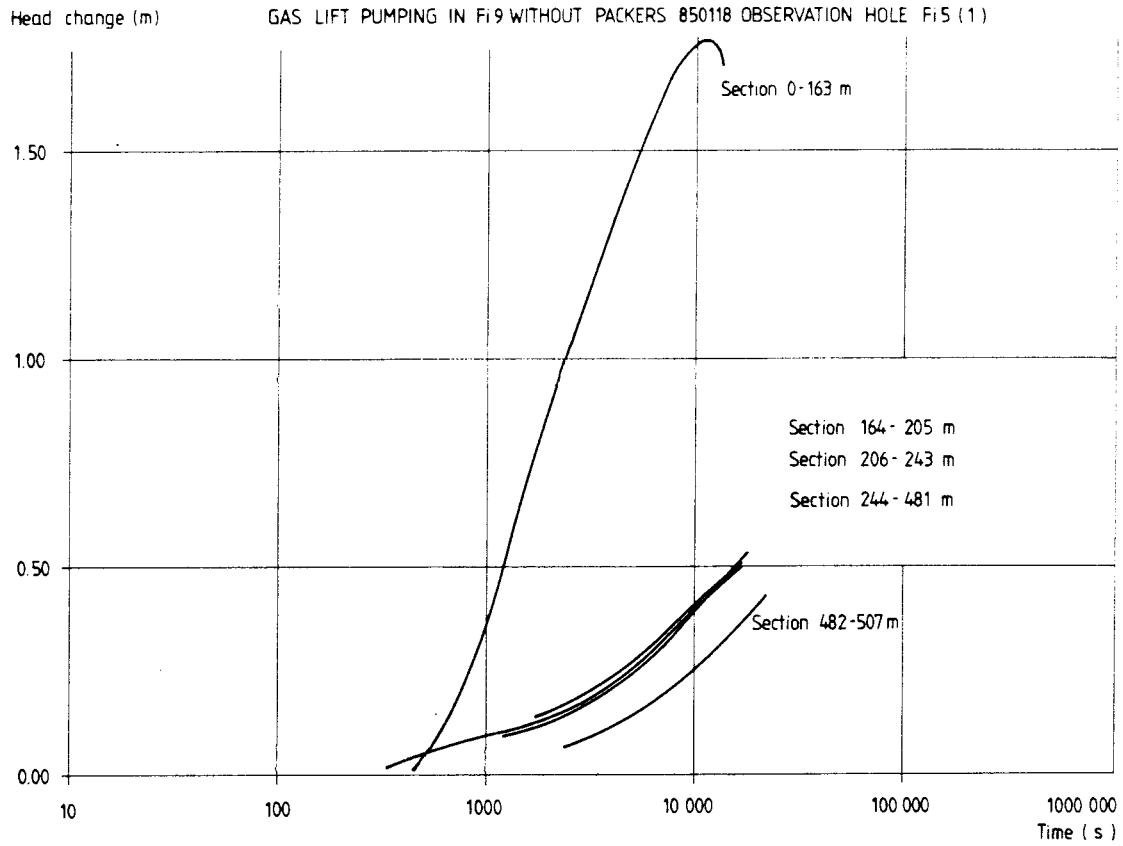


Figure 8.9 Interference test without packers 85 01 18.
Head change graphs from Fi 5.

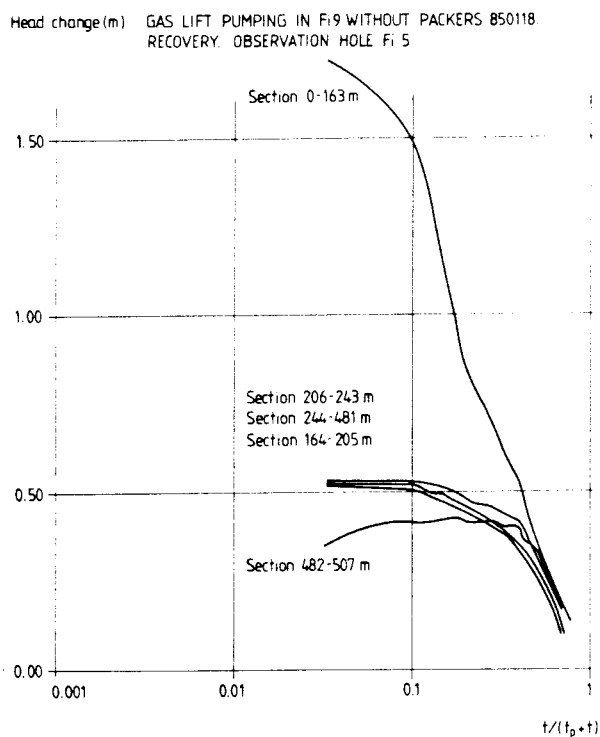


Figure 8.10 Interference test without packers 85 01 18.
Head change graph (recovery) from F1 5.

Table 8.5 Hydraulic conductivity ($\cdot 10^{-6}$ m/s) in F1 5
according to different test methods.

Section	Injection	Pumping-H	Recov.-H	Pumping-D
0-163	0.64 *	1.2	1.7	0.98
164-205	17	17	8.1	3.9
206-243	24	17	9.0	4.3
244-481	1.8	2.7	1.2	0.67
482-507	0.36	24	16	0.016

* This value is calculated for the section 50-163 m

H Homogeneous-isotropic evaluation model

D Double-porosity evaluation model

8.1.8 Gas-lift pumping, with packers. Methods

During the chemistry programme of this project, water samples were taken within Zone 2. The Uranine content of the water samples was very high, indicating that the sampled section was highly contaminated with drilling fluid (see chapter 10). In order to clean Zone 2 as effectively as possible and to regain "natural" groundwater, a "directed" gas lift pumping between packers was therefore attempted. The cleaning of the borehole was the primary aim of the pumping, but at the same time the boreholes Fi 5, Fi 6 and HFi 1 were equipped for piezometric monitoring. The purpose was to make pressure registrations, if the gas-lift pumping between packers showed to be technically sufficiently good to be used as a pumping test method.

The gas-lift pumping equipment with packers is described in figure 8.11. The procedure during pumping is similar to that from pumping without packers. The hydrostatic pressure for the level where the gas is injected into the aluminium pipe from the injected section (approximately the upper packer position) is calculated. A sufficient overpressure of gas versus the hydrostatic pressure is generated. During the pumpings described below, an overpressure of 700-1 000 kPa (recorded on the gas-regulator at the ground) was used. The gas lifts the water in the aluminium pipe to the ground surface. This creates a negative pressure in the pipe contra the aquifer. Water flows into the pipe through the infiltration holes just underneath the upper packer and is continuously transported to the ground surface. The water is collected in one or several tanks and is pumped away from the infiltration area. The ground water pressure in the pumped section of the borehole is registered during the test.

Two gas-lift pumpings according to this method were executed in March 1985 (85 03 01 and three days later, 85 03 04). The packer spacing was 85 m (150-235 m). One series of N_2 -gas bottles was emptied at each pumping. A gas dp (overpressure) of 700 kPa was used at the first occasion. The time needed to empty the gas bottles was 6 h 40 min. An almost continuous flow of approximately 1 250 l/hour (0.3472 l/sec) was measured.

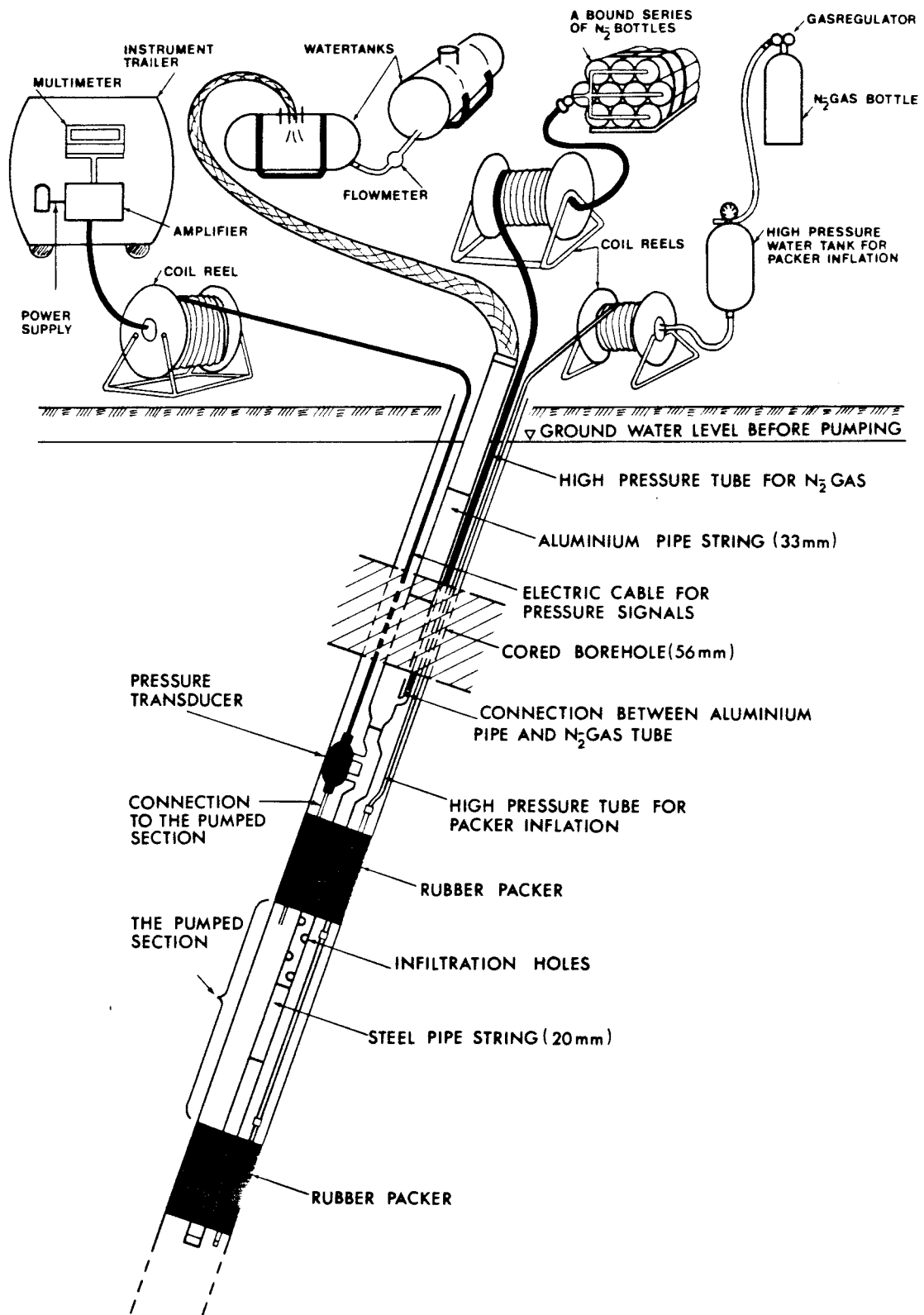


Figure 8.11 Equipment for gas lift pumping with packers.

This means, that 8.3 m^3 were emptied from the section. The corresponding figures at the second pumping were 1 000 kPa, 5 h 40 min, 1 260 l/hour (0.3500 l/sec) and 7.1 m^3 .

Water sampling for chemical analysis including the content of Uranine were performed during both pumpings. Piezometric registrations in five sections in Fi 5 and in five sections in Fi 6 were also made as well as manual measurements of the drawdown in three sections of HF1 1. Unfortunately, during the test the pressure transducer in Fi 5 failed, and therefore the results from Fi 5 are excluded.

8.1.9 Gas-lift pumping with packers. Results

Flow and pressure responses in the well borehole Fi 9

Figure 8.12 summarizes some of the results from the two gas-lift pumpings. The upper diagram shows the flow rate and the total volume. Small variations in the flow rate can be observed. The flow measurements were made intermittently. Using continuous measurements, a more detailed picture of the flow rate variations should result. The graph below shows the water pressure on a linear scale in the sealed off section during pumping. An interesting feature is the sudden pressure drop from about 1 320 kPa to about 1 180 kPa, which occurs after approximately five hours of pumping on the 1:st of March (85 03 01) and after only one hour on the 4:th of March (85 03 04). The third graph is a histogram showing the Uranine content of the pumped water versus time. The chemical conditions are discussed in chapter 10 and 11. It can immediately be concluded that the attempt to clean the borehole from drilling fluid failed, since the Uranine content raised almost continuously during the first day of pumping, from 27 g/l to 50 g/l. The level during the second day was constantly high (42 g/l). A much longer gas-lift pumping would have been necessary to achieve decreasing Uranine values.

In order to calculate the values of hydraulic conductivity in the different tested sections according to Jacob's method, head change graphs versus time in a lin-log scale were made.

In fig. 8.13(1) the head change in the pumped section 150-235 m in Fi 9 during the gas lift pumping 85 03 01 is plotted versus log time. The K-values for the different parts of the curve are calculated. The value for the flat, lower part of the curve, $3.7 \cdot 10^{-6}$ m/s, can be compared to the corresponding value from the injection tests, $4.4 \cdot 10^{-6}$ m/s. The steep part of the curve gives a conductivity value two orders of magnitude lower. The last part of the curve results in approximately the same K-value as for the first part. Figure 8.13(2) shows the corresponding graph for the pumping 85 03 04. The K-values are identical with the previous diagram for the flat

GAS LIFT PUMPING Fi 9

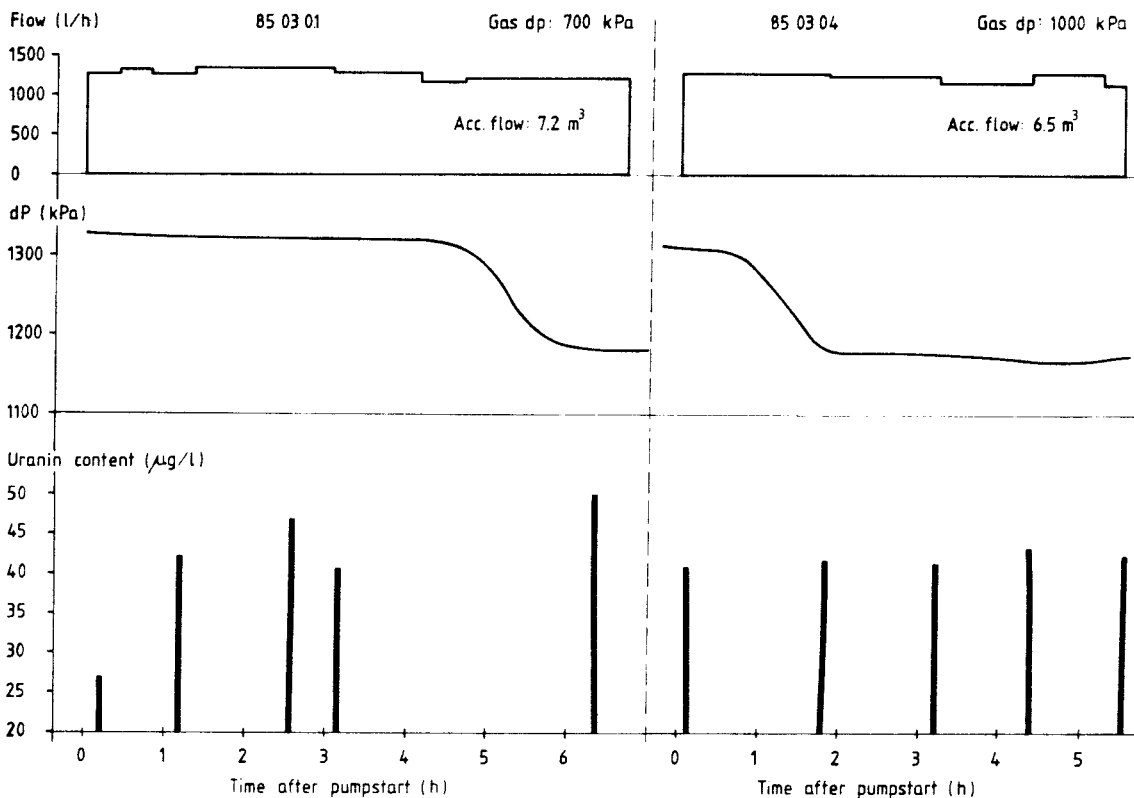
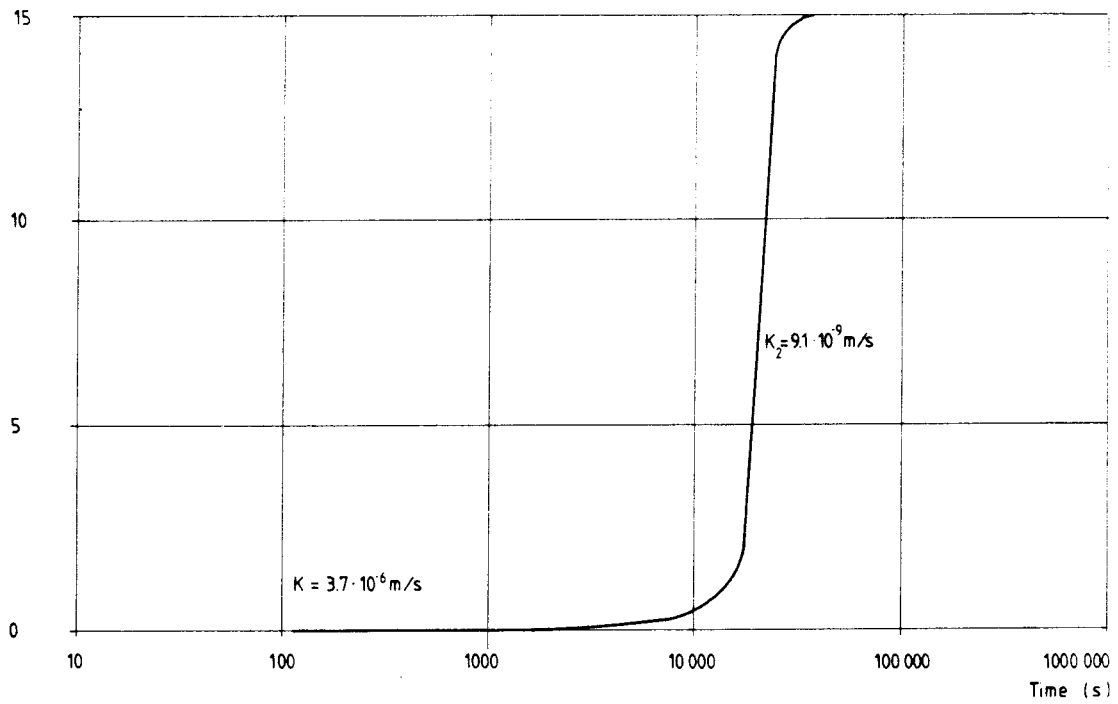


Figure 8.12 Summary of some of the results of the gas lift pumpings 85 03 01 and 85 03 04.

Head change (m) GAS LIFT PUMPING IN F19 WITH PACKERS 850301. SECTION 150 - 235 m (1)



Head change (m) GAS LIFT PUMPING IN F19 WITH PACKERS 850304. SECTION 150 - 235 m (2)

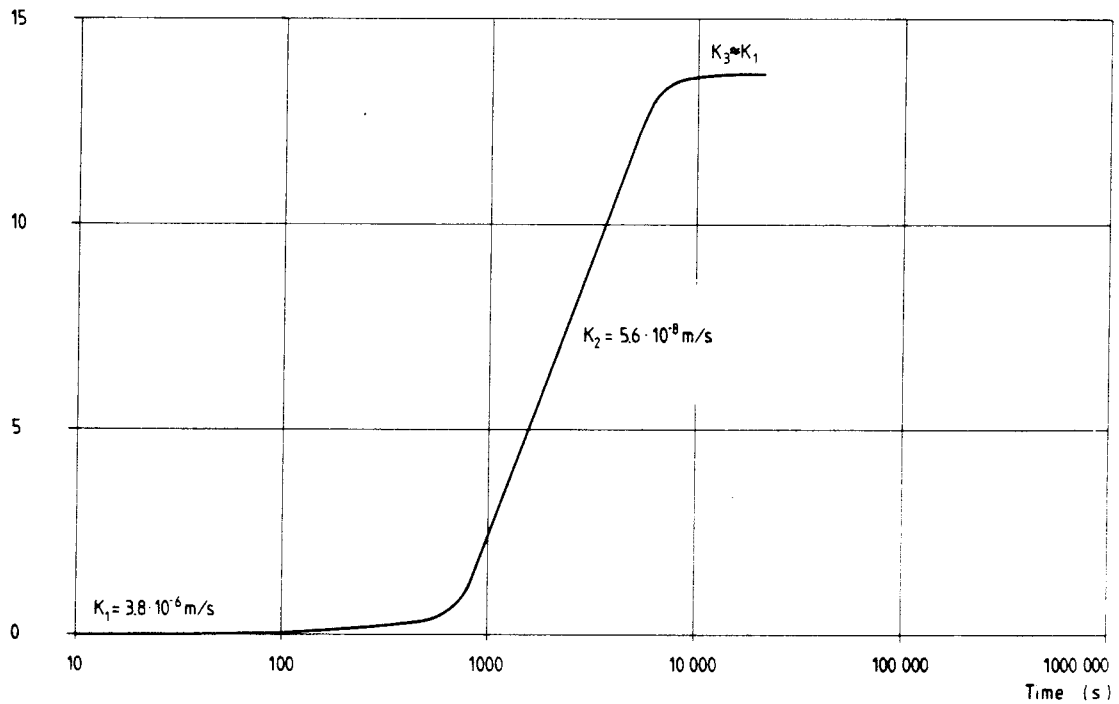


Figure 8.13 Interference test with packers 85 03 01 and 85 03 04. Head change graph from the pumped section 150-235 m in F1 9.

parts of the curves and half an order of magnitude higher for the steep part.

Pressure responses in borehole HFi 1

In figure 8.14 the head change versus time for three sections in HFi 1 during the pumping 85 03 01 are plotted in a lin-log graph 8.14(1) (for evaluation according to Jacob's method) and a log-log graph 8.14(2) (for evaluation according to the double porosity model). The curves show similar slopes, but there is a time lag for the response between the different sections. This is probably an effect primarily depending on the different distances between observation sections and the pumped section in Fi 9. The responses in HFi 1 from the test three days later are illustrated in figure 8.15. All sections react somewhat earlier than at the first test. The slopes for the respective sections are very similar except for section 0-35 m. However, a longer testing time might have resulted in a steeper slope also for this curve.

Using the double porosity model for interpretation of the test 85 03 01, the response in section 91-129 m is assumed to represent the fracture zone. The responses in section 0-35 m and 36-90 m are more difficult to analyze. They were, however, also assumed to represent fracture zones. Evaluation according to the double porosity model was not performed for the pumping 85 03 04, because the data curves have no characteristic shape to analyse with type curves. In table 8.6 the conductivity values for the three tested sections in HFi 1 according to the different test and evaluation methods are compared (also the results from pumping without packers are included).

The values from the two occasions of gas-lift pumpings with packers (evaluated with Jacob's method) are very similar. This is expected, since they represent the same volume of bedrock as well as the same test and evaluation methods. The K-values from the homogeneous-isotropic evaluation model seem to be overestimated, especially in the upper sections, compared both with the single-hole injection tests and the double porosity evaluation. The biggest difference between different methods

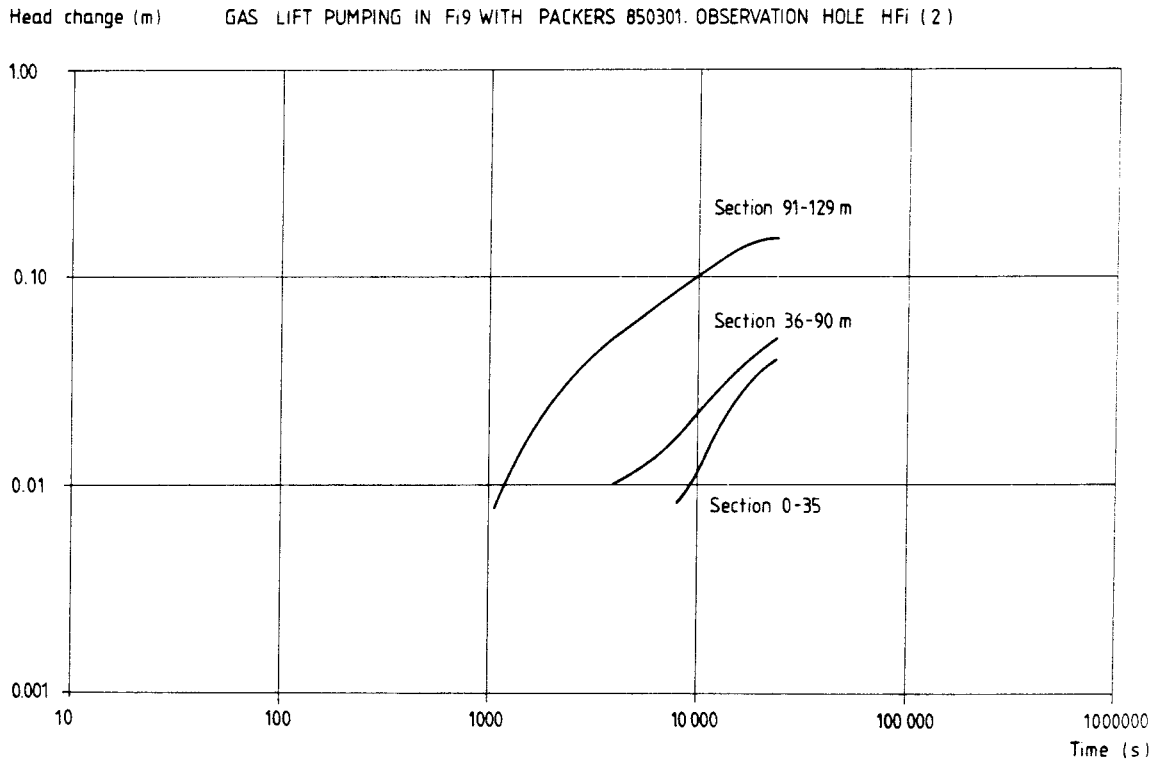
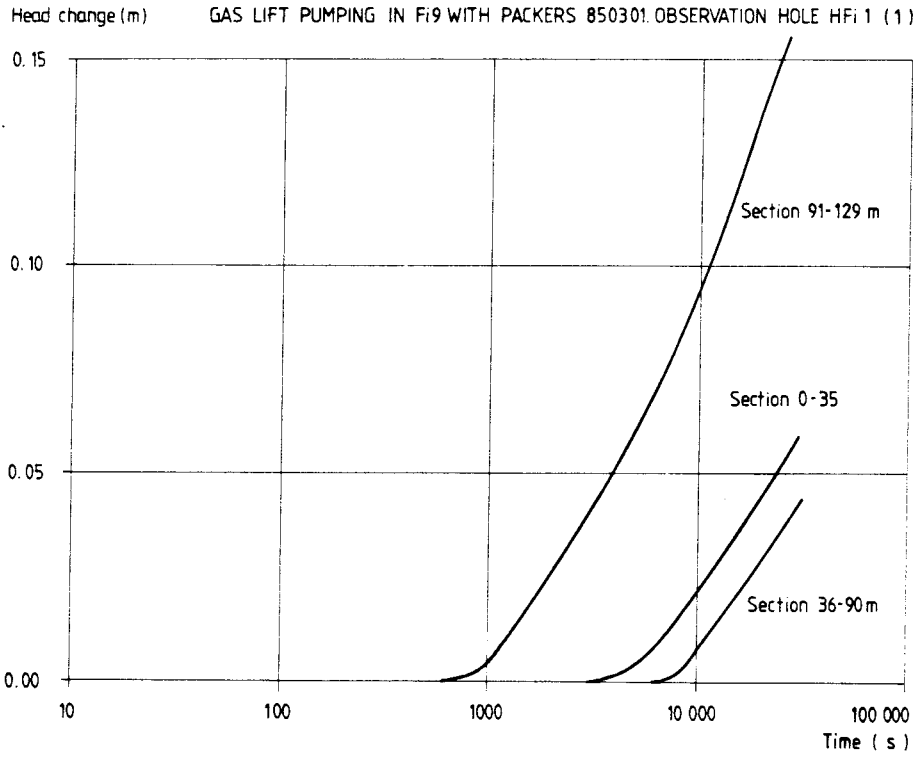


Figure 8.14 Interference test with packers 85 03 01.
Head change graphs from HFi 1.

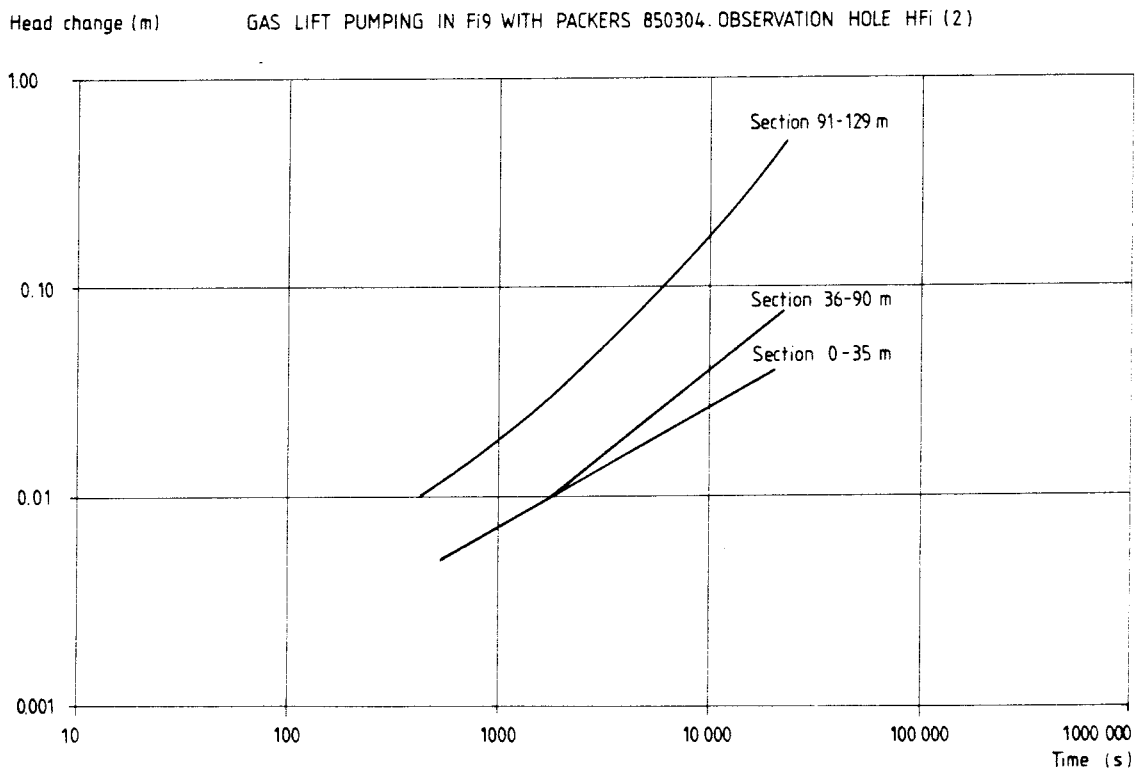
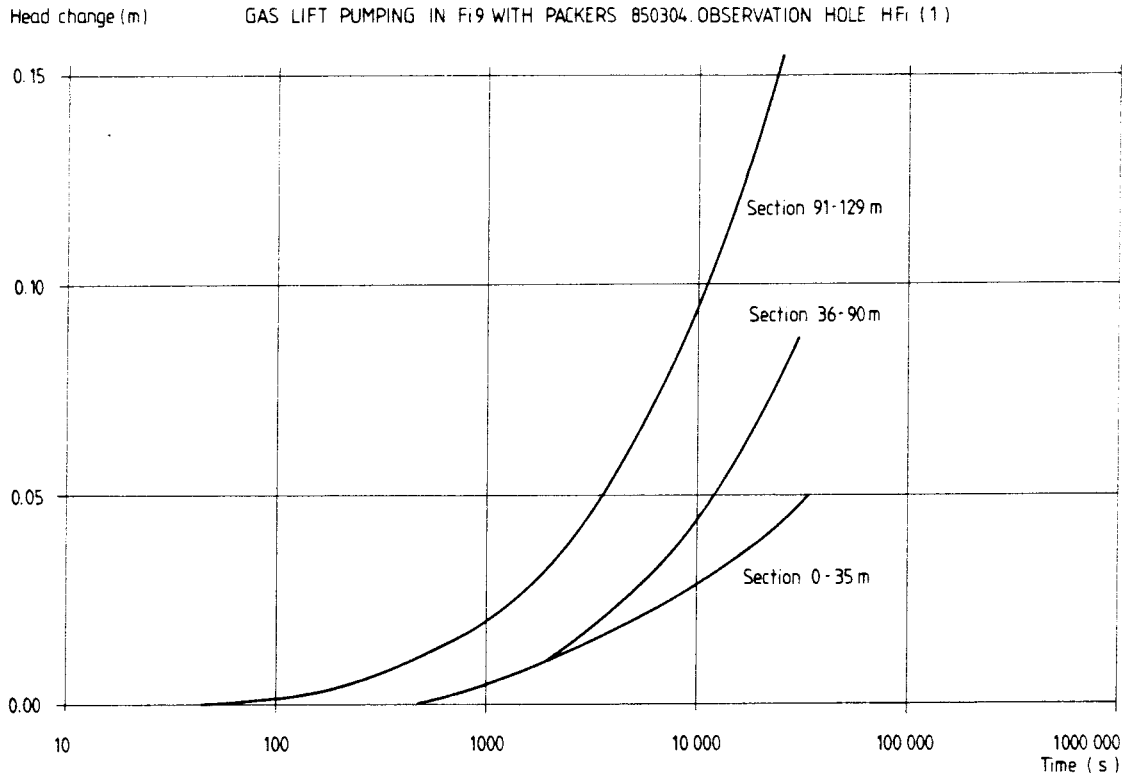


Figure 8.15 Interference test with packers 85 03 04.
Head change graphs from HFi 1.

occurs in section 0-35 m. The injection tests result in a K-value of $5.9 \cdot 10^{-7}$ m/s, whereas the gas-lift pumping with packers 85 03 04, evaluated according to Jacob's method, gives a significantly higher value, $3.8 \cdot 10^{-5}$ m/s.

Table 8.6 Hydraulic conductivity (m/s) in three sections of HFi 1 according to different test and evaluation methods.

	Section 0-35 m	Section 36-90 m	Section 91-129 m
Inj. tests	$5.9 \cdot 10^{-7}$ *	$1.8 \cdot 10^{-6}$	$1.7 \cdot 10^{-5}$
Gas lift pumping without packers (H)	$9.7 \cdot 10^{-6}$	$6.2 \cdot 10^{-6}$	$2.2 \cdot 10^{-5}$
"- (D)	$5.3 \cdot 10^{-6}$	$4.1 \cdot 10^{-6}$	$1.6 \cdot 10^{-5}$
Gas lift pumping with packers 0301 (H)	$2.4 \cdot 10^{-5}$	$1.5 \cdot 10^{-5}$	$1.2 \cdot 10^{-5}$
"- (D)	$2.3 \cdot 10^{-6}$	$1.5 \cdot 10^{-6}$	$9.6 \cdot 10^{-6}$
Gas lift pumping with packers 0304 (H)	$3.8 \cdot 10^{-5}$	$1.1 \cdot 10^{-5}$	$1.1 \cdot 10^{-5}$

* This value is calculated for the section 4-35 m

H Homogeneous-isotropic evaluation model

D Double porosity evaluation model

Pressure responses in borehole Fi 6

The pressure graphs for borehole Fi 6 are shown in figures 8.16 - 8.19. Most sections in Fi 6 exhibit straight line responses in the log-log diagram. This indicates that the test time is too short for evaluation of these sections according to the double porosity model (radial flow has not been established during the test). Therefore, only estimates of the hydraulic parameters can be performed. Assuming that the responses are representative for the fracture Zone 2 in the sections 0-202 m, 203-211 m, 212-262 m and 263-400 m, the hydraulic conductivity values shown in table 8.7 can be estimated. The response in section 542-691 m is assumed to represent the rock matrix.

An interesting detail from the pressure graphs is the section 542-691 m (figures 8.17 and 8.19). During pumping the response is slow and of small amplitude compared with the rest of the sections. After pumping, during the first phase of recovery, the water pressure continues to decrease for about 4 hours and 45 min during the first pumping and for about 4 hours and 50 min the second time. First after that, the pressure starts to build up again.

The conductivity values of the five borehole sections in Fi 6 according to different test and evaluation methods are illustrated in table 8.7. The most obvious conclusion that can be drawn from the table is the lower conductivity values from the injection tests compared with the values from the gas lift pumpings. If only the calculations from the interference tests are compared, it can be noticed, that the evaluation with the double porosity model in most sections gives lower conductivity values.

Table 8.7 Hydraulic conductivity ($\cdot 10^{-6}$ m/s) in five sections of Fi 6 according to different methods.

	Sect. 0-202m	Sect. 203-211m	Sect. 212-262m	Sect. 263-400m	Sect. 542-691m
Inj.tests	0.072 *	0.25	5.1	0.5	0.022
Gas lift pump. with packers 0301 (pump.)(H)	0.52	2.0	8.5	2.1	4.7
Gas lift pump. with packers 0301(pump.)(D)	0.57	15	2.3	0.85	0.058
Gas lift pump. with packers 0301 (recov.)(H)	1.1	32	6.3	1.6	1.9
Gas lift pump. with packers 0304 (pump.)(H)	2.0	69	13	3.2	4.6
Gas lift pump. with packers 0304 (recov.)(H)	0.8	Data loss	Data loss	1.5	1.4

* This value is calculated for the section 60-202 m

H Homogeneous-isotropic evaluation model

D Double porosity evaluation model

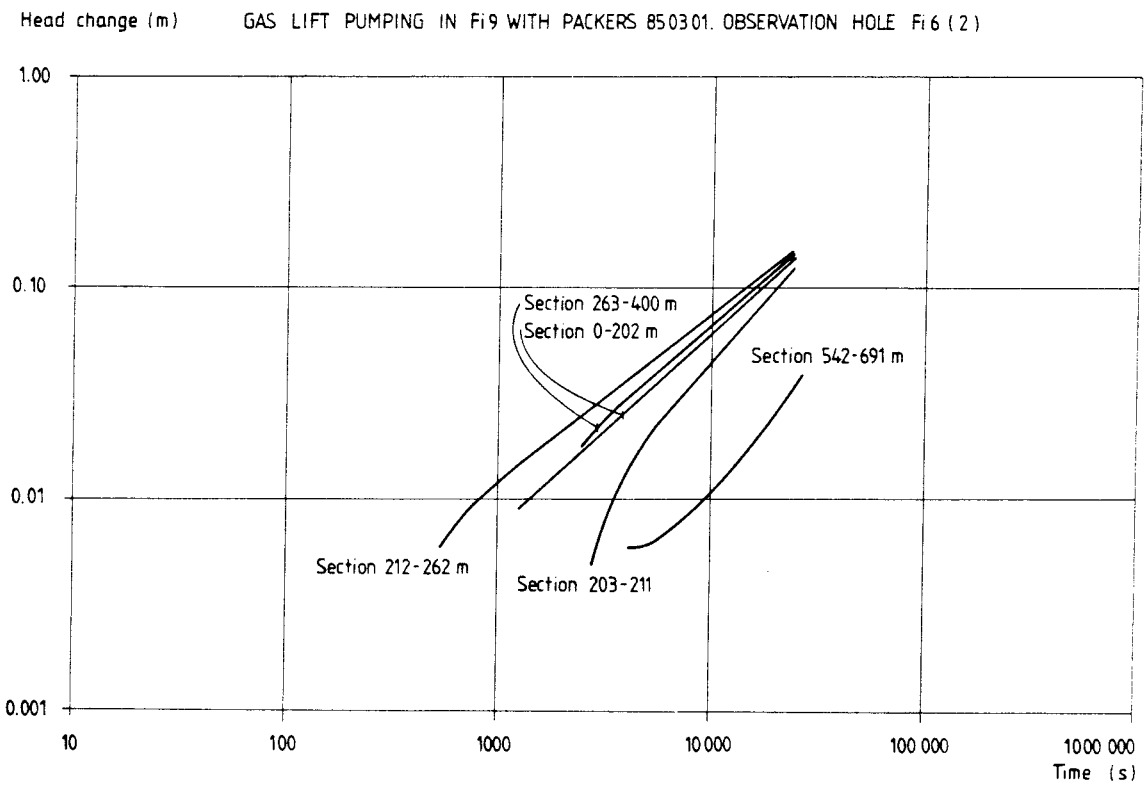
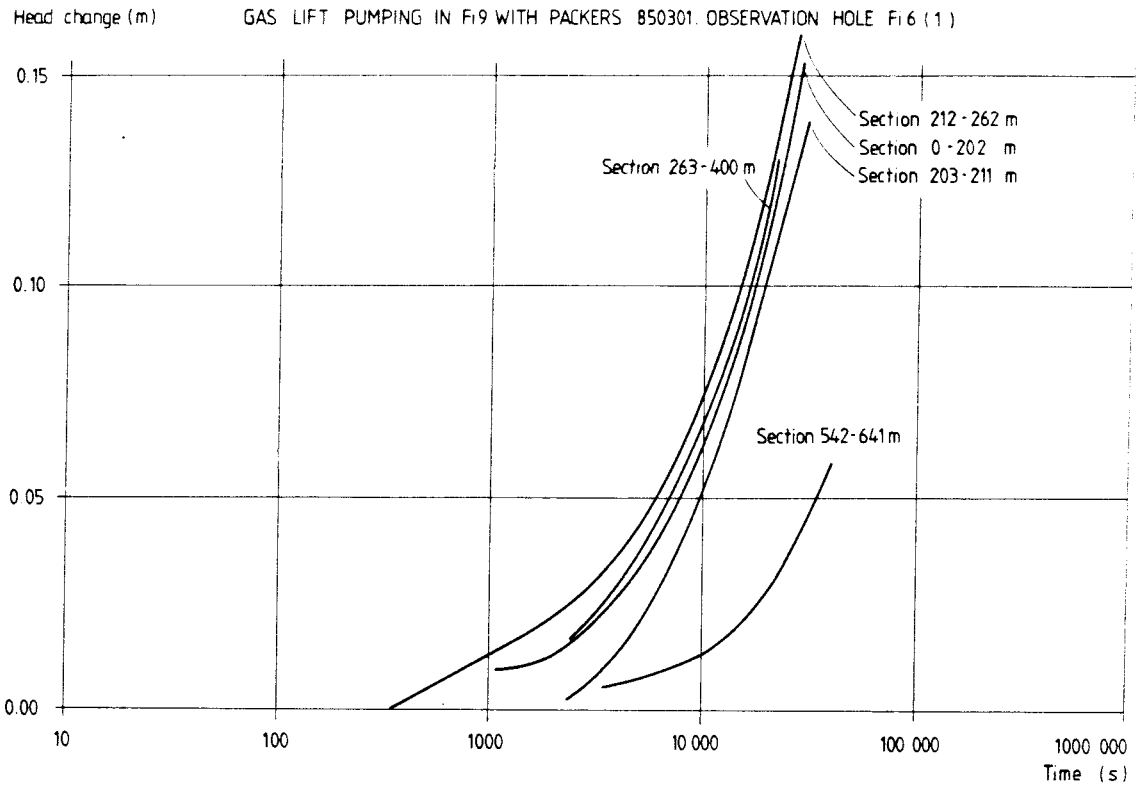


Figure 8.16 Interference test with packers 85 03 01.
Head change graphs from F1 6.

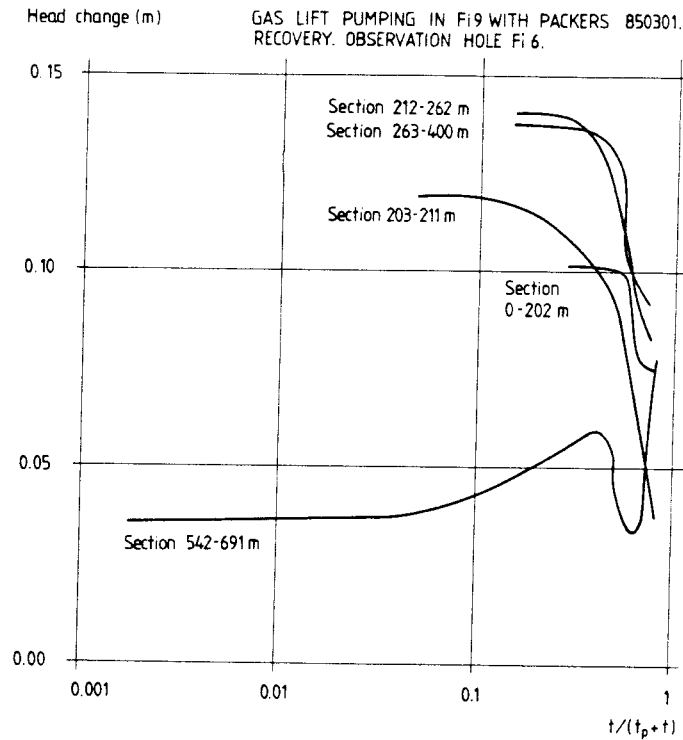


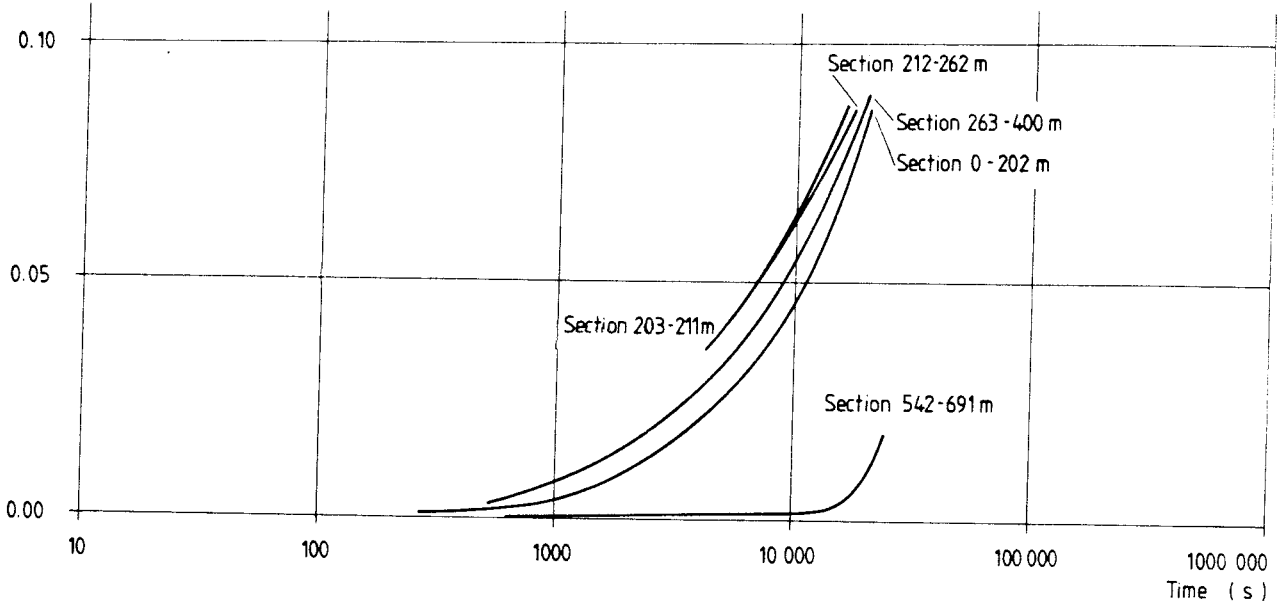
Figure 8.17 Interference test with packers 85 03 01.
Head change graph (recovery) from F1 6.

8.1.10 Interference tests. Conclusions

The following conclusions about the interference tests can be drawn:

- 1) The gas-lift pumping technique proved to be successful for performing interference tests, especially the pumping between packers.
- 2) The interference tests established hydraulic connections in Zone 2 between all five investigation boreholes at distances up to 450 m.

Head change (m) GAS LIFT PUMPING IN Fi9 WITH PACKERS 850304. OBSERVATION IN HOLE Fi 6 (1)



Head change (m) GAS LIFT PUMPING IN Fi9 WITH PACKERS 850304. OBSERVATION HOLE Fi 6 (2)

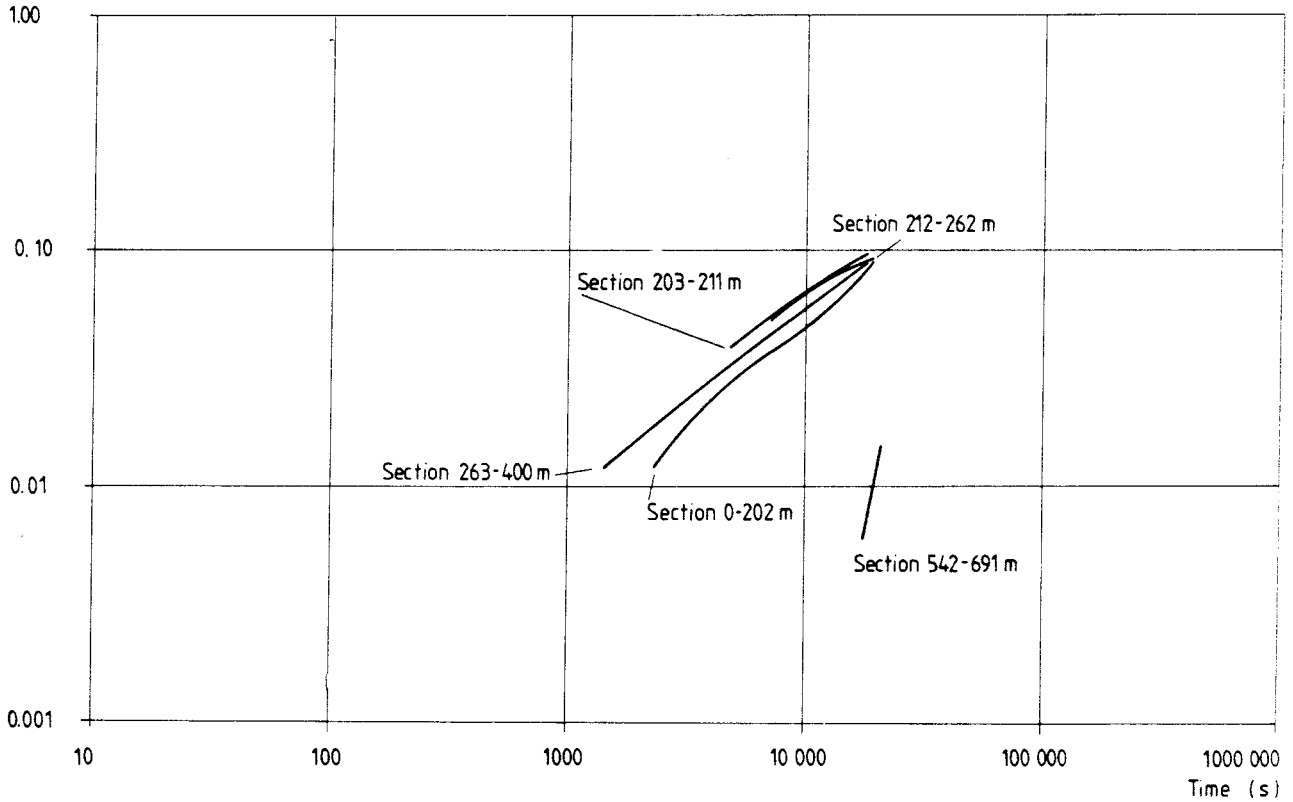


Figure 8.18 Interference test with packers 85 03 04.
Head change graphs from Fi 6.

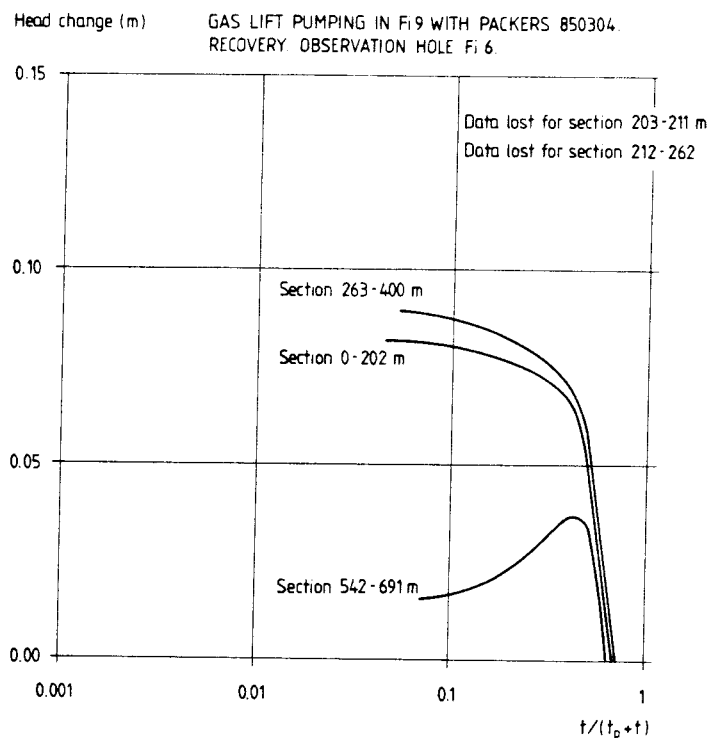


Figure 8.19 Interference test with packers 85 03 04.
Head change graph (recovery) from F1 6.

- 3) The packer configuration in relation to the fracture zone geometry was not perfect due to lack of adequate information at the time being.
- 4) The test time was too short for a complete evaluation of all observation sections according to the double porosity model.
- 5) In spite of the problems mentioned in point 3 and 4, the conductivity values interpreted according to the double porosity model were better in agreement with the injection test values.
- 6) The K-values according to Jacob's method seems to be overestimated in most sections. This is in agreement with theoretical considerations (Streltsova, 1984).

8.2 Estimates of specific storage.

The specific storage was calculated from the interference tests for all sealed off sections according to:

$$S_s = \frac{2.25 \cdot K \cdot t_0}{r^2} \quad (8-3), \text{ Cooper and Jacob (1946)}$$

where S_s = specific storage coefficient (m^{-1})

K = hydraulic conductivity of the section (m/s)

t_0 = time for intersection of head change curve with the abscissa in a lin-log graph (s)

r = distance from pump well to obs sect. (m)

The sections in HFi 1 and Fi 5 were calculated using the K-values determined with Jacob's method from the gas-lift pumping without packers, whereas for the sections in Fi 6 the corresponding K-values from the pumping with packers 85 03 01 were used.

The results are illustrated in table 8.8 and figure 8.20, which is a crossplot of hydraulic conductivity versus specific storage in a log-log graph.

Since the values of hydraulic conductivity according to the evaluation with Jacob's method are somewhat doubtful, the S_s -values suffer from the same shortcomings. Therefore, S_s -values were also calculated according to the double porosity evaluation model. Using this model, the specific storage coefficient is calculated as follows:

$$S_s = \frac{4 \cdot K \cdot t_m}{r^2} \quad (8-4), \text{ Walton (1970)}$$

where t_m = the time value at the match-point in the log-log diagram (s)

(The other symbols as in 8-3.) Since there are some uncertain-

ties about the interpretation of the K-values, as mentioned above, the S_s -values for some sections are excluded. The calculated values of specific storage are illustrated in table 8.9 and figure 8.20.

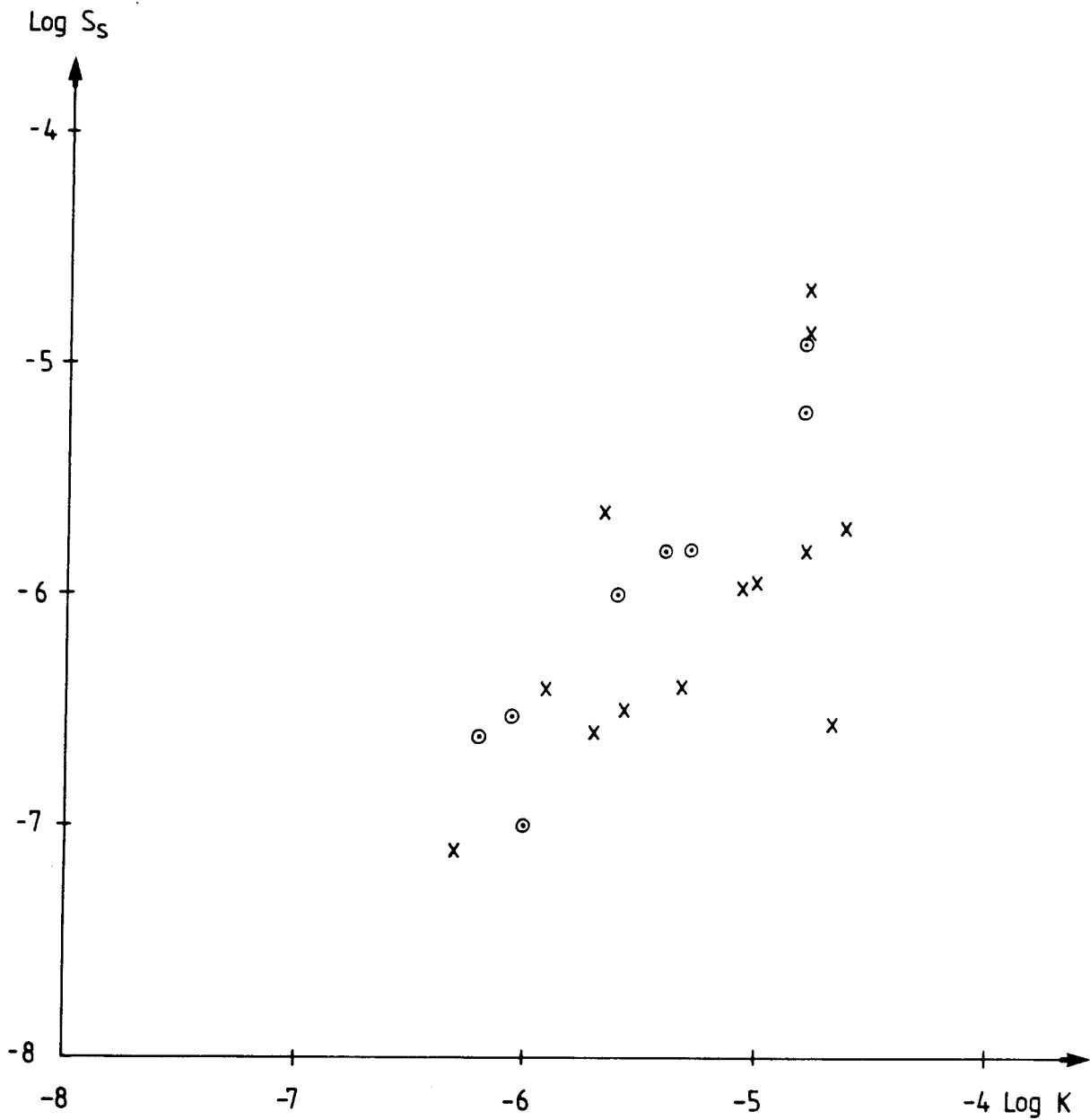
Table 8.8 Specific storage coefficient for sections in HFi 1, Fi 5 and Fi 6. Homogeneous-isotropic evaluation.

Borehole	Section m	Specific storage m^{-1}
HFi 1	0- 35	$1.2 \cdot 10^{-6}$
HFi 1	36- 90	$1.6 \cdot 10^{-6}$
HFi 1	90-129	$2.9 \cdot 10^{-7}$
Fi 5	0-163	$4.1 \cdot 10^{-7}$
Fi 5	164-205	$2.2 \cdot 10^{-5}$
Fi 5	206-243	$1.4 \cdot 10^{-5}$
Fi 5	244-481	$3.2 \cdot 10^{-7}$
Fi 5	482-507	$2.0 \cdot 10^{-6}$
Fi 6	0-202	$7.9 \cdot 10^{-8}$
Fi 6	203-211	$2.5 \cdot 10^{-7}$
Fi 6	212-262	$1.1 \cdot 10^{-6}$
Fi 6	263-400	$2.3 \cdot 10^{-6}$
Fi 6	542-691	$4.1 \cdot 10^{-7}$

If only those borehole sections which are clearly situated within Zone 2 are accounted for (90-129 m in HFi 1, 164-205 m and 206-243 m in Fi 5, 203-211 m and 212-262 m in Fi 6), the range of the specific storage coefficient for Zone 2 is about $3 \cdot 10^{-7} - 3 \cdot 10^{-5} m^{-1}$ according to the homogeneous-isotropic evaluation and about $1 \cdot 10^{-5} - 4 \cdot 10^{-4} m^{-1}$ using the double-porosity evaluation model.

Table 8.9 Specific storage coefficient for sections in HF1 1, F1 5 and F1 6. Double porosity evaluation.

Borehole	Section m	Specific storage m^{-1}
HF1 1	0- 35	$1.7 \cdot 10^{-6}$
HF1 1	36- 90	$1.5 \cdot 10^{-6}$
HF1 1	91-129	$1.3 \cdot 10^{-5}$
F1 5	0-163	$9.2 \cdot 10^{-8}$
F1 5	164-205	-
F1 5	206-243	-
F1 5	244-481	-
F1 5	482-507	-
F1 6	0-202	$2.4 \cdot 10^{-7}$
F1 6	203-211	$6.3 \cdot 10^{-6}$
F1 6	212-262	$9.9 \cdot 10^{-7}$
F1 6	263-400	$3.0 \cdot 10^{-7}$
F1 6	542-691	-



x = Homogeneous-isotropic evaluation model

o = Double porosity evaluation model

Figure 8.20 Cross-plot of specific storage coefficient, S_s , versus hydraulic conductivity, K , according to homogeneous-isotropic and double porosity evaluation models.

9. PIEZOMETRIC MEASUREMENTS

9.1 Background

When this project started in October 1984, there were no earlier made piezometric registrations in the Brändan area. In order to obtain data of the natural groundwater heads at different depths, piezometric equipments were installed in F1 5 and F1 6. Piezometric monitoring was also made during hydraulic events caused by drilling, pumping and injecting water.

9.2 Equipment

The piezometric equipment is thoroughly described in Almén et al. (1983). The main components can be studied in figure 9.1. With a system of packers, five different sections in the borehole can be sealed-off and the groundwater head in each section measured by scanning. The number of packers used can exceed five, but measurements are possible in a maximum of five sections. The packer spacing can be chosen arbitrarily.

When a measurement is to start, the power to the probe is automatically switched on, and a solenoid valve opens. Hereby a connection is established by a pressure tube to the first measurement section. (All other connections are closed.) After a few seconds, two measurements are subsequently made and the values are sent to the microcomputer (so called "Piezomac"). The Piezomac compares the two values, and one is accepted, if the difference is within a certain range. Then the first valve closes and the second opens etc. The time between measurements (scan time) is optional, between 1 minute and 17 hours. The measurement range is 500 kPa for the transducer used and the serial measurement values are obtained at a resolution of 0.03 kPa (0.003 m watercolumn). Since the probe is situated approximately 20 m below the groundwater table in the borehole (far from the sealed off sections), the measured values do not represent the hydrostatic pressure in the sections (with the exception of the one between the groundwater table and the uppermost packer). Instead they represent the pressure relations

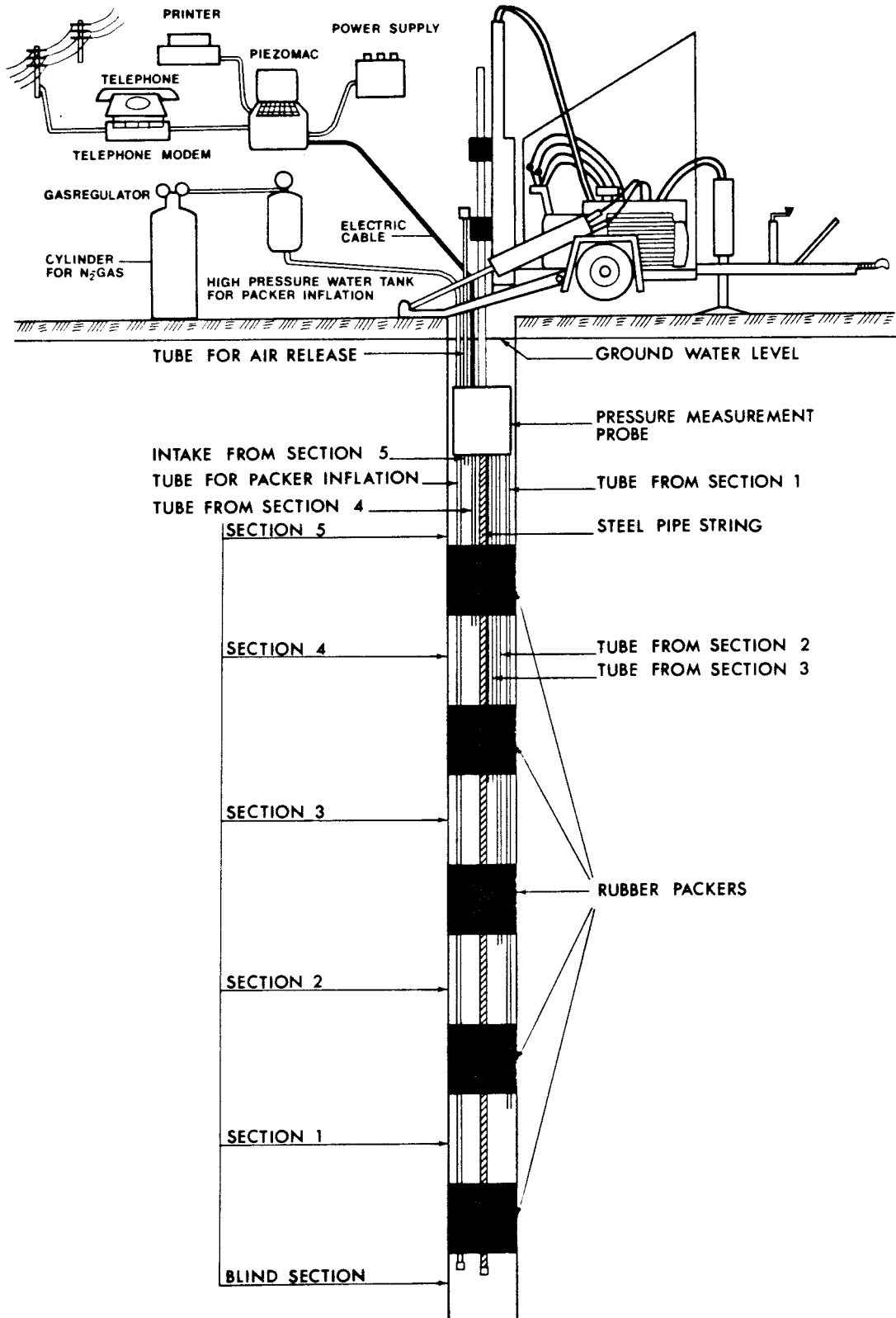


Figure 9.1 Equipment for piezometric measurements.

between the different sections, if the hydrostatic pressure increase with depth is excluded. Assuming, that there are no density variations with depth in the aquifer, the pressure values can be recalculated to groundwater head (m.a.s.l.).

The piezometric data are stored in the piezomac and transferred either to a printer, a tape or via a telephone modem to a macrocomputer in the office for further treatment.

9.3 Methods

Based on existing data from core logging, geophysical logging and water injection tests, five sections in each borehole were chosen for piezometric measurements. The purpose was to isolate different "units" in the bedrock from each other, mainly presumed fracture zones of high hydraulic conductivity from more undisturbed rock. The instrumentation was completed at the end of October 1984 and the measurements started the last of October (85 10 31) in Fi 5 as well as in Fi 6. The selected measurement sections are illustrated in figure 9.2 and in table 9.1. With the more detailed knowledge of the geology of the area, which exists today, the packer spacing would have been chosen somewhat differently. As can be seen in the table, the packers in Fi 6 were moved 10 m upwards at one occasion due to a suspicion, that the lowermost packer had been placed in the middle of a minor fracture zone. This was confirmed by later investigations.

Before packer inflation, measurements were made during 8 days in Fi 5 and 4 days in Fi 6 to achieve stable pressure values after the disturbance of the pressure conditions caused by the lowering of the equipments into the boreholes. The pressure values before inflation are used in order to check if valves, tubes etc. are correct, or if there are density variations or streaming water along or across the borehole. The pressure values from the different sections before packer inflation should be identical if no instrumental errors exist, if no density differences with depth occur in the hole and if there is no natural strong flow of water in the borehole.

Table 9.1 Piezometric sections in Fi 5 and
Fi 6 (m below top of casing).

Fi 5	Fi 6 841031-850219	Fi 6 850220-850417
0 - 163	0 - 212	0 - 202
164 - 205	213 - 221	203 - 211
206 - 243	222 - 272	212 - 262
244 - 481	273 - 410	263 - 400
482 - 507	411 - 551 *	401 - 541 *
508 - 751 *	552 - 691	542 - 691

* = "blind" section (i.e. no measurements are made).

The values before packer inflation can also be used as a reference level, which is compared to the measured values after packer inflation (section 9.4).

Precipitation and atmospheric pressure affect the piezometric pressure and was therefore measured during the project. A Hellman gauge was used as a pluviograph and a mechanical barometer registered the pressure. Also a piezometric probe was placed upon the ground for double-checking the atmospheric pressure. The pressure values from this probe were used to subtract the atmospheric pressure from the piezometric pressure. The piezometric graphs therefore represent piezometric pressure values (recalculated to head values), which are corrected for the atmospheric pressure variations.

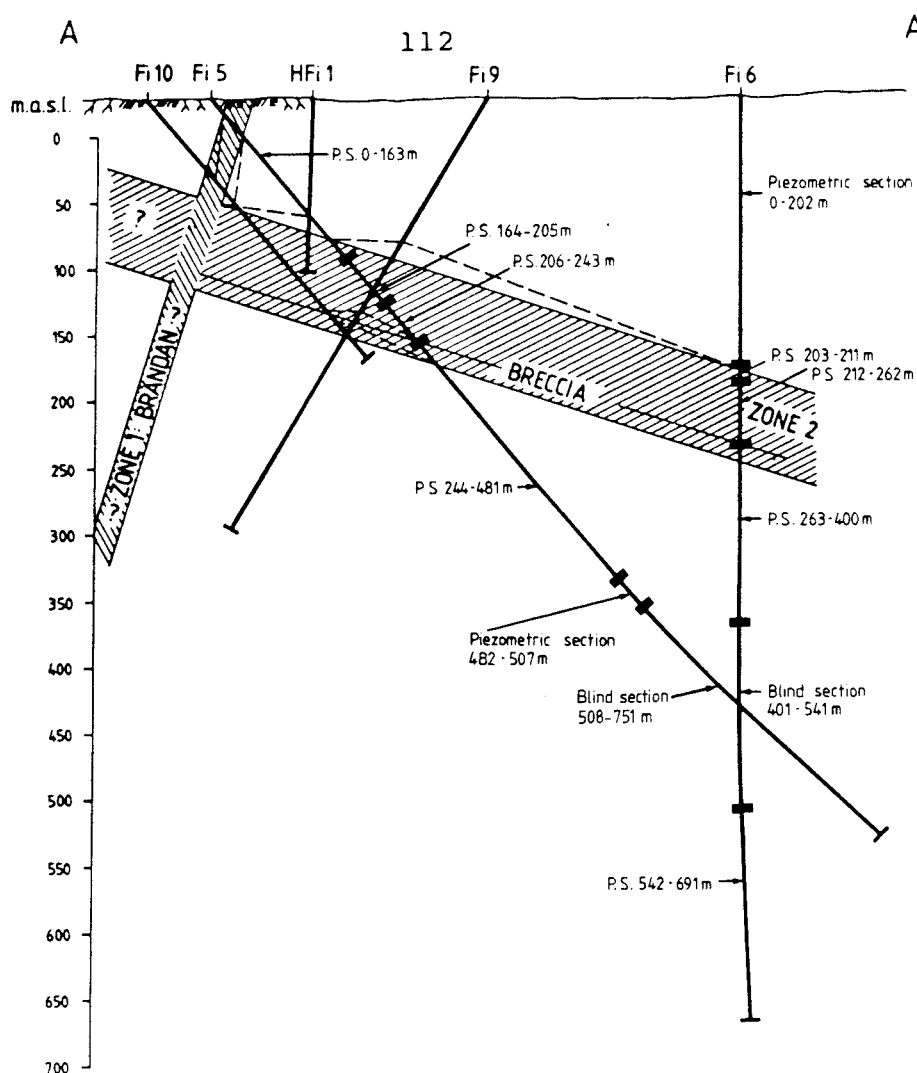


Figure 9.2 Packer configuration during the piezometric measurements.

9.4 Results

The resulting data were stored as printer lists and also in a computer. This made plotting of graphs of the type shown in the figures 9.3, 9.4, 9.6 and 9.7 possible. The head values in the graphs are given in metres above sea-level (m.a.s.l.). The values are only approximately correct, since the pressure transducers were not calibrated towards independent values of the water column above the pressure transducers (level of groundwater table). Measuring of the groundwater table reveals, that the error at the beginning of December 1984 is about -0.2 m for Fi 5 and about + 1.0 m for Fi 6. However, the transducer in Fi 5 and especially the one in Fi 6 were also drifting with time. One month later the error had grown to about -0.8 m in Fi 5 and to 3.8 m in Fi 6. A big "jump" occurs

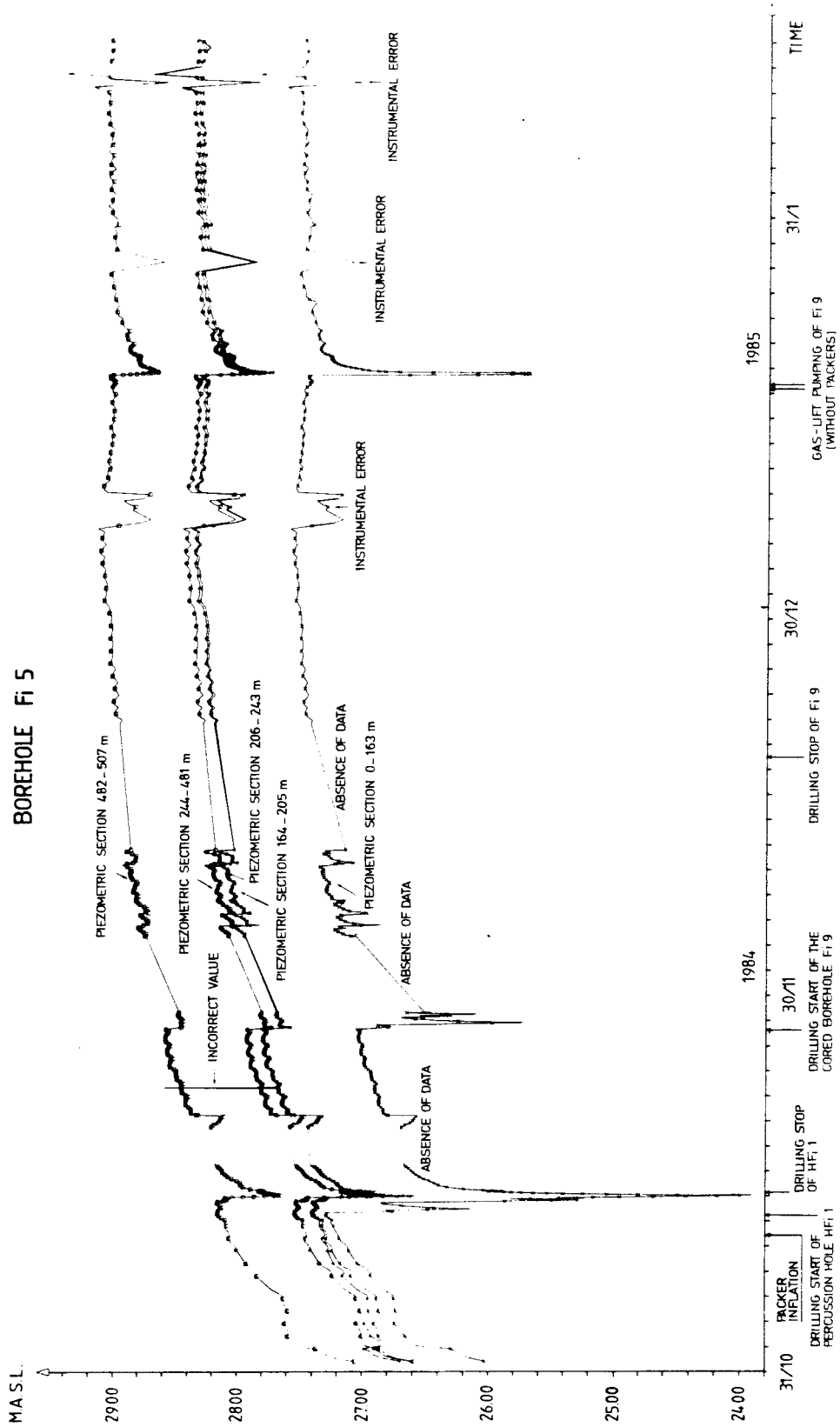


Figure 9.3 Results from the piezometric measurements in Fi 5.

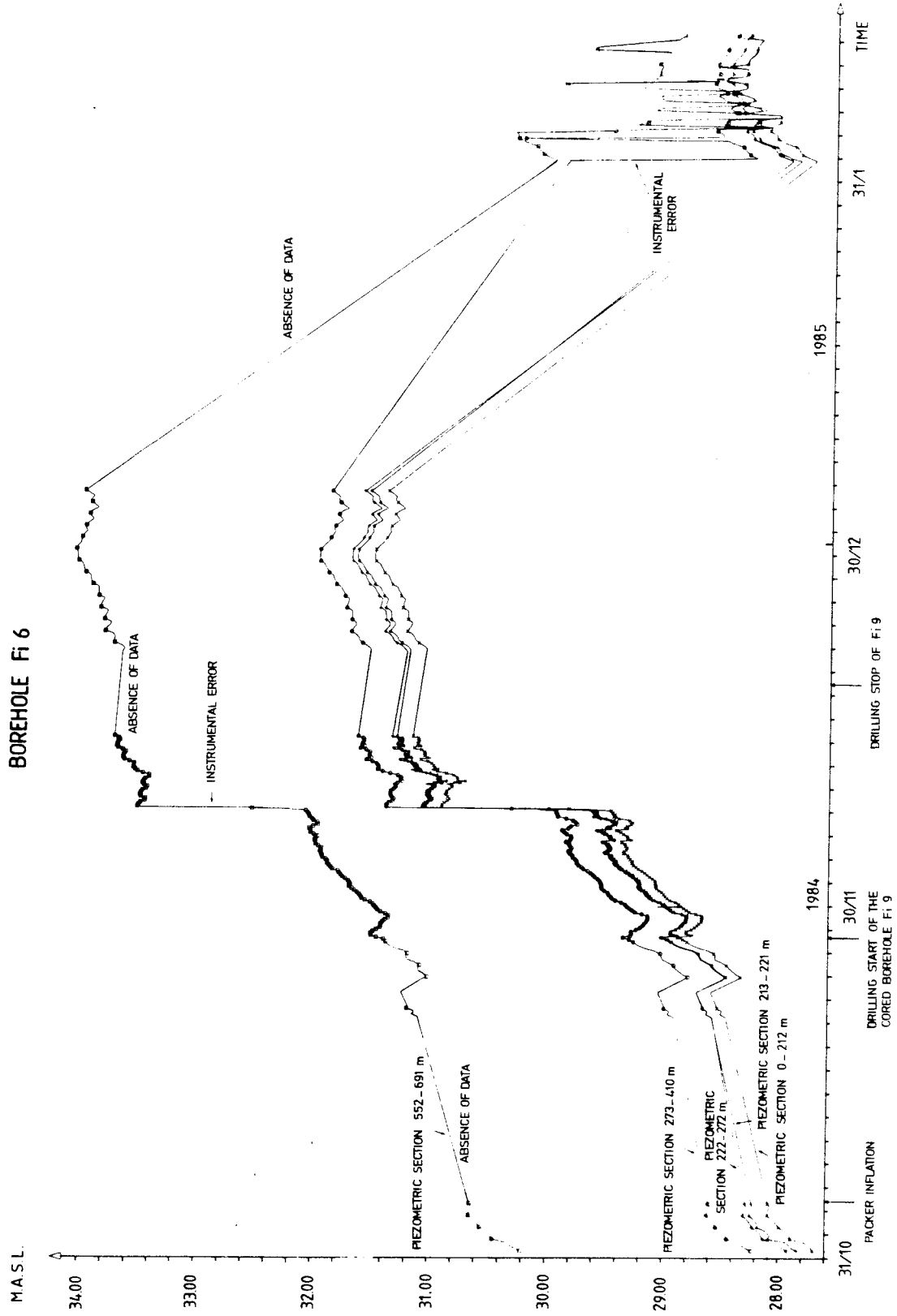


Figure 9.4 Results from the piezometric measurements in Fi 6.

in F1 6 on the 8:th of December. After that date, the transducer drift seems to be of minor importance. However, the pressure differences between the sections in the same borehole are not influenced by the drift in absolute pressure. The pressure relations between the holes can, on the other hand, not be established.

The tendency of increasing pressure values during the first two months of registration is mainly caused by the transducer drift but to some degree also by rising groundwater levels due to precipitation. Other obvious features illustrated in the figures 9.3 and 9.4 are the instrument problems during rather long periods of time, especially in F1 6, and hydraulic disturbances from drilling and pumping.

9.4.1 Groundwater head conditions in F1 5 and F1 6

As mentioned in section 9.3, the pressure values from the different sections before packer inflation ought to be identical, if there are no density variations or heavy local streaming in the borehole fluid (or instrument failure). The graphs in the figures 9.3 and 9.4 clearly illustrate, that the values are far from identical in F1 5 and F1 6 respectively. The deeper a section is situated in the borehole, the higher the piezometric pressure appears to be. The apparent piezometric increase with depth is caused by the density difference between the distilled water, which is pressed into the tubes between the measurement sections and the probe in order to evacuate air bubbles, and the surrounding saline water, that prevails in the borehole (chapter 6 and 11). The density of the borehole water is also an effect of temperature and water pressure. It is however assumed, that those parameters change almost identically with depth in the borehole fluid and in the tubes. Therefore they do not have any influence on the density differences.

Since the salt content at different levels is roughly known from the resistivity logs, an estimation of the theoretical pressure increase was made. Table 9.2 compares the estimated pressure increases with the measured ones. It should be

Table 9.2 Calculated and measured increases of piezometric pressure (m watercolumn) with depth, due to increasing salinity, in relation to the upper section in Fi 5 and Fi 6 respectively.

Borehole sections	Theoretical	Measured
Fi 5 section 0-163 m	0.00	0.00
section 164-205 m	0.04	0.14
section 206-243 m	0.13	0.22
section 244-481 m	0.22	0.30
section 482-507 m	0.58	0.88
Fi 6 section 0-212 m	0.00	0.00
section 213-221 m	0.16	0.14
section 222-272 m	0.20	0.20
section 273-410 m	0.45	0.52
section 552-691 m	1.98	2.55

emphasized, that the theoretical calculations do not take into consideration minor variations in salinity, that can be seen in the geophysical logs.

The measured values are in most cases higher than the theoretical. The greatest relative difference in Fi 5 occurs in section 164-205 m and in Fi 6 in section 552-691 m. The cause for the deviations may be, that the resistivity logs suffer from some errors, or that locally flowing water creates a hydrodynamic pressure, which differs somewhat from the hydrostatic pressure. The geophysical loggings can to a certain extent be checked by water sampling, although the sampling points are very scarce. The water sampling in Fi 5 and Fi 6 indicates a higher salinity than the resistivity logs. For instance, the water samples from the level 398 m in Fi 6 have a total salinity of 9 000 - 9 300 ppm and those from the level 688 m 9 600 - 9 700 ppm. The resistivity logs show values of 7 000 - 7 500 ppm. To nullify the discrepancy in section 552-691 m between

theoretical and measured values of piezometric pressure before packer inflation demands a salinity of about 9 800 ppm in the input calculations. In other words, if the water sampling values had been used instead of the resistivity log values of salinity, the discrepancy had been very small. If the salinity values from the water sampling in F1 5, which are about 2 500 ppm higher than the values from the resistivity log, should be used, the discrepancy would change signs but remain in (roughly) the same order of magnitude. The effects of streaming water in the boreholes are probably not measurable.

When the packers are inflated, the piezometric pressure relations between the sections change somewhat. The changes might theoretically be a combined effect of changing density, flow and head conditions. It is however assumed, that the groundwater in the bedrock in the vicinity of the borehole has the same density variations as the borehole water, and that the flow conditions in the borehole are the same before and after packing off. Whether these assumptions are fully correct or not, cannot be completely verified. The change in piezometric pressure can best be illustrated, if the "salinity effect" is subtracted from the total measured pressure differences after packer inflation. Figure 9.5 shows the result of this operation, where every section value has been related to the piezometric pressure in the upper, freshwater section (in other words, the groundwater table in the open borehole) one day before packer inflation. The operation has not been performed for the total time sequence, and therefore the figure refers only to one specific moment. In F1 5 it refers to one day after packer inflation, before any artificial disturbance has been created by drilling, pumping etc. Instrument problems in F1 6 unfortunately prohibited measurements shortly after packer inflation. Instead, one day during a relatively stable period without activities in January 1985 was chosen for comparison with the conditions before packer inflation.

Figure 9.5 indicates, that all sections have positive piezometric pressures in relation to the background value. This cannot be true for a complete borehole. Positive values ("out-flow sections") ought to be balanced by negative values ("in-

flow sections"). In this case the explanation can be either the fact that there is one "blind", unmeasured, section in every borehole or, more likely, the general positive transducer drift, which is obvious during the actual period.

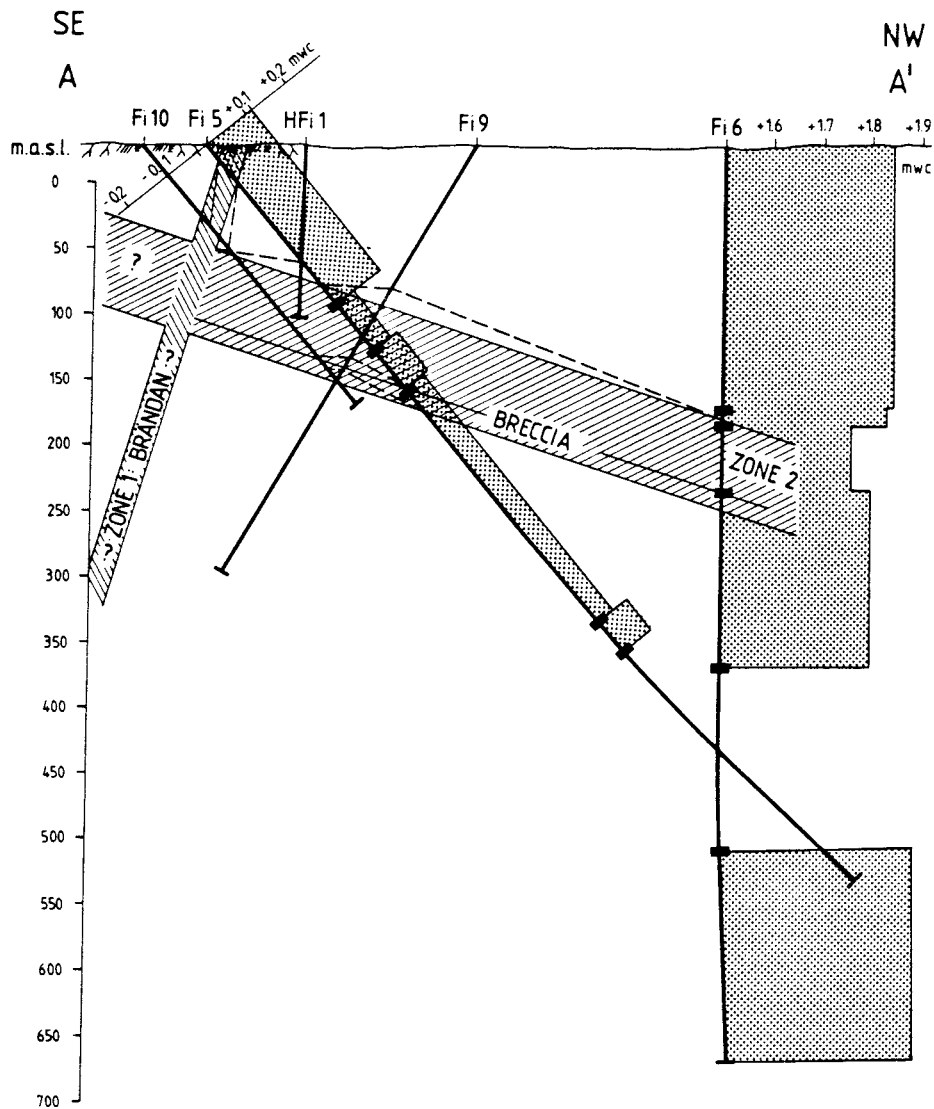


Figure 9.5 The piezometric pressure distribution in the boreholes Fi 5 and Fi 6.

The most interesting conclusion drawn from figure 9.5 is the pressure relations between the measured sections. Two things are obvious. The first is the small differences between the sections. In F1 5 the maximum gradient between two sections is 0.07 m (0.007 kPa). In F1 6 the corresponding value is 0.13 m (0.013 kPa). Secondly, the Zone 2 coincides with the point of lowest head in both boreholes. This indicates, that the subhorizontal Zone 2 drains both the overlying and underlying bedrock. If this is correct, the zone is a structural barrier in the rock, which prevents or diminishes the mixture of superficial fresh groundwater with deep saline water. There might in fact be two separate circulation cells for fresh water and saline water.

9.4.2 Piezometric registrations of artificial hydraulic events

Piezometric monitoring was also made during hydraulic events caused by drilling, pumping and injecting water. The aim was to determine hydraulic connections between boreholes.

Looking at the piezometric graphs in figure 9.3 and 9.4, the first "hydraulic event" is the drilling of the percussion borehole HF1 1. During percussion drilling, water is intermittently pressed out from the borehole by compressed air. Between the flushings, the water level is recovering. The percussion drilling can thus be regarded as a huge pumping test, although the outflow in this case was uncontrolled. The drilling of the 129 m deep vertical borehole took place (with a few breaks) from the afternoon on the 12:th of November 1984 (84 11 12) to the morning on the 14:th of November (84 11 14). Unfortunately, instrument failure in F1 6 prevented registrations in that borehole. The details in the F1 5 graph from that occasion is enlarged in figure 9.6.

When the drilling had reached 51 m, water was flushed from the hole. A very distinct response is observed in the uppermost section 0-162 m in F1 5, while a hardly noticeable drawdown occurs in the sections below. This indicates a hydraulic connection in the near-ground rock between HF1 1 and F1 5. At the

drilling depth of 90 m the response in the uppermost section of F1 5 is more accentuated, while the other sections are only slightly influenced. Not until the drilling reaches about 100 m, there is a "break through" for the deeper sections in F1 5, which shows, that the borehole at 100 m penetrates a highly conductive hydraulic unit of considerable thickness. This unit was later interpreted as the Zone 2.

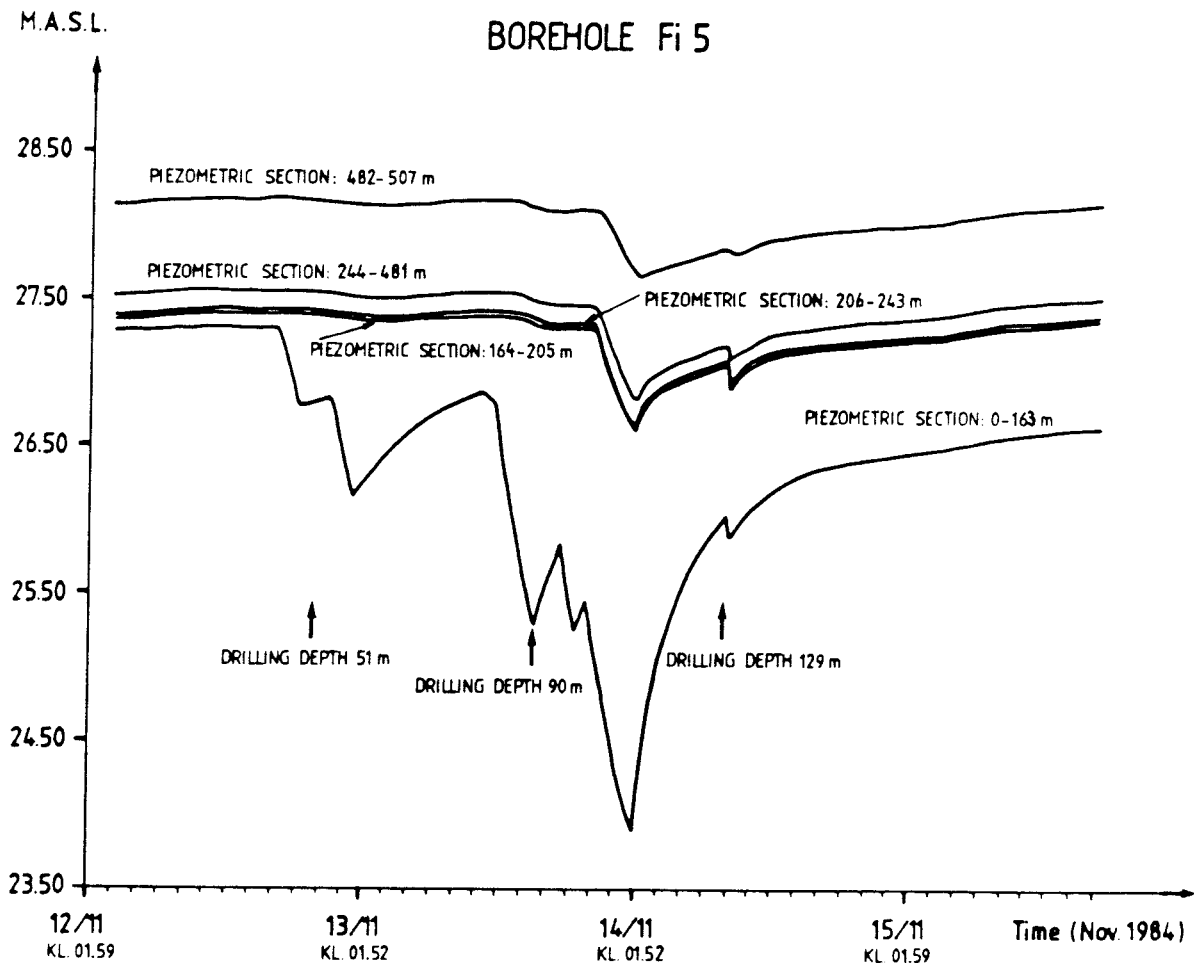


Figure 9.6 The piezometric registrations in F1 5 of the drilling of percussion hole HFi 1.

The second important event is the drilling of the cored borehole F1 9. Drilling fluid was taken from the percussion borehole HF1 1. The water was pumped into a 5 m³-tank and samples were taken for chemical analysis. A tracer, Uranine, was then added. In total, 13 tanks were used during the drilling (chapter 10). When filling up the first tank, it was noticed that the water was saline. In order to avoid contamination of the superficial, freshwater part of the bedrock with saline water, a packer was installed at the level 57-58 m in HF1 1, and non-saline water was pumped from above the packer. Later, when borehole F1 9 was expected to reach the part with saline water, the packer was removed, and saline water was again pumped from Zone 2 at the bottom of the percussion borehole.

Unfortunately, instrument failure in both F1 5 and F1 6 during the core drilling made the registrations incomplete. The details from the piezometric graphs in figure 9.3 and 9.4 during the pumpings 84 11 27 to 84 11 29 are enlarged in figure 9.7.

A strong response was observed in the uppermost section of F1 5 while pumping from above Zone 2 in HF1 1 (with the packer at 57 m). Only very small responses occurred in the deeper test sections of F1 5 and in all sections of F1 6. However, when pumping from the lower part of HF1 1 (Zone 2), all piezometric sections in both cored boreholes were affected, except for the lowermost section of F1 6.

These observations show, that there is a good hydraulic connection between different boreholes intersecting Zone 2 for distances greater than 450 metres. They also show, that the hydraulic connections between the superficial parts of the bedrock (above Zone 2) and the deeper parts (Zone 2 and below) are weak.

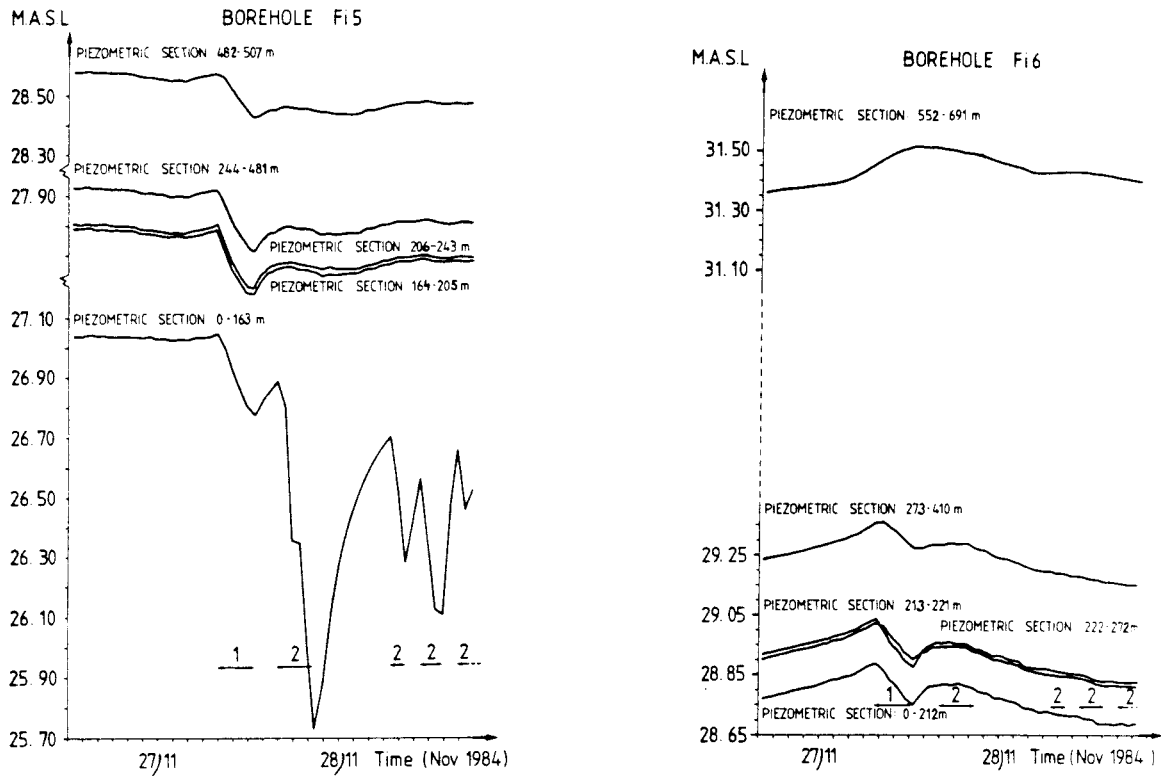


Figure 9.7 The piezometric registrations in F1 5 and F1 6 of the pumpings in HF1 1 without a packer (1), (pumping from Zone 2) and with a packer at the level 57 m (2), (pumping from the near-surface rock).

10. DRILLING FLUID AND DRILLING DEBRIS

The drilling of a cored borehole creates a change in groundwater head and in water chemistry due to the injection of drilling fluid into the fracture system of the rock mass. These disturbances can be studied in other boreholes and may indicate hydraulic connections. In the preceding chapter, observations made of changes in hydraulic head due to drilling are described. The section below discusses some disturbances in the groundwater chemistry due to drilling.

10.1 Drilling fluid and tracers

In order to calculate the component of drilling fluid in a water sample, the drilling fluid has to be labeled with a tracer. The tracer should have the following qualities:

- easy to handle
- easy to detect and analyze
- non-sorbing
- low background
- no reaction with original water

In the Brändan area, an organic dye was considered to be the most suitable tracer. Drilling fluid for the cored boreholes F1 5 and F1 6, drilled 1978-79, were labelled with the fluorescent dye Rhodamine WT. In order not to interfere with Rhodamine the fluorescent dyes Uranine (sodium fluorescein) and Amino G Acid were chosen for boreholes F1 9 and F1 10 respectively. The concentration of Uranine, shown in table 10.1, was chosen after measuring old water samples from boreholes F1 5 and F1 6 and samples from the percussion hole HF1 1. The governing criterium was to measure a dilution to 0,1% of the initial concentration. The initial concentration of Amino-G Acid was, due to shortage of time, chosen from background values reported by Smart and

Laidlaw (1977). A Sequoia-Turner 450 filter fluorometer was used for the analyses.

Table 10.1 Initial concentrations, C_0 , of chosen tracers.

Borehole	Tracer	C_0 (ppm)
Fi 5	Rhodamine WT	2
Fi 6	Rhodamine WT	2
Fi 9	Uranine	1.0
Fi 10	Amino-G Acid	2.0

The drilling fluid was labeled by mixing a small amount of concentrated tracer solution into the 5m^3 storage tanks for drilling fluid. Samples were taken from the non-labeled incoming HFi 1 water and from the storage tanks after mixing. The results from the sampling of HFi 1 water are presented in table 10.2 and figure 10.1. The table also shows the volumes pumped from HFi 1 at each time, the total volume pumped into Fi 9 and the drilling depth interval in Fi 9.

When drilling in the non-saline superficial part of the bedrock (see chapter 11), drilling fluid was pumped from the upper 57 m in HFi 1, where a packer had been installed. At about 150 m drill depth the packer was removed, and saline water was pumped in order to use natural saline water as drilling fluid. After removal of the packer and pumping about 10m^3 , the concentration of Uranine in HFi 1 increased rapidly, as can be seen from figure 10.1. This indicates a hydraulic connection between Fi 9 and HFi 1 in the Zone 2, somewhere between 150 and 210 m borehole length, figure 10.2. An attempt was made to estimate the hydraulic conductivity of the Zone 2 from the tracer breakthrough. However, this attempt was not successful due to the difficulty of determining the hydraulic gradient during the

drilling of F1 9 and the intermittent pumping in HF1 1.

Table 10.2 Volumes, V, and concentrations, C, of Uranine and Rhodamine WT in HF1 1-water.

Date	V HF1 1** (m ³)	V F1 9*** (m ³)	Drill depth (m)	C Uranine (ppb)	C RdWT (ppb)
28/11	5.0	5.0	12 - 57	0.52	1.0
28/11	5.0	10.0	57 - 102	0.41	0.9
29/11	5.5	15.5	102 - 142	0.42	1.0
3/12	5.0	20.5	142 - 173	0.48	0.8
5/12*	5.0	25.5	173 - 203	0.39	3.6
6/12	5.0	30.5	203 - 232	0.33	3.6
10/12	5.0	35.5	232 - 255	1.12	3.5
10/12	5.0	40.5	255 - 281	3.10	3.3
11/12	5.0	45.5	281 - 305	4.50	3.3
12/12	5.0	50.5	305 - 326	6.70	3.2
13/12	5.0	52.5	326 - 335	9.40	-
17/12	5.0	57.5	335 - 357	13.60	3.4
18/12	5.0	62.5	357 - 376	16.20	3.3

* Packer at 57 m depth removed.

** Volume pumped from HF1 1.

*** Total volume pumped into F1 9.

The water from HF1 1 was also analyzed for Rhodamine. The results presented in table 10.2 shows that the concentration of Rhodamine is 3-4 times higher in the saline water compared to the non-saline. This might imply that the drilling fluid from the drilling of boreholes F1 5 and/or F1 6 during 1978 has not been washed out from the area. There is also a possibility that the natural background of Rhodamine is higher in the saline water than in the non-saline water.

The drilling fluid used for F1 10 was, for practical reasons, pumped from the upper 40 m of HF1 1 and instead of pumping at

short intervals the pumping was continuous at a low pumping rate (0.32 l/s). Unfortunately, the background values were much higher than expected from literature data, 0.1 ppm for Amino G Acid, which implied that a dilution to 5 % could be measured. There were no indications of tracer transport from F1 10 to the upper part of HFi 1. This implies, that there is no direct hydraulic connection between the upper part of HFi 1 and borehole F1 10.

During the drilling of F1 9 and F1 10, records of drilling fluid loss versus depth were kept. These records can be used as indications of high conductive zones. As can be seen from figure 10.3 the agreement between high conductive zones and increasing drilling fluid loss is rather good for borehole F1 9.

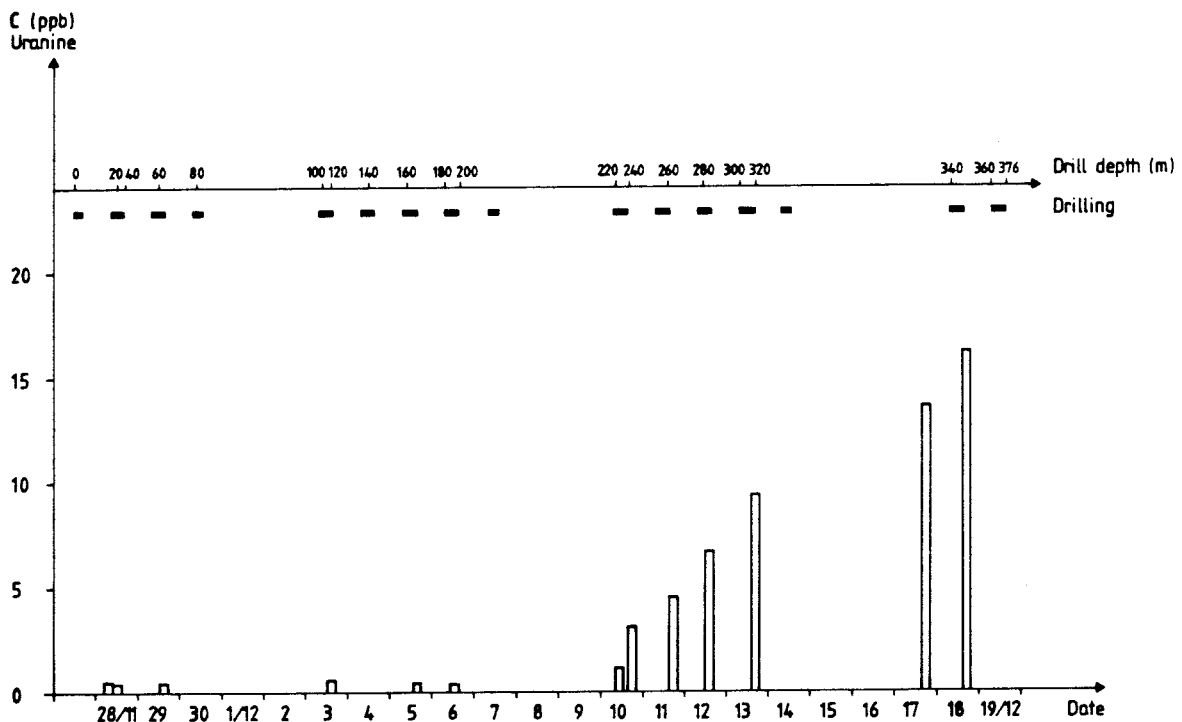


Figure 10.1 Concentration of Uranine in water pumped from borehole HFi 1 versus date and drill depth.

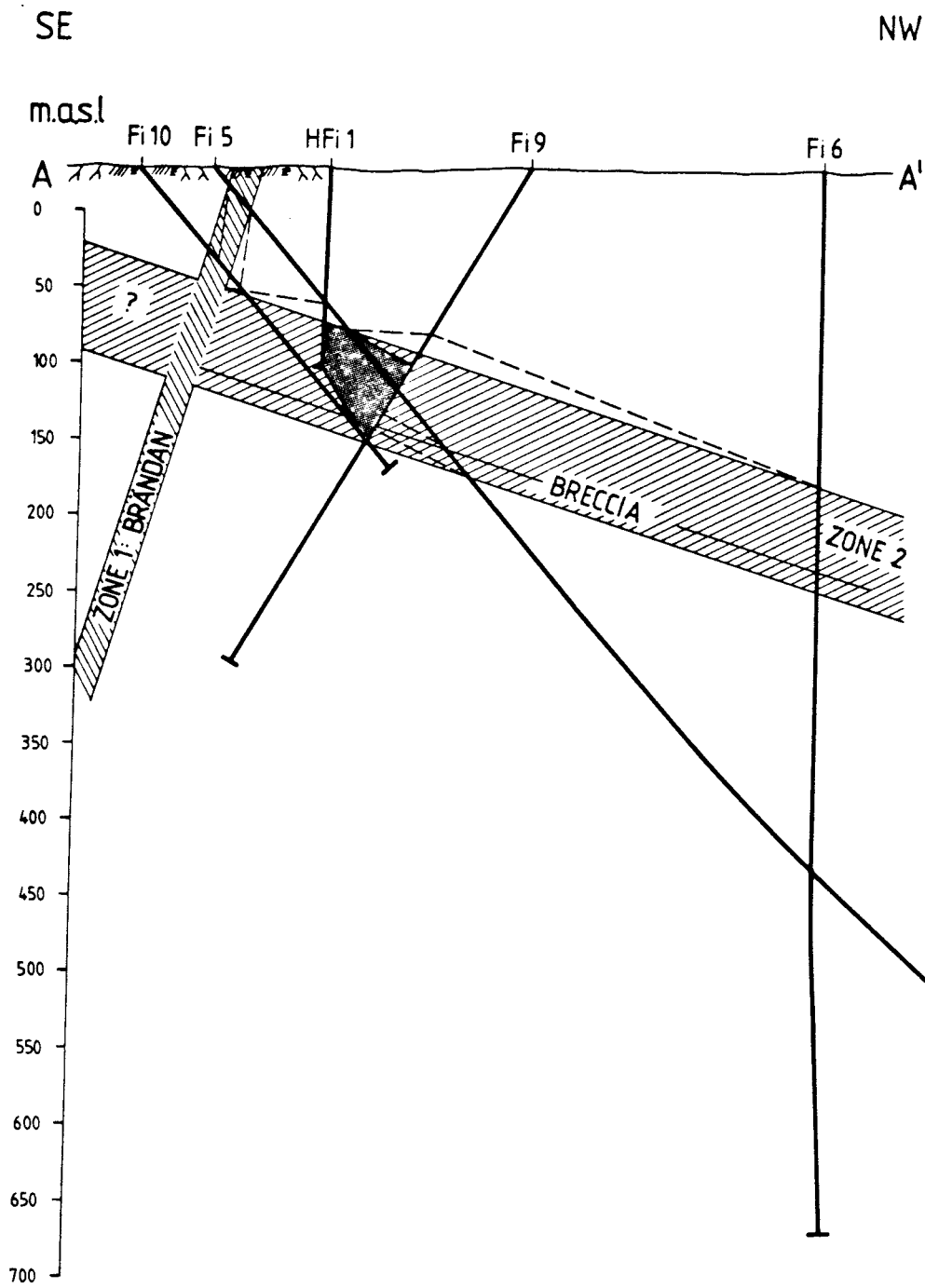


Figure 10.2 Possible area of transport between boreholes Fi 9 and HFi 1.

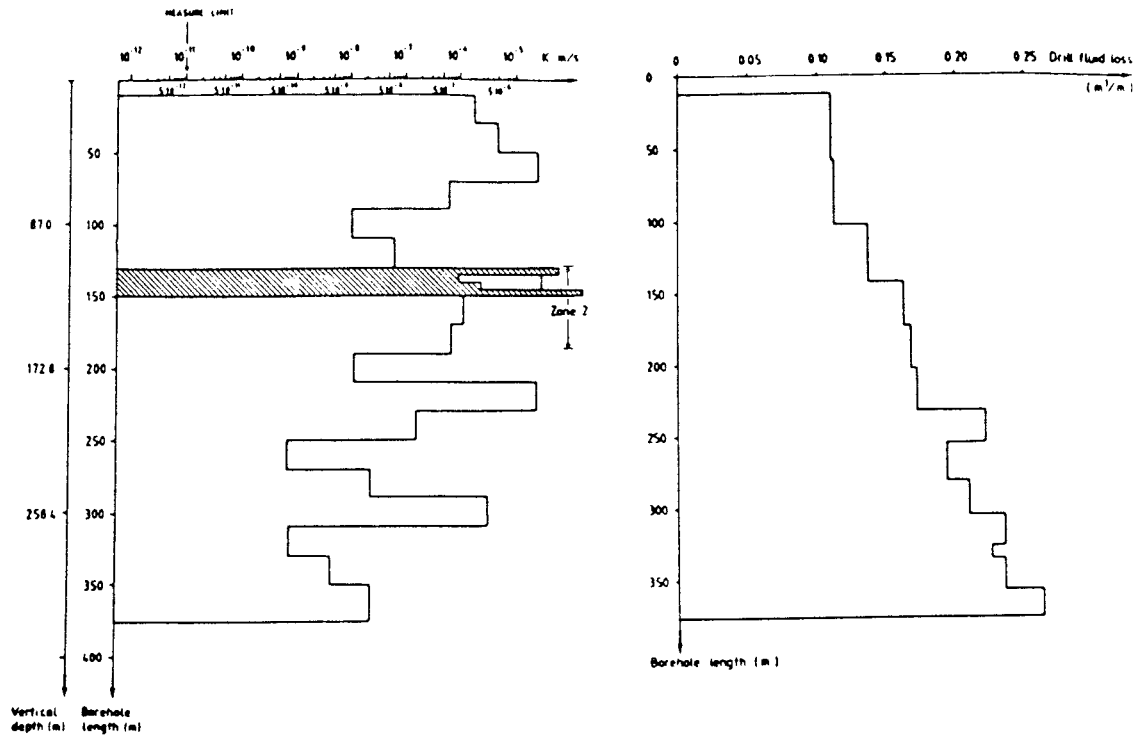


Figure 10.3 Comparison between hydraulic conductivity and drilling fluid loss versus depth in borehole F1 9.

10.2 Water sampling and collection of drilling debris during gas-lift pumping

During the gas-lift pumping of borehole F1 9, water samples were collected for analysis of Uranine and drilling debris content in order to study the recovery rate of these. This is of great interest to know, as the purpose of a gas-lift pumping is to clean the borehole from drilling water and debris. The first gas-lift pumping was performed from the whole borehole F1 9 as described in chapter 8. The initial concentration of Uranine during pumping was very low, due to the dilution of the surface water in the borehole, but it rapidly (whithin one minute)

reached a maximum value of 80 ppb and then slowly decreased as the pumping proceeded, figure 10.4.

Gas-lift pumpings 2 and 3 were performed in the section 150-235 m borehole length in Fi 9, i.e. from the sub-horizontal Zone 2. In this case the Uranine content was almost constant (50 ppb) despite the fact that a total volume of 15.4 m³ or 73 section volumes was pumped out during 13 hours. This is probably due to the good mixing and large volumes of drilling fluid injected into the high conductive zone.

The total amount of drilling fluid recovered from the gas lift pumpings was determined by integrating the concentration versus

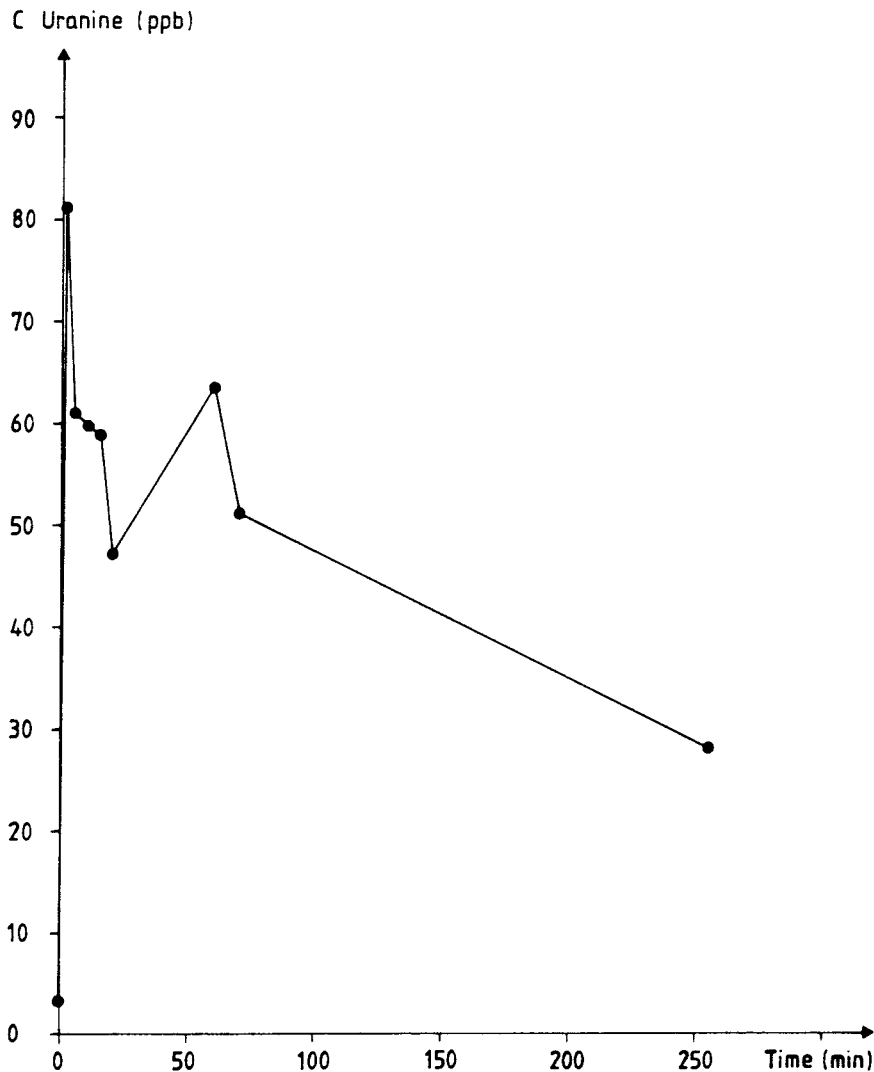


Figure 10.4 Uranine content versus time from gas-lift pumping of Fi 9 without packers.

time curves and knowing the pumping rate. The result was that only 3 % of the 62.5 m³ drilling fluid, injected into Fi 9, was recovered. This result shows the difficulty of cleaning a borehole, especially the high conductive zones, from drilling fluid by short gas-lift pumpings.

The content of drilling debris in the water samples were determined by filtering the water, drying and weighing the dry substance. The results in table 10.3 show a very rapid decrease from 24 g/l to 0.36 g/l during five minutes of pumping.

Table 10.3 Drilling debris content in water samples from gas-lift pumping in borehole Fi 9.

Time (min)	Drilling debris content (g/l)
0	24.0
1	1.9
5	0.36
10	0.25
15	0.23
20	0.22
60	0.05
80	0.03
250	0.01

By integrating in the same way as described above, a total drilling debris recovery of 5 kg was determined. This is a very low figure, as the total amount of drilling debris produced from a core drilling of 376 meter is about 1000 kg. During the drilling of Fi 9, the drilling fluid was flowing out from the borehole down to 134 m drilling depth. Assuming that all of the drilling debris was recovered to this depth and that about 15 m at the bottom of the borehole was filled with sedimented drilling debris, still about 500 kg of the drilling debris have been flushed out into the fracture system resulting in a maximum recovery ratio of 1 % from the gas-lift pumping.

11. WATER CHEMISTRY

Studies on the groundwater chemistry in the Finnsjön area constitute only a small part of the overall programme. However, their importance in helping to unravel the bedrock hydraulics cannot be underestimated. In addition, the timing of the programme in relation to the SKB test site investigations as a whole, provided the opportunity to implement some ideas that had been under discussion for some time (i.e. improvements in sampling).

11.1 Earlier hydrochemical studies in the Finnsjön area

During earlier site investigations (1981/82) a total of seven boreholes were sampled for groundwater characterization. These results are presented by Hultberg et al. (1981) and Laurent (1982). The chemical parameters have been discussed by Allard et al. (1983) and the geochemical association between the groundwater and the fracture minerals by Tullborg and Larson (1982).

Not all data are available from these earlier investigations, for example, no oxidation potential measurements are presented. In general, however, the results distinguish two major types of groundwater: saline and non-saline, with the former usually increasing in extent with depth. The groundwater chemistries appear to emphasize saline groundwaters from three of the boreholes (F1 5, 6 and 8; figure 3.1) whereupon chloride concentrations ranged from 2500-5900 mg/l. Low tritium contents (< 3 - 7 TU) and old ^{14}C ages (ca 5500 - 10 000 years) also typify these waters thus establishing them as representative and free from major contamination (i.e. from near-surface fresh water and drilling fluid). In contrast, F1 4 and 7 exhibit higher tritium (3 - 14 TU) and younger ^{14}C ages (ca 4000 - 6000 years) which, together with smaller concentrations of chloride (ca 30 - 650 mg/l), indicate varying degrees of contamination from other sources. The two boreholes which would appear to represent only non-saline water (F1 1 and 2) are characterized

by high to very high tritium (38 - 50 TU) and correspondingly low ^{14}C ages (ca 2000 - 4000 years). These waters are thus highly contaminated by surface to near-surface derived water and not representative for the measured holes.

These waters show, therefore, that although the salinity of holes F1 5, 7 and 8 is beyond dispute, the remaining holes which are non-saline to weakly saline in character, may in fact prove to be more saline than originally suspected. In some respects it was therefore surprising that recent borehole logging (see chapter 8) supported the reported groundwater salinities. However, the hydraulics of the borehole environments are not quantitatively known, especially open-hole effects, so that surface-derived non-saline water may still dominate to the depths measured.

These earlier investigations also presented trace element analyses for several of the boreholes (F1 1, 4, 5 and 7). Interestingly the most saline borehole (F1 5) also showed appreciable amounts of lithium and boron. Such enrichments, together with chloride, have been considered to result from rock/water interaction processes over long time periods (Edmunds et al. 1983).

11.2 Water chemical investigations in the Brändan area

Present water chemical investigations in the Brändan area have involved:

- surface water analyses
- analysis of source water used for drilling purposes
- deep hole groundwater analysis

11.2.1 Surface Water

This was limited to only one sample which was considered to be representative of the recharge environment; the location was a small stream in the small valley where the Zone 1 (Brändan) outcrops, some 200 metres from borehole F1 9 and about 50 metres from F1 5 (figure 3.1).

The chemistry of the water (table 10.1) is typical for a surface environment, i.e. moderately acidic (pH 5.9), low conductivity (4.12 mS), and generally low amounts of dissolved ions. The tritium content (31 ± 2 TU) is normal for recharge water in this part of Sweden. The stable isotope content (D = -80.5 ppt; $^{18}\text{O} = -12.1$ ppt) are usual for meteoric waters in this area (Saxena, 1984).

11.2.2 Drilling Source Water

For drilling purposes, shallow groundwater of similar properties as the groundwater to be sampled (i.e. pH, Eh etc), is obtained by drilling a percussion hole in the near-vicinity of the hole to be sampled. By taking water from depths of around 100 m it is hoped that a reasonably compatible water can be obtained to cause the minimum contamination. To assess the degree of potential contamination it is therefore extremely important to quantify the composition of the drilling component. Furthermore, percussion hole drilling is a simplified form of "booster hole" drilling, a technique which is being considered in the near future for groundwater sampling and chemical characterization. A crude test as to the efficiency of such a method was therefore attempted.

Simulation booster hole groundwater sampling was carried out whilst drilling the percussion borehole HF1 1, figure 3.2. Sampling was crude and entailed collecting water as soon as a water conducting zone was encountered. A series of five samples were taken within a vertical depth of approximately 130 m. Contamination is present (seen as abnormally high amounts of Al^{2+} , $\text{Fe}(\text{T})$ and Fe^{2+}), but the results (table 4.13.1) show promise in that the contact between non-saline and saline groundwater could be fairly sharply defined. This is clearly seen by comparing sample HF1 1D (98.6 m) with HF1 1E (129 m) whereupon the chloride content increases from 9 to 1100 mg/l. The importance of this was realized later when it was impossible to achieve non-saline water for drilling purposes from depths greater than 50 m from the same hole. Thus, had sampling been carried out after drilling, as normally happens, the upper detected saline groundwater level would be erroneous.

Water for drilling purposes was taken from the percussion borehole. The intention was that as hole Fi 9 was being drilled through the estimated thickness of bedrock to the level of suspected salinity, which coincides with the sub-horizontal Zone 2, non-saline drilling water should be used. It was hoped that this would reduce the risk of groundwater contamination prior to the sampling of Fi 9. Systematic analysis of the drilling water was carried out and the results are represented by HFi 1 F-L (table 11.1). It can be seen that the non-saline samples (HFi 1F-H) never quite achieved the water compositions represented by samples HFi 1 B-E, and these were only possible after packing off the hole at 57 m. The saline drilling water samples (HFi 1I-L), used for depths greater than Zone 2, were satisfactory although HFi 1L showed a decrease of chloride which suggests contamination from higher non-saline levels around the packer system.

Presented in table 11.1 are some isotope data relating to tritium and the stable isotopes. The tritium data show that apart from the surface sample already referred to, the other three samples show a marked decrease. The low contents present in HFi 1C and E (5 and 4 TU respectively) may be accounted for by minor contamination of surface water during sampling. This is supported by the below detection amount in HFi 1K (< 3 TU) which has been collected after continuous pumping from the hole thus reducing the risk of a surface water component. Oxygen isotope data (figure 11.1) from the same four localities show little variation (-12.1 to -12.8 ppt) and are consistent for other borehole measurements in the Finnsjön area (Saxena, 1982). The deuterium data ranges from -88.4 to -76.2 ppt which is similar in range to other SKB test-site areas (Smellie et al. 1985). Comparison between HFi 1C and K show negligible differences, although they represent the extremes of non-saline and saline water. Saline groundwaters compared with non-saline from the other test-sites often show depletions of the stable isotopes. The absence at Finnsjön may be due to non-saline contamination (as suggested on a small scale by the tritium data) or that both groundwater varieties are of a similar palaeoclimatic origin. More data are required.

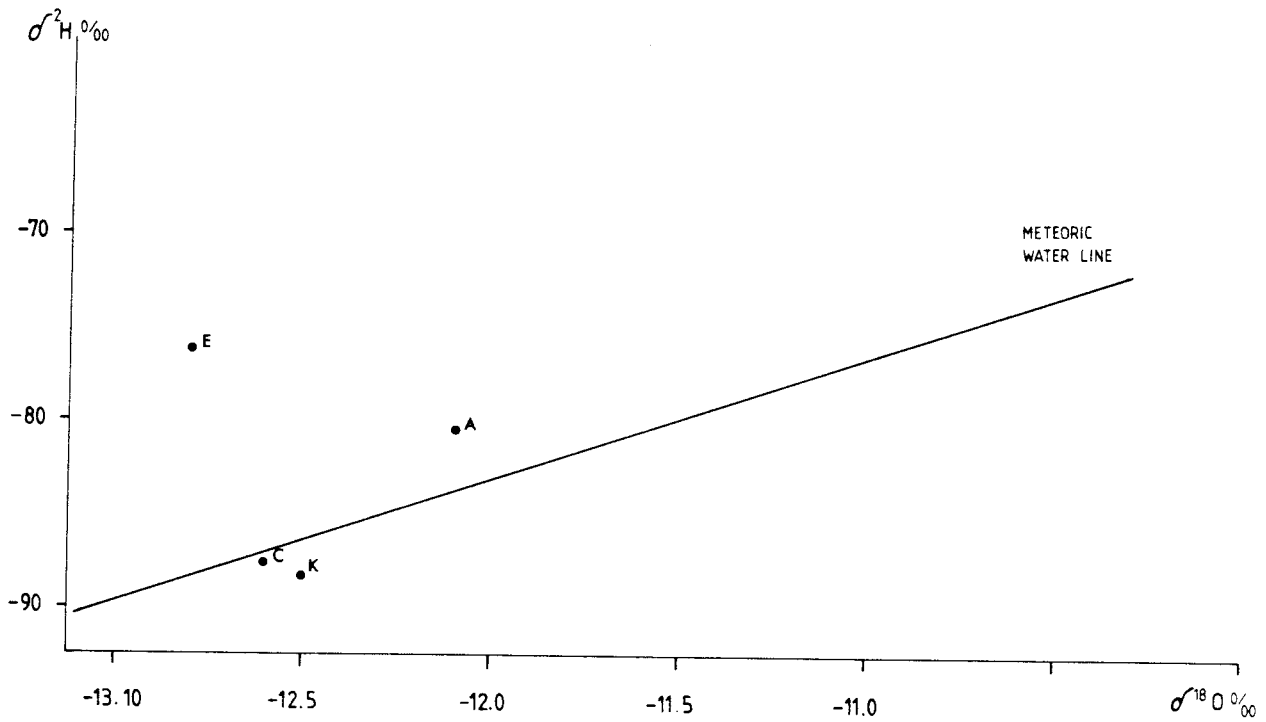


Figure 11.1 ^{18}O and deuterium compositions of nearsurface to shallow ground waters from percussion borehole HFi 1.

11.2.3 Deep Hole Groundwater Analysis

Borehole sampling procedures and the equipment used are described by Almén et al. (1983), Wikberg et al. (1983) and summarised by Smellie et al. (1985). Most of the standard chemical analyses presented here have been carried out on site by the mobile chemical laboratory. Selected samples were also analysed for tritium and radiocarbon.

Four levels were sampled in F1 9; at 94 m, 114 m, 182 m and 360 m. Sampling was duplicated at 182 m (the sub-horizontal fracture Zone) prior to and subsequent to the gas-lift pumping (see chapter 8). The overall objectives of the hydrochemical sampling programme was to:

- chemically characterize the saline and non-saline groundwaters intercepted by borehole F1 9.
- compare the groundwater composition at the 182 m level before and after gas-lift pumping.
- compare the water chemistries with the earlier hydrochemical investigations carried out in the Finnsjön area.
- speculate on the presence and origin of the saline groundwater

11.3 Chemistry of the groundwaters

Average compositions from the four sampled levels are presented in table 11.1.

Table 11.1 Chemical analysis of surface, near-surface, and ground waters from borehole Fi 9 and nearvicinity.

Table 1: Chemical analysis of surface, near-surface, and ground waters from borehole Fi9 and near-vicinity.

Sample	HFi1A	HFi1B	HFi1C	HFi1D	HFi1E	HFi1F	HFi1H	HFi1I	HFi1J	HFi1K	HFi1L	KBS	KBS	KBS	KBS
Depth (metres)	Surface	11	38.6	98.6	129	<57	<57	>80	>80	>80	>80	94	114	182	360
pH	5.9	8.5	7.9	8.4	8.0	8.2	8.1	7.7	8.0	8.1	7.8	7.3	7.5	7.7	7.4
C(mSm)	4.12	23.2	44.9	48.9	402	78.1	67.4	586	560	495	478	270	656	860	1410
Eh(mV)	-	-	-	-	-	-	-	-	-	-	-	-245	-300	-212	-
HCO3-	7	290	300	330	320	300	320	210	210	200	220	285	116	150	32
Ca	5.9	11	4.9	10	160	35	26	410	460	460	370	115	-	970	1691
Mg	0.81	2.3	18	3.4	27	7.2	6.4	73	85	74	59	16	-	91	84
Na	2.6	87	94	95	350	190	230	270	830	830	770	415	-	1020	1510
K	0.44	7.7	15	4.8	7.5	7.6	6.8	12	12	11	10	5.8	-	15	7.4
SO4	4.7	1.6	0.7	0.9	8.7	7.6	4.2	170	160	140	150	175	-	225	326
F	0.13	3.1	2.7	2.7	1.8	2.6	2.5	1.6	1.7	1.8	1.5	3.4	-	7.2	1.1
Cl	2	16	11	9	1100	120	58	1500	1700	1700	520	680	2125	2700	5150
Br	-	-	-	-	-	-	-	-	-	-	-	2.03	-	13.5	27.10
I	<0.01	0.03	0.01	0.01	0.01	0.01	0.01	0.02	0.02	0.02	0.02	0.01	-	0.03	0.07
PO4	0.01	0.63	0.06	0.08	0.05	0.14	0.06	0.03	0.07	0.04	0.02	.001	.002	.003	.004
Si	2.8	3.1	4.8	3.9	2.0	11	11	5.7	2.8	2.5	2.5	7.6	-	4.6	7.6
NO3	0.28	0.22	0.03	0.18	0.02	0.01	0.01	0.01	0.03	0.18	0.03	0.02	-	0.14	0.01
NO2	.006	.078	.006	.004	.004	.006	.002	.001	.006	.002	.004	.001	-	.002	.001
Al	0.8	100	59	6.3	5.3	2000	1600	61	9	14	9	0.02	-	0.02	0.18
Fe(T)	0.97	230	59	6.3	5.3	1.1	1.1	0.71	0.79	0.76	0.70	0.52	0.35	0.94	0.35
Fe2+	0.58	150	1.3	0.2	0.12	0.2	0.29	0.07	0.04	0.03	0.05	0.13	0.36	0.19	0.05
Mn	0.06	3.3	0.83	0.14	0.56	0.11	0.10	0.58	0.59	0.58	0.55	0.19	0.45	0.82	0.36
TOC	62	68	13	19	13	9.5	13	18	6.3	5.8	5.1	18	-	6.3	1.0
U (ppm)	-	-	-	-	-	-	-	-	-	-	-	2.1	-	1.6	8.2
A.R.	-	-	-	-	-	-	-	-	-	-	-	4.1	-	3.1	5.0
δ2H (ppt)	-80.5	-	-87.7	-	-76.2	-	-	-	-	-88.4	-	-	-	-	-
δ18O (ppt)	-12.1	-	-12.6	-	-12.8	-	-	-	-	-12.5	-	-	-	-	-
Tritium (TU)	31	-	5	-	4	-	-	-	-	< 3	-	8	-	<3	<3
14C (years)	-	-	-	-	-	-	-	-	-	-	-	-	-	12205	-

Anal. HFi1A = surface recharge water; HFi1B-HFi1E = percussion borehole for drill water source; HFi1F-HFi1L water used for drilling; KBS: 94m-KBS:360m = average values for groundwater sampled from different levels in borehole Fi9.

N.B. Concentrations in mg/l unless otherwise noted.

Level 94 m

This level was considered suitable for a non-saline groundwater sample, figure 11.2, being located sufficiently above the Zone 2. The analyses show, however, that the lower-derived saline water has contaminated the sampling level to the extent of up to 680 mg/l Cl. As explained above, the initial non-saline groundwater (anals. HF1 1B-D) was never again achieved. Other contaminating features include high amounts of Ca^{2+} , Na^{2+} and SO_4^{2-} . The redox character is markedly reducing ($\text{Eh} = -245$ mV) although the dissolved uranium content is fairly high (2.1 ppb) and probably typical of shallow groundwaters in this area. The presence of a near surface or shallow water component is supported by a significant tritium content (8 TU). Compared to other shallow groundwater samples (HF1 1B-L) which have an average pH of around 8.1, a pH value of 7.3 would appear to be unusually low and is most likely a further indication of contamination from deeper-derived saline waters (pH values ranging from 7.3-7.8).

In summary, this level is characterized by waters which represent:

- shallow non-saline groundwaters representative for this depth.
- strong saline component derived from deeper levels.
- significant young, near-surface component derived from higher levels.

Level 114 m

This level is located just above the sub-horizontal fracture Zone. Only limited analyses are available. These are adequate to show that the groundwater is slightly more reducing ($\text{Eh} = -300$ mV) and that the pH is still low (7.5). Salt water mixing is even more apparent, i.e. 2125 mg/l Cl^- , and lower amounts of HCO_3^- (down to 116 mg/l from 285 mg/l).

Level 182 m

This sampling point is located within the sub-horizontal fracture Zone which is hydraulically connected to the boreholes HF1 1, F1 5 and F1 6, and to the Zone 1, figure 3.2. In comparison to the two upper levels, the general chemistry shows a steadily increasing saline component, i.e. increasing Ca^{2+} , Na^+ , SO_4^{2-} , Br^- and Cl^- , and a corresponding reduction in HCO_3^- and TOC. Although still reducing ($E_h = -212$ mV), it is less so than the above levels; the pH value of 7.7 is still lower than perhaps expected. The dissolved uranium content is moderately high (1.6 ppb) and the $^{234}\text{U}/^{238}\text{U}$ activity ratio is high (3.1) indicating widespread disequilibrium in the groundwater environment. An age of 12 200 years is indicated by the ^{14}C data. This level was sampled prior to and subsequent to gas-lift pumping. No significant changes in the chemistry of the waters are apparent.

In conclusion, this water composition is probably reasonably representative for the sub-horizontal Zone 2 which represent the groundwater transition from intermediate non-saline to deeper saline types. As indicated by the absence of tritium (< 3 TU), no younger, near surface component is present.

Level 360 m

This sampling point is well within the saline horizon and is clearly evident from the chemistry which indicates a Ca-Na-Cl groundwater with appreciable Br^- , SO_4^{2-} , and Mg^{2+} . Low TOC typifies a deep groundwater environment and no significant tritium (< 3 TU) indicate the absence of a younger, near-surface component. In common with the higher levels the pH is low (7.4), no Eh values have been quoted because the respective measuring electrodes showed wide variations. The dissolved uranium content is very high (8.2 ppb) and the $^{234}\text{U} / ^{238}\text{U}$ activity ratio of 5.0 indicates widespread disequilibrium due to excess ^{234}U accumulated by alpha recoil processes during long groundwater residence periods. The low pH values and the variation of Eh values are not believed to be an instrumental fault, but a consequence of the saline waters.

11.4 Discussion of results

A graphic representation of the results is presented in figures 11.2 - 11.4. The distinction between the non-saline and saline waters, via a transition zone of mixing as evidenced by the sub-horizontal Zone 2, is clearly visible. This is readily indicated by the conductivity measurements. The pH in contrast shows a perceptible decrease with depth which is contrary to that normally indicated by groundwater at increasing depths. This is not only true for Finnsjön, but also for saline groundwaters in other areas such as Finland and Canada (Fritz and Frøpe, 1982, Hyyppä, 1984). As suggested above, measurement of such parameters such as pH and Eh may be somewhat suspect in such saline environments.

Of the cations, Ca^{2+} , Na^+ and Mg^{2+} shows marked increases with depth. K^+ is less emphasised. Of the anions, HCO_3^- typically decreases with depth accompanied by sympathetic increases of Cl^- and SO_4^{2-} , increases of Br^- are also present. Although not presented, monitoring of S^{2-} shows an increase within Zone 2. This can reflect a greater percentage of pyrite (Chapter 5.7) available as a fracture mineral, and hence in contact with reactive groundwaters, along this zone.

In general, the overall picture is fairly simple and the presence of saline groundwater corresponds to the earlier hydrochemical investigations in the Finnsjön area. Of particular interest in the present work is the function of Zone 2, which appears to represent a structural/hydraulic barrier to the bed-rock groundwater cells of circulatory movement. Downward moving non-saline groundwater flow will preferentially spread out along Zone 2 rather than continue to deeper levels mixing with, and eventually washing out the older salt water. Similarly, the more sluggish upward moving salt water will do likewise. Zone 2 will therefore be a horizon along which groundwaters of considerable age differences will come into contact and mix with one another (note a groundwater age of 12 205 years was obtained from Zone 2).

The presence of deep saline groundwaters in crystalline basement rocks is not uncommon. Occurrences have been documented from the Canadian and Fenno-Scandian shield areas, and from the Carnmenellis granite in S.W. England (Fritz and Frøpe (1982), Hyyppä (1984), Edmunds et al. (1984), Nordstrom (1985)). The salinity of these waters have been attributed to one or more processes which include: a) relict ancient marine water, b) residual igneous/metamorphic fluids, c) rock/water interactions, and d) release of fluids during the mechanical rupture of fluid inclusions.

The origin of the saline groundwater in the Finnsjön area is debatable. Allard et al. (1983) have allocated a residual igneous/metamorphic fluid origin, although partial mixing with Yoldia/Littorina seawater (maximum age of 10 000 years) was not ruled out. Investigations of saline waters in Central Sweden (Nordstrom, 1985) have shown that whilst the majority of the shallow wells examined are of relict Baltic seawater origin, some of the deep groundwaters, such as those from Stripa, are believed to be genetically different with a significant component being derived from the breakdown of fluid inclusions.

Being able to classify saline water as marine or non-marine is based on chemical ionic signatures such as Br/Cl, I/Cl, Ca/Mg, Mg/Cl, Ca/Cl, Na/Cl, K/Cl and SO_4/Cl . The Br/Cl ratio is considered to provide the most definitive evidence for a marine origin. Table 11.2 lists the ionic ratios from various salt water localities, inclusive of Finnsjön. It can be shown that depending on which ionic ratio is compared, the Finnsjön saline waters share certain characteristics with the Yoldia and the more recent Skåne relict seawaters, the 'non-marine' Stripa groundwaters, and the Finnish groundwaters which are mostly considered to be derived from relict marine waters. It would therefore be reasonable to suggest that, bearing in mind the geographical location of the Finnsjön area during the Yoldia/Littorina marine transgressions, and the relatively old age indicated for the Finnsjön saline waters which appear to pre-date these transgressions (e.g. a ^{14}C age range of 9350 - 15 150 years is indicated by groundwaters of < 3 TU), the Finnsjön groundwaters exhibit the following characteristics:

- water that is derived from the Yoldia/Littorina marine transgressions
- residual igneous/metamorphic fluids
- fluids derived from the mechanical breakdown of fluid inclusions

Because of the long residence times of these various bedrock fluids, especially those which are non-marine derived, significant rock/water interactions have more than likely occurred, thus further modifying the chemistry of the groundwaters. In this respect the greater lithium and boron contents of the most saline groundwaters (i.e. 0.05 ppm and 0.80 ppm respectively, when compared to younger shallow groundwaters of 0.008 ppm and 0.50 ppm respectively) could have resulted from limited alteration of biotite and plagioclase feldspar. Such alteration, together with the production of chloride, may have influenced the groundwater salinity to some small degree. Long groundwater residence times are supported by the high $^{234}\text{U}/^{238}\text{U}$ activity ratios resulting from an excessive build-up of ^{234}U by alpha recoil processes.

Although based on limited data, some speculative ideas on the derivation of salt water in the area of immediate study can be forwarded. The various stages of development may be:

- prior to approximately 10 000 years ago the water matrix of the bedrock at depth was heterogeneously saline due to the accumulation of residual igneous/metamorphic fluids, fluid inclusion influences, and limited rock/water interactions.
- during the marine transgressions of the Yoldia (approx. 7000-8000 years ago) and the later Littorina (approx. 2500-5500 years ago) the area became saturated with marine saline waters.
- following isostatic uplift and exposure of the landmass, the near-surface marine water was gradually flushed out and replaced by fresh water. The depth of this flushing out process

would have depended on the regional and local hydrogeology. In this respect the presence of major structural weaknesses (i.e. porous and permeable horizons, faults and shears etc.) will act as hydrological barriers resulting in the entrapment of salt water at higher levels than would otherwise be expected. As horizontal fracture zones are a feature of the Finnsjön area, and particularly illustrated in the area of study, their influence on the groundwater hydraulics has been clearly demonstrated.

The situation to-day is that the sub-horizontal Zone 2 and the adjoining steeply dipping Zone 1 have effectively trapped groundwater of a high saline character at a level which is only about 100 m from the bedrock surface. Zone 2 represents a zone of hydraulic mixing and the waters above and below represent extremes of composition. This local pattern can probably be extended regionally in the Finnsjön area. It can therefore be speculated that saline water exists throughout the bedrock, and its depth of occurrence is to a large degree dependent on the dip and sub-aerial extent of these large-scale sub-horizontal and near-vertical fracture/shear zones.

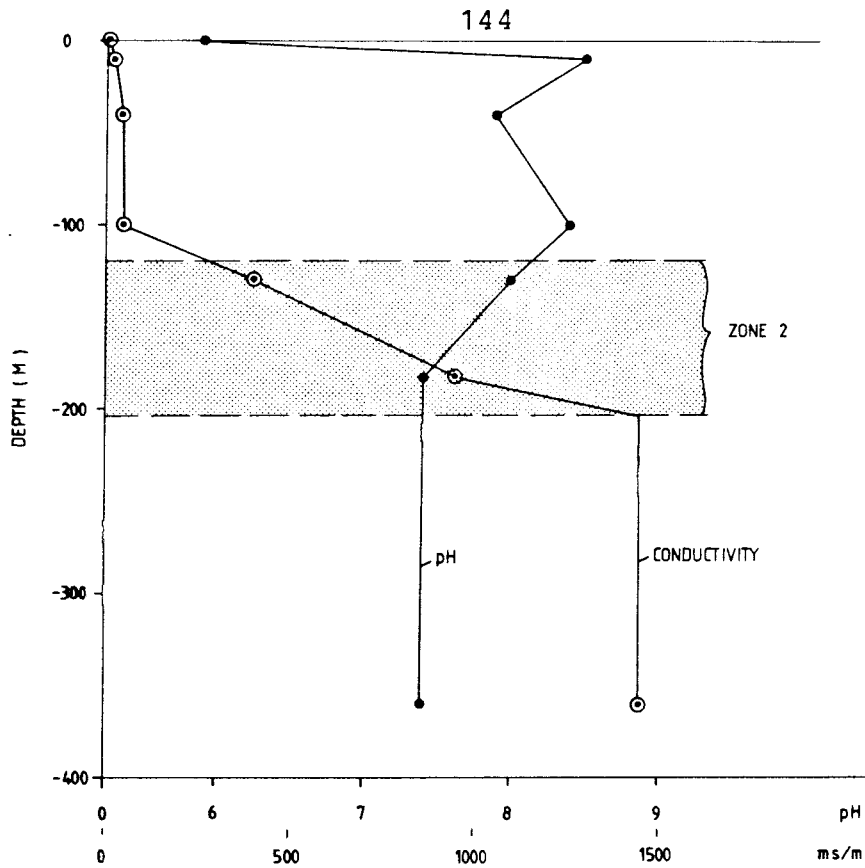


Figure 11.2 Variation of pH and conductivity with depth (boreholes HFi 1 and Fi 9).

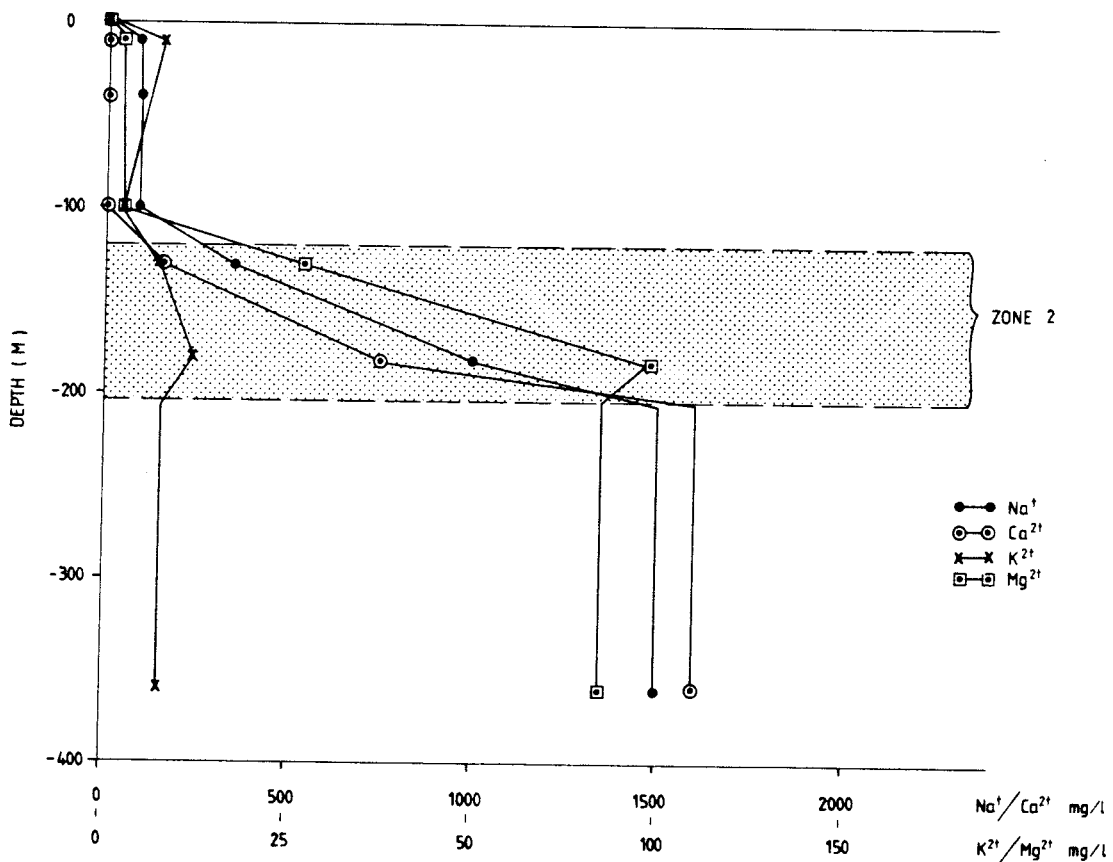


Figure 11.3 Variation of selected cations with depth (boreholes HFi 1 and Fi 9).

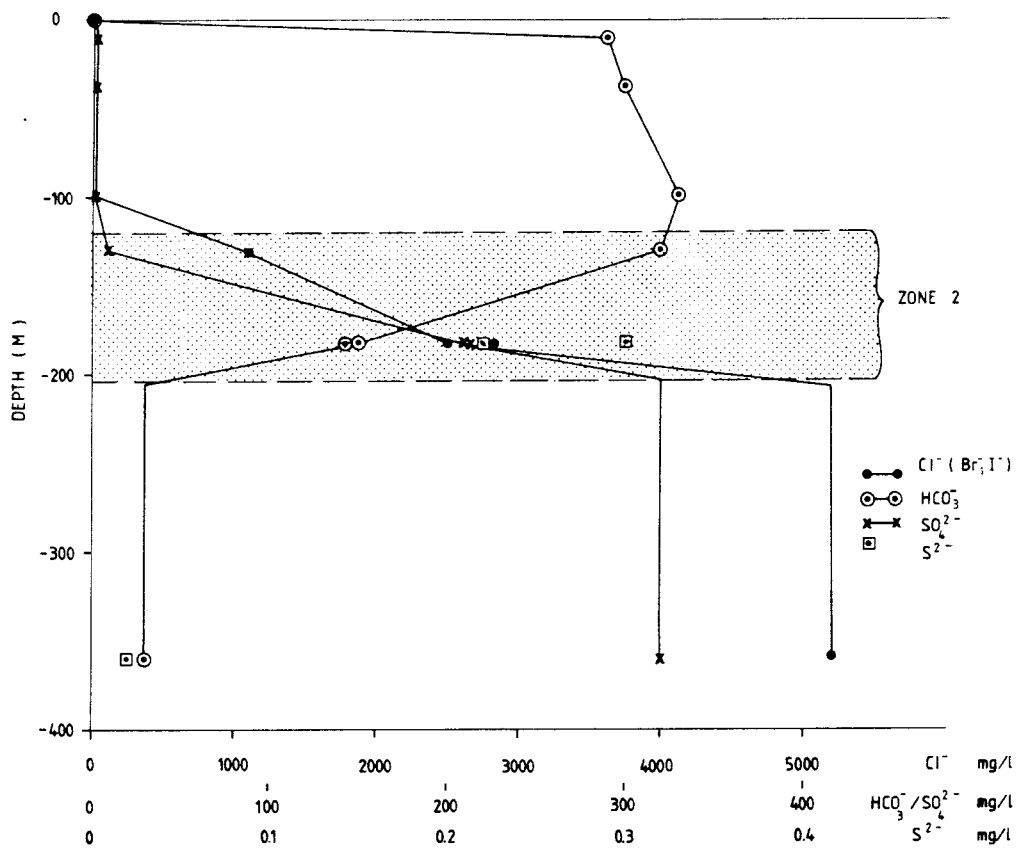


Figure 11.4 Variation of selected anions with depth (boreholes HFi 1 and Fi 9).

Table 11.2 Ion ratios (by weight) of saline waters and the Finnsjön groundwaters.

Table 2: Ion ratios (by weight) of saline waters and the Finnsjön groundwaters.

Sample Type	Br/Cl	I/ClX10 ⁶	Ca/Cl	Mg/Cl	Ca/Cl	Na/Cl	K/Cl	SO ₄ /Cl
<u>Seawater</u>	0.00347	3.1	0.32	0.067	0.021	0.55	0.0206	0.14
<u>Baltic Water</u>	0.00342		0.32	0.067	0.022	0.55	0.0205	0.14
<u>Yoldia Seawater</u>	0.00342	163	4.7	0.052	0.072	0.74	0.0308	0.125
<u>Skåne Brines</u>	0.0055	40-53	22	0.012	0.20	0.50	0.011	0.023
<u>Finnsjön</u>								
Fi5	-	-	18	0.018	0.32	0.26	0.001	0.06
Fi6	-	-	25	0.013	0.33	0.26	0.005	0.06
Fi8	-	-	425	0.001	0.38	0.21	0.002	0.03
Fi9	0.00526	135	20	0.016	0.32	0.29	0.001	0.06
<u>Stripa</u>								
V1-V2	0.0107	446	451	0.00107	0.23	0.47	0.0040	0.11
N1	0.0105	359	108	0.0069	0.48	0.68	0.011	0.016
E1	0.0047	192	56	0.016	0.83	1.56	0.048	0.354
<u>Shallow Wells</u>	0.0024	330	6.7	0.94	7.1	1.17	0.39	2.3
<u>Surface Waters</u>	0.0077	1300	4.8	0.40	1.77	0.65	0.21	2.1
<u>Finnish Groundwaters</u>								
Kalajoki	-	-	28	0.013	0.36	0.30	0.007	-
Jurmo	-	-	3.5	0.058	0.21	0.48	0.020	-
Ahvenanmaa	-	-	4.5	0.056	0.25	0.34	0.009	-

11.5 Conclusions of the water chemistry studies

This limited hydrochemical study of the Finnsjön area has resulted in the following interesting points:

- sampling during the drilling of a percussion borehole (i.e. a crude simulation of the "booster hole" method) has been demonstrated to be an promising method for hydrochemical purposes.
- the success of selecting saline and non-saline groundwaters for drilling F1 9 is largely unknown.
- systematic sampling of drilling water during drilling was not possible because of the very fractured, permeable nature of the Finnsjön bedrock. No drilling water was recycled and therefore no indication as to water/hole chemical reactions was possible.
- the saline water encountered at such shallow levels has been trapped by the fracture geometry of the investigated area. These medium to large-scale structures have functioned as hydrologic barriers to the flushing out and replacement of the saline water by non-saline groundwaters.
- the presence or absence of saline water throughout the Finnsjön region, and its occurrence at different levels within the bedrock, is largely determined by the structural geometry.
- the Finnsjön saline groundwaters comprise waters resulting from the Yoldia/Littorina marine transgressions, from residual igneous/metamorphic fluids, from fluids released from the mechanical rupture of fluid inclusions, and from rock/water interactions over long residence times.

12. CONCLUSIONS

The aim of the first phase of the Fracture Zone Project was to select a fracture zone in one of the SKB study sites, suitable for detailed studies regarding hydraulic properties, transport mechanisms and rock stability. The first phase also includes a preliminary geoscientific characterization in order to assess the suitability of the selected fracture zone and to obtain data for the design of the detailed studies.

After a selection process, where about 50 fracture zones were compared, the Brändan fracture zone within the Finnsjön study site was selected for preliminary characterization. The investigations were at first concentrated to this zone. However, after the discovery of a major subhorizontal fracture zone, which appeared to have a strong influence on the hydrology and groundwater chemistry, the major part of the investigations was focused on the subhorizontal fracture zone.

Zone 1, the Brändan fracture zone, is 20 metres wide, strikes NNE and dips about 75 degrees towards east. The fracture zone is from geophysical ground surveys traceable for at least 1 km. The zone is intersected by two boreholes and displays a high frequency of coated and sealed fractures. The high fracture frequency together with hematitization of fractures clearly define the zone. The hydraulic conductivity of the zone varies between $1.2 \cdot 10^{-6}$ and $4.8 \cdot 10^{-5}$ m/s measured by single-hole water injection tests at vertical depths between 57 and 76 m.

Zone 2 is about 70 metres wide and strikes N-S with a westerly dip of about 17 degrees. However, since the zone is only defined in boreholes situated at a more or less straight line, the precise orientation is uncertain. The zone is intersected by at least 5 boreholes, thereby showing a minimum lateral extent of about 450 m. The boreholes intersect the upper part of the zone at 100-200 m. Zone 2 represents an old ductile shear zone, which has been reactivated by brittle deformation. Several sections, 2-5 m wide, with mylonitic to cataclastic deformation

characterize the zone. The frequency of coated fractures for the Zone 2 varies greatly, while the frequency of sealed fractures is high in all boreholes.

The radar measurements confirm the existence and orientation of Zone 2. The width of the zone, as indicated from the distribution of sealed fractures, coincides in general with a decrease in velocity and a penetration loss for the radar waves. This is caused by high porosity of the bedrock in connection to the zone.

Zone 2 has in most boreholes two maxima of hydraulic conductivity, one at the upper border, another at the lower border of the zone. Within these high conductive sections, several values higher than 10^{-4} m/s have been measured. Between the two high conductive parts, there is a low conductive section, $3 \cdot 10^{-9}$ - $7 \cdot 10^{-7}$ m/s. Interference tests show a well established hydraulic connection in Zone 2 between all five investigation boreholes. Hydraulic conductivity and storativity determined from interference tests gave somewhat different results according to the evaluation method used. Evaluation according to a double porosity model resulted in similar values of hydraulic conductivity in most sections as those determined from water injection tests. When a homogeneous-isotropic model was used, the conductivity values seemed to be overestimated. The specific storage coefficient for Zone 2 according to the double porosity model evaluation gave values ranging between $1 \cdot 10^{-5}$ and $4 \cdot 10^{-4}$ m^{-1} .

From hydrochemical investigations in two boreholes, a distinction between non-saline and saline waters, via a transition zone of mixing in Zone 2, was clearly visible. Geophysical logging showed, that the same conditions prevail in all boreholes intersecting Zone 2. The saline water encountered at such shallow levels might have been trapped by the geometry and character of the fracture zones of the investigated area. Piezometric measurements revealed, that Zone 2 has a somewhat lower groundwater pressure compared with the surrounding bedrock. Thus, two circulating groundwater systems, one above and another below Zone 2, appear to exist. Both are drained into the Zone 2.

The saline groundwater might comprise waters resulting from the Yoldia/Littorina marine transgressions, from residual igneous/metamorphic fluids, from fluids released from the mechanical rupture of fluid inclusions, and from rock/water interactions over long residence times.

Both Zone 1 and Zone 2 fulfil most of the characteristics considered favourable for the Fracture Zone Project. However, the amount of data, and thus the reliability, is much higher for Zone 2 than for Zone 1. The subhorizontal Zone 2 displays a high hydraulic conductivity in all boreholes penetrating the zone together with a well established hydraulic connection between the different boreholes. This is also shown by the tracer test performed in connection to drilling of borehole F1 9. Water chemistry studies and piezometric measurements indicate, that the zone is hydraulically active under undisturbed conditions. All these facts speak in favour of choosing Zone 2 for detailed studies regarding hydraulic properties and transport mechanisms.

There are a number of other factors that have an influence on the suitability for detailed studies of a specific fracture zone. For instance: accessibility, high degree of outcrops, high hydraulic gradient, homogenous bedrock, few interfering minor fracture zones and the possibility of making surface fracture studies at the outcropping part of the fracture zone. Also most of these factors speak in favour for the Zone 2. One exception is the hydraulic gradient, which is low. Concerning the possibility to make surface fracture studies, a strongly fractured and tectonized area has been discovered at the calculated outcropping of the zone. However, since the precise orientation of Zone 2 is uncertain, and since another fracture zone has been interpreted to be located in the same area, further investigations are needed to confirm the location of the outcropping of zone 2.

REFERENCES

- Allard, B., Larson, S-Å. and Tullborg, E-L. (1983): Chemistry of deep groundwaters from granitic bedrock. KBS Technical Report 83-59.
- Almén, K-E., Ekman, L., Olkiewicz, A., 1978: Försöksområdet vid Finnsjön. Beskrivning till berggrunds- och jordartskartor. SKBF-KBS Teknisk Rapport 79-02.
- Almén, K., Andersson, O., Hansson, K., Johansson, B.E., Nilsson, G., Wikberg, P., and Åhagen, H. (1983): Final disposal of spent nuclear fuel - equipment for site characterization. KBS Technical Report TR 83-44.
- Brotzen, O., Duran, O., Magnusson, K-Å. (1980): Evaluation of geophysical borehole studies. Report Prav 4.14. Stockholm.
- Carlsson, L., B. Gentzchein, G. Gidlund, K. Hansson, T. Svensson and U. Thoregren (1980): Supplementary permeability measurements in the Finnsjön area (In Swedish). KBS Technical report TR 80-10.
- Carlsson, L. and Gidlund, G. (1983): Evaluation of the hydrogeological conditions at Finnsjön, and Hesselström, B., Supplementary geophysical investigations of the Stårnö peninsula. SKBF-KBS Technical Report TR 83-56.
- Carlsson, L. and Winberg, A. (1983): Model calculations of the groundwater flow at Finnsjön, Fjällveden, Gideå and Kamlunga. SKBF-KBS Technical Report 83-45.
- Carlsson, L. and Olsson, T. (1985): Hydrogeological and hydrogeochemical investigations in boreholes - injection - recovery tests and interference tests. Stripa project, internal report 85-09.

- Cooper, H.H. and Jacob, C.E. (1946): A generalized graphical method for evaluating formation constants and summarizing well-field history. Trans. Amer. Geoph. Un. Vol. 27, No. IV., August 1946.
- Duran, O. (1984): Borehole in situ measurements of Eh, pH, pS^{2-} and temperature. SGAB IRAP-84022.
- Edmunds, W.M., Andrews, J.N., Burgess, W.G., Kay, R.L.F., and Lee, D.J. (1984): The evolution of saline and thermal groundwaters in the Carnmenelles granite. Mineral. Mag. 48, 3. pp. 407-424.
- Evans, S. and Bergman, R. (1981): Uranium and radium in Finnsjön - an experimental approach from calculation of transfer factors. SKBF-KBS Teknisk Rapport 81-10.
- Fischer, H.B., List, E.J., Koh, R.C.Y., Imberger, J. and Brooks, N.H. (1979): Mixing in Inland and Coastal Waters, pp. 443-449. Academic Press Inc., New York.
- Fritz, P. and Frøpe, S.K. (1982). Saline groundwaters in the Canadian Shield - A first overview (1982). Chem. Geol. 36, pp. 179-190.
- Gidlund, G. (1978): Analyser och åldersbestämningar av grundvatten på stora djup. KBS Teknisk Rapport 62.
- Gustafsson, E. and Klockars, C-E. (1981): Studies on groundwater transport in crystalline rock under controlled conditions using nonradioactive tracers. SKBF-KBS Teknisk Rapport 81-07.
- Hult, A., Gidlund, G., Thoregren, U., Magnusson, K-Å. and Duran, O. (1978): Permeabilitetsbestämningar, Geofysisk borrhålmätning. KBS Teknisk Rapport 61.
- Hultberg, B., Larson, S-Å. and Tullborg, E-L. (1981): Grundvatten i kristallin berggrund. SGU Arbetsrapport.

- Hyypä, J. (1984): Sammansättningen hos grundvattnet i Finlands berggrund. Rapport YJT-84-10 (Finska Kraftbolagens Kommission för Radioaktivt Avfall).
- Jacobsson, J-Å. (1980): Resultat av kompletterande jordartssonderingar i Finnsjöns undersökningsområde 1979. SGU Arbetsrapport 1980-02-22.
- Jacobsson, J-Å. (1980): Resultat av brunnsinventering i Finnsjöns undersökningsområde 1979. SGU Arbetsrapport 1980-02-26.
- Jacobsson, J-Å. and Larsson, N-Å. (1980): Hydrologisk ytkartering av Finnsjöns undersökningsområde. SGU Arbetsrapport 1980-03-06.
- Jämtlid, A., Magnusson, K-Å. and Olsson, O. (1981): Elektriska mellanhålmätningar i Finnsjön. Rapport Prav 4.23.
- Kamb, B.W., (1959): Theory of preferred crystal orientation developed by crystallization under stress. Journal of Geology, Vol. 67, No 2, pp. 153-170.
- Larson, S.Å. (1980): Sprickmineralogisk litteraturstudie. Rapport Prav 4.13.
- Larsson, N-Å. and Svenson, T. (1980): Nederbördsdata från Finnsjöns undersökningsområde februari - september 1979. SGU Arbetsrapport 1980-01-30.
- Larson, S.Å., Tullborg, E-L. and Lindblom, S. (1981): Sprickmineralogiska undersökningar. Rapport Prav 4.20.
- Laurent, S. (1982). Analysis of groundwater from deep boreholes in Kräkemåla, Sternö and Finnsjön. KBS Technical Report 82-23.
- Magnusson, K-Å. and Duran, O. (1984): Comparative study of geological, hydrological and geophysical borehole investigations. SKBF-KBS Technical Report 84-09.

- Moreno, L., Neretnieks, I. and Klockars, C-E. (1983): Evaluation of some tracer tests in the granitic rock at Finnsjön. SKBF-KBS Teknisk Rapport 83-38.
- Nordstrom, K. (1985): Hydrogeological and hydrochemical investigations in boreholes - Geochemical and isotope characterisation of the Stripa groundwaters. Andrews et al. Stripa Report.
- Olsson, O., O. Forslund, L. Lundmark and E. Sandberg and L. Falk (1985): The design of a borehole radar system for detection of fracture zones. NEA symposium on In Situ Experiments in Granite Associated with the Disposal of Radioactive Waste, Stockholm, (in press).
- Olkiewicz, A., S. Scherman and K-A. Kornfält (1979): Supplementary bedrock investigations in the Finnsjön and Karlshamn areas (In Swedish): KBS Technical Report 79-05.
- Saxena, R.K. (1984): Surface and groundwater mixing and identification of local recharge - discharge zones from seasonal fluctuations of 180 in groundwater in fissured rock. Division of Hydrology, Uppsala University, Sweden.
- Scherman, S. (1978): Förarbeten för platsval, berggrundsundersökningar, and Klockars, C-E., Persson, O. (1978): Berggrundsvattenföihållanden i Finnsjöområdet nordöstra del. KBS Teknisk Rapport 60.
- Skagius, K. and Neretnieks, I. (1982): Diffusion in crystalline rocks of some sorbing and nonsorbing species. SKBF-KBS Teknisk Rapport 82-12.
- Skagius, K. and Neretnieks, I. (1983): Diffusion measurements in crystalline rocks. SKBF-KBS Teknisk Rapport 83-15.
- Smart, P.L. and Laidlaw, I.M.S. (1977): An evaluation of some fluorescent dyes for water tracing. Water Resources Research Vol. 13 no. 1, pp. 15-33.

- Smellie, J.A.T., Larsson, N. and Wikberg, P. (1985): Hydrochemical investigations in crystalline bedrock: Experience from the SKB testsites in Sweden. (In preparation).
- Streltsova, T.D. (1983): Well Pressure Behaviour of a Naturally Fractured Reservoir. Society of Petroleum Engineers Journal, October 1983.
- Streltsova, T.D. (1984): Buildup Analysis for Interference Tests in Stratified Formations. Journal of Petroleum Technology, February 1984.
- Stokes, J. and Thunvik, R. (1978): Investigations of groundwater flow in rock around repositories for nuclear waste. KBS Teknisk Rapport 47.
- Swan, G. (1977): The mechanical properties of the rocks in Stripa, Kråkemåla, Finnsjön and Blekinge. KBS Teknisk Rapport 48.
- Tullborg, E-L. and Larson, S.Å. (1982): Fissure fillings from Finnsjön and Studsvik, Sweden. Identification chemistry and dating. SKBF-KBS Teknisk Rapport 82-20.
- Walton, W.C., (1970): Groundwater Resource Evaluation. Mc Graw-Hill Book Company, New York.
- Wiman, E., (1930): Mineralized fissures and the succession of fissure filling. Bull. Geol. Inst. Uppsala 23, pp. 89-98.
- Wickman, F.E., Åberg, G. and Levi, B. (1983): Rb-Sr dating of alteration events in granitoids. Contrib. Mineral. Petrol. Vol. 83, pp. 358-362.
- Wikberg, P., Grenthe, I. and Axelsen, K. (1983): Redox conditions in groundwaters from Svartboberget, Gideå, Fjällveden and Kamluge. KBS Technical Report TR 83-40.

List of SKB reports

Annual Reports

1977–78

TR 121

KBS Technical Reports 1 – 120.

Summaries. Stockholm, May 1979.

1979

TR 79–28

The KBS Annual Report 1979.

KBS Technical Reports 79-01 – 79-27.

Summaries. Stockholm, March 1980.

1980

TR 80–26

The KBS Annual Report 1980.

KBS Technical Reports 80-01 – 80-25.

Summaries. Stockholm, March 1981.

1981

TR 81–17

The KBS Annual Report 1981.

KBS Technical Reports 81-01 – 81-16.

Summaries. Stockholm, April 1982.

1982

TR 82–28

The KBS Annual Report 1982.

KBS Technical Reports 82-01 – 82-27.

Summaries. Stockholm, July 1983.

1983

TR 83–77

The KBS Annual Report 1983.

KBS Technical Reports 83-01 – 83-76

Summaries. Stockholm, June 1984.

1984

TR 85–01

Annual Research and Development Report 1984

Including Summaries of Technical Reports Issued during 1984. (Technical Reports 84-01–84-19)
Stockholm June 1985.

1985

TR 85-20

Annual Research and Development Report 1985

Including Summaries of Technical Reports Issued during 1985. (Technical Reports 85-01-85-19)
Stockholm May 1986.

Technical Reports

1986

TR 86-01

I: An analogue validation study of natural radionuclide migration in crystalline rock using uranium-series disequilibrium studies

II: A comparison of neutron activation and alpha spectroscopy analyses of thorium in crystalline rocks

JAT Smellie, Swedish Geological Co, A B MacKenzie and RD Scott, Scottish Universities Research Reactor Centre
February 1986

TR 86-02

Formation and transport of americium pseudocolloids in aqueous systems

U Olofsson
Chalmers University of Technology, Gothenburg, Sweden
B Allard
University of Linköping, Sweden
March 26, 1986

TR 86-03

Redox chemistry of deep groundwaters in Sweden

D Kirk Nordstrom
US Geological Survey, Menlo Park, USA
Ignasi Puigdomenech
Royal Institute of Technology, Stockholm, Sweden
April 1, 1986

TR 86-04

Hydrogen production in alpha-irradiated bentonite

Trygve Eriksen
Royal Institute of Technology, Stockholm, Sweden
Hilbert Christensen
Studsvik Energiteknik AB, Nyköping, Sweden
Erling Bjergbakke
Risø National Laboratory, Roskilde, Denmark
March 1986